University of Misan

College of Science

Department of Chemistry

Preparation, Characterization, Biological Activity and Molecular Docking Study of Some New Aniline Derivatives

A thesis

Presented to the College of Science\University of Misan

in fulfillment of the thesis requirement for the degree of Master of Science

in Chemistry

By

Zahraa Sabah Shamkhi

B.Sc. Chemistry / Misan University 2021

Supervisor

Prof. Dr. Kareem Salim Abbas

Asst. Prof.Dr. Yusra Sebri Abdul-Saheb

2025

Acknowledgement

Above all else, I want to express my great thanks to ALLAH for helping me to present this thesis. I wish to express my sincere gratitude and great appreciation to my Supervisors **Prof. Dr. Kareem Salim Abbas and Asst. prof.Dr. Yusra Sebri Abdul-Saheb** for their guidance and their encouragement throughout this work. I'm greatly indebted for the assistance given to me by Head and staff of Chemistry Department, College of Science, Misan University.

I thank, Dr. Usama Ali Muhsen, and Dr. Ali Taha Saleh for their assistance.

Finally, all appreciation and respect to my family (my dear father and mother, my sisters and brothers) for their encouraged.

List of Contents

LIST OF TABLES

LIST OF EQUATIONS

LIST OF SCHEMES

LIST OF FIGRUES

LIST OF ABBREVIATIONS

Abbreviations Symbols	Definition
AIDS	Acquired immunodeficiency syndrome
$BCSC_S$	Breast cancer stem cells
^{13}C-NMR	Carbon (13) Nuclear Magnetic Resonance
cm^{-1}	Wave Number Unit
3D	3 Dimensional
DMF	Dimethylformamide
DHPS	Dihydropteroate synthase
DCM	Dichloromethan
DPEA	N, N-Diisopropylethyl amine
et.al	et alia
Et_3N:	Triethyl amine
70 EV	70 Electric volt
ETOAc	Ethyl acetate
FT-IR	Fourier transform infrared spectroscopy
Gr+	Gram positive
Gr-	Gram negative
G	Gram
H	Hour
^1H-NMR	Proton (1) Nuclear Magnetic Resonance
HIV	Human immunodeficiency virus
IZ	inhibition zone
IC_{50}	half-maximal inhibitory concentration
LIHMDS	Lithium hexamethyldisilazide
M.P	Melting point

MOE	Molecular Operating Environment
MIC	Minimum inhibitory concentration
MeCN	Acetonitrile
MBC	Minimum bactericidal concentration
MWI	microwave irradiation
MTT	Methyl thiazolyldiphenyl-tetrazolium bromide
Ml	Milliliter
NBS	N-Bromosuccinimide
Nm	Nanometer
PDB	Protein Data Bank
Ph	Phenyl group
PPM	part per million
r.t	Room temperature
RMSD	Root mean square deviation
TLC	Thin layer chromatography
TMSCI	Chlorotrimethylsilane
TCT	2,4,6-Trichloro-1,3,5-triazine
TBAB	Tetrabutylammonium bromide
TMS	Tetra methylsilane
TAP	1,3,5-triazo-2,4,6-triphosphorine
THF	Tetrahydro furane
T_3P	Propanephosphonic acid anhydride
UV	Ultraviolet
Δ	Chemical shift in NMR
$^{\circ}C$	Degree Celsius
μg/ml	Microgram/Ml
%	Percentage

Abstract

The study has been divided into Four main parts:

The first part involves the synthesis of some benzamide derivatives (A1-A6) by the reaction of *p*-substituted aniline or o-tolidine with 4-chlorobenzoyl chloride in the presence of 1,4-dioxane as solvent.

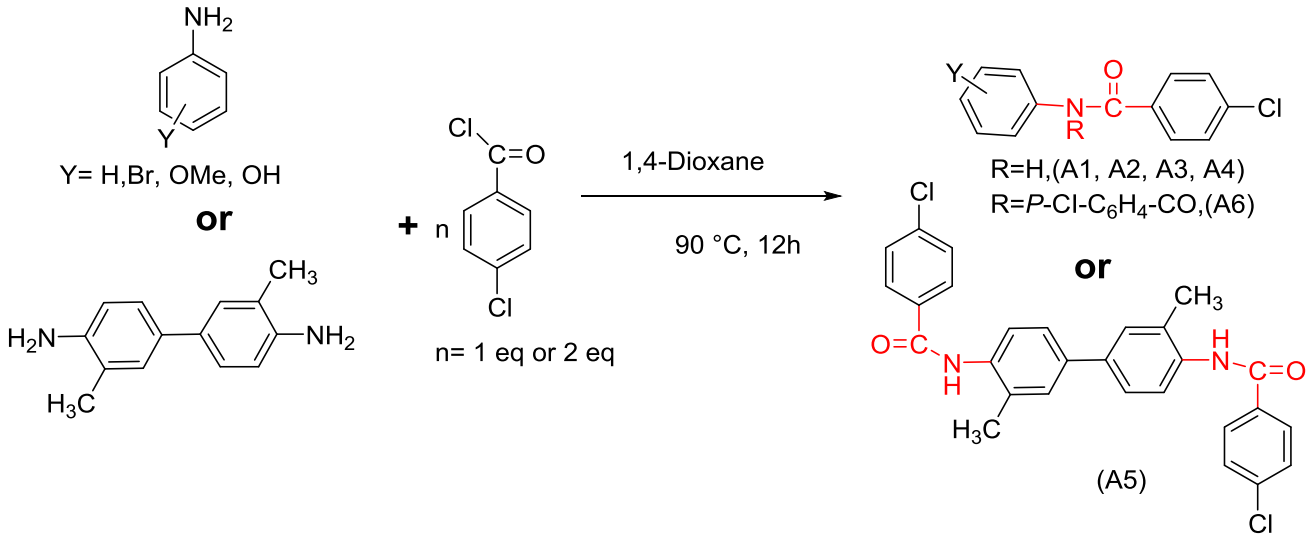

The second part shows, some sulfonamide derivatives(B1-B5) are synthesized through the reaction of p-substituted aniline or o-tolidine with *p*-toluene sulfonyl chloride using DCM as solvent and Et_3N: as catalyst.

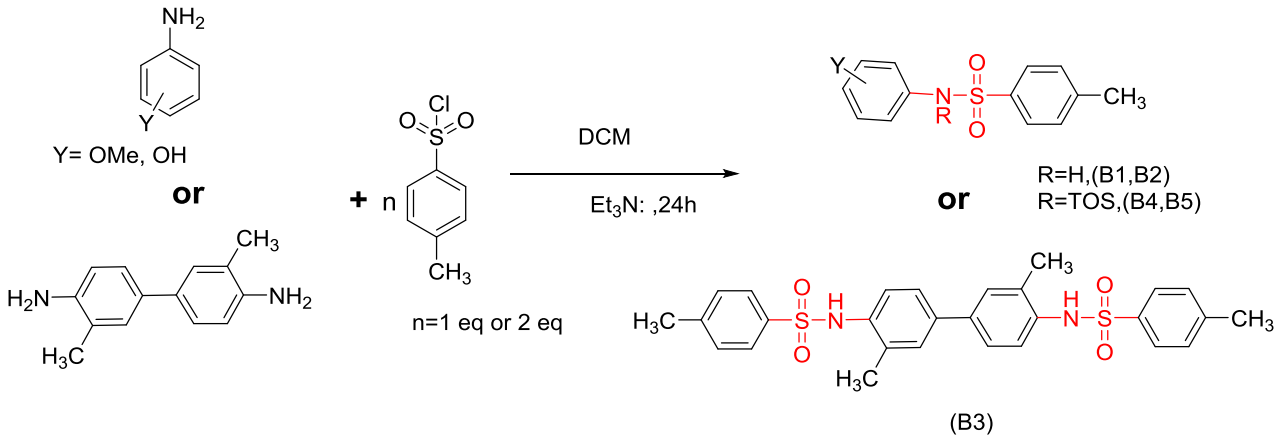

The third part describes the synthesis of some allyl derivatives (C1-C3) by mixing A1, B2 or o-tolidine with allyl bromide and potassium carbonate in acetone/H_2O.

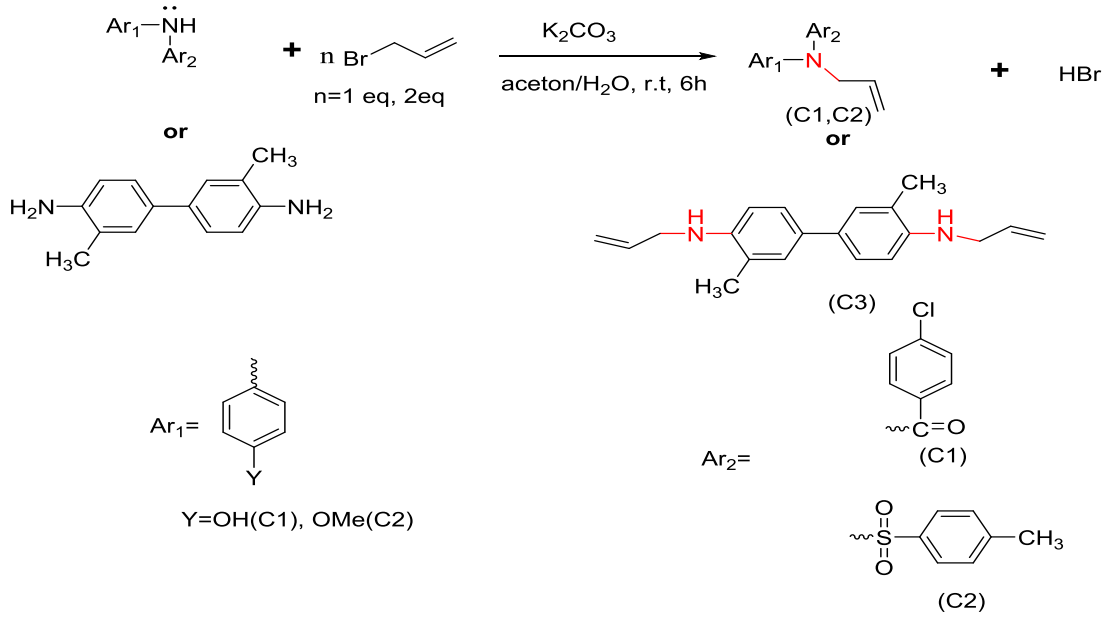

Benzamide, sulfonamide and allyl derivatives are characterized by some physical measurements, such as melting points, thin layer chromatography besides the spectroscopic techniques, FT-IR, ^{1}H-NMR, ^{13}C-NMR and mass spectrometry. The study shows that all the data and values obtained from physical and spectroscopic measurement confirmed the validity of the structures of the derivatives prepared in this study.

The fourth part: comes up with the molecular docking of the prepared compounds which is studied by using a program (MOE 2015.10) to analyze the ability of these compounds to inhibit breast cancer, by binding them to a single protein (PDB: 3eqm) and compounds (A1, A5, B2, B5, C1) shows good activity. Subsequently, the biological activity of these compounds is estimated after the synthesis for compounds and characterized by different chemical methods, including anticancer and antioxidant activity, these activities were determined in vitro using the

cytotoxicity assay (MTT cell viability assay) in MCF-7 Cells to detect the anticancer activity, and DPPH assay (IC_{50}) for scavenging action against free radicals to antioxidant activity determination. In this study, the MCF-7 cell line was used to assay the antiproliferative activity of different compounds, The cytotoxic impact of (A1, A2, A3, A4, A5, B4, B5) on the breast cancer cell line (MCF-7) was determined, the cytotoxic effect of (A1, A2, A3, A4, A5, B4, B5) in concentration ranged from (7.4-600) µg/ml on MDA-MB-231 cells. In addition, The IC_{50} values were used to compare the antiradical scavenging activity of different analyzed samples with those of standard antioxidant compound. The IC_{50} values cleared that A1 compound exhibited the highest antiradical scavenging activity with the lowest IC_{50} value (6.9 µg/mL), while the A2 had the lowest capacity to scavenge the radical with the highest IC_{50} value (31019.2 µg/mL).

1. Introduction

1.1. Amides

A type of chemical compounds have a functional group that is made up of a carbonyl group bound to a carbon on one side and a nitrogen on the other, carboxylic acid derivatives in the acid's (-OH) has been swapped out for (-NR_2), where R is any of the following: (H, alkyl, or aryl). Similar to amines, amides are categorized as "primary", "secondary" or "tertiary" based on how much of nitrogen has been substituted with carbon[1].

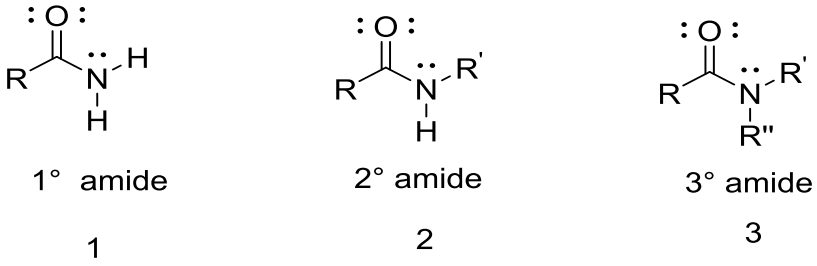

The simplest amides are derivatives of ammonia in which one hydrogen atom has been replaced by an acyl group. The ensemble is generally represented as ($RCONH_2$) and is described as a primary amide (1). Closely related and even more numerous are secondary amides (2) which can be derived from primary amines ($R'NH_2$) and have the formula ($RCONHR'$). Tertiary amides (3) are commonly derived from secondary amines ($R'R''NH$) and have the general structure ($RCONR'R''$) **Figure 1.1**[1].

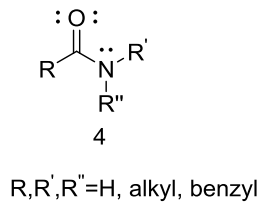

Figure 1.1: Chemical structure of amide.

Based on the type of nitrogen substituents and overall structure, amides can also be subclassified as cyclic (lactams), aromatic (benzamides or anilides), or aliphatic (acetamide). As demonstrated in the examples below, aromatic amides (5) have at least one aromatic ring substituent, whereas aliphatic amides (6) have simple hydrocarbon substituents (alkyl groups). A cyclic structure with an amide group is present in lactams (7).[1]

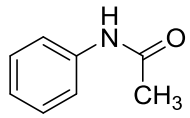

Aromatic amide

5

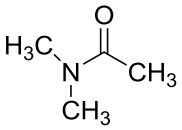

Aliphatic amide

6

Lactam(Cyclic amide)

7

For instance, molecules like proteins are vital to almost every biological action, including enzymatic catalysis (because almost all known enzymes are proteins), hemoglobin transport and storage, antibody defense against infection, and collagen mechanical support. Because all three of the (O-C-N) chain atoms in an amide are reactive, they serve as a valuable moiety in organic compounds and are therefore essential to medicinal chemists. A few of the amides found in are (8,9) nature.[2]

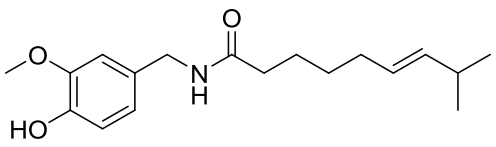

8

Capsaicin

Found in red and green chili peppers

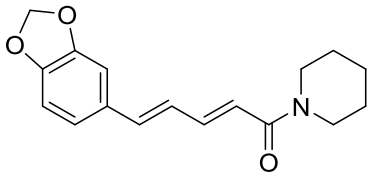

9

Piperine

Component of white and black pepper

Carboxamides are the most prevalent type of organic amides, while phosphoramides and sulfonamides are also recognized as significant amide types. Amides are widely used as structural materials in both nature and industry. Amide synthesis can be done in a lot of ways. The simplest way to create an amide is to combine an amine and a carboxylic acid or reacting the acyl chloride with the intended amine (a process known as aminolysis), coupling reactions with acyl chlorides can generate amide bonds, as seen in **Equation 1-1**[3].

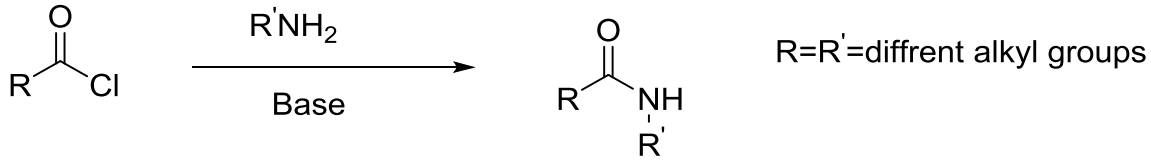

Equation 1.1: Amide preparation (aminolysis).

However, acyl chlorides are often robust enough to be coupled to amines under aqueous conditions, such as in the presence of NaOH (Schotten–Baumann conditions) **Equation 1.2** [4].

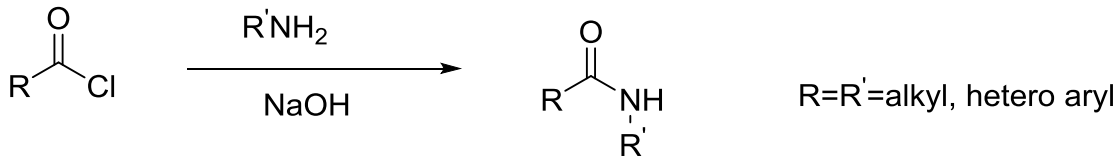

Equation 1.2: Amide preparation (Schotten-Baumann).

Couplings are typically performed in inert dry solvents, in the presence of a non-nucleophilic tertiary amine (Et_3N:, *i*Pr_2NEt) (also called Hunig's base), or N-methyl morpholine). An additional base is typically required to trap the formed HCl and prevent the amine from being converted into its unreactive HCl salt.[5]

Because of its simplicity, sustainability, and cleanliness, photocatalysis has become a potent technique for the creation of (C-C and C-N) bonds in recent years **Equation 1.3** [6].

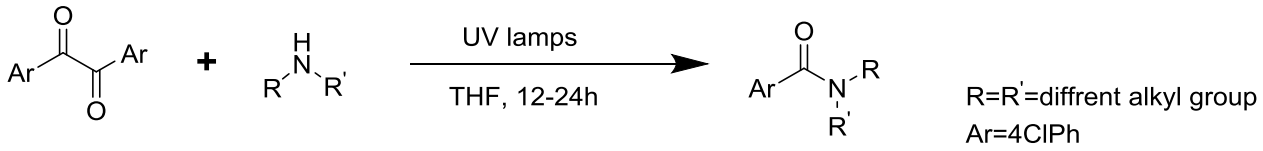

Equation 1.3: Amide preparation (Photocatalysis).

A series of methods for metal-catalyzed synthesis of amides have been well developed **Equation 1.4**[7].

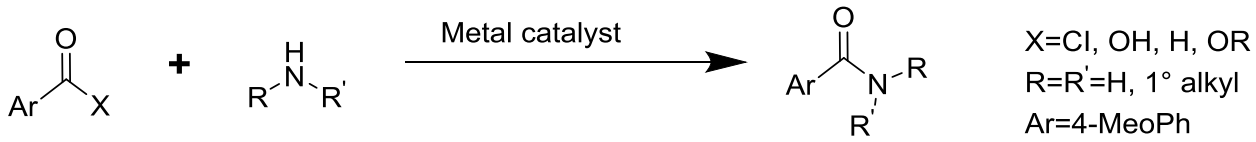

Equation 1.4: Amide preparation (metal-catalyzed).

N-formylation of amines with glyoxylic acid provides formamides in good yields. The reaction tolerates a wide range of functional groups under metal free and base free conditions. In addition, large-scale experiments and high chemo-selectivity have shown great potential application of this strategy **Equation 1.5**.[8]

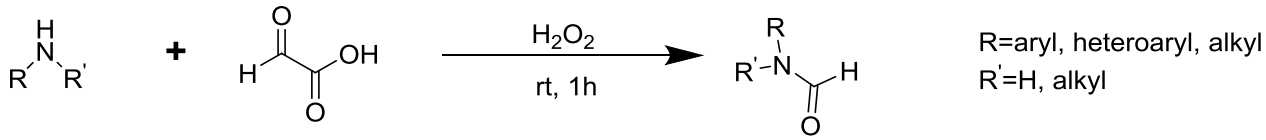

Equation 1.5: Amide preparation (N-formylition).

1.2. Benzamides

Benzamide is an organic molecule **Figure1.2**

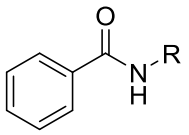

Benzamide
R=H, alkyl, aryl, benzyl group

Figure 1.2: Chemical structure of benzamide.

Benzamides are significant structural components in a wide variety of chemicals isolated from natural sources that may have biological activity. Benzamides are amide of benzoic acid or any of its byproducts; some of its derivatives are pharmaceuticals. Although nowadays benzamides have largely been replaced by 5-HT3-antagonists, they are still used in post-chemotherapy nausea and vomiting as an adjunct agent for delayed emesis. Benzamide analogs screening revealed that metoclopramide (10) is one of the most effective drugs in blocking vomiting [264]. Metoclopramide has been used clinically for the suppression of moderate-to-severe chemotherapy nausea and vomiting. High doses of metoclopramide have been combined with dexamethasone as antiemetic for highly emetogenic chemotherapy. It is also an advantageous antiemetic for Parkinson's disease patients for whom it was used to prevent L-DOPA-induced emesis . [9]

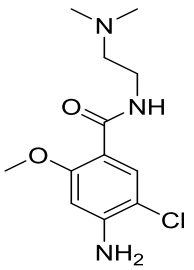

10
Metoclopramide

1.2.1. Applications of benzamide derivatives

The comprehensive medicinal chemistry database revealed that the carboxamide group appears in more than 25% of known drugs. Benzamides (11) have been reported to possess in vitro antibacterial activity. These benzamides exhibit optimal antimicrobial activity against *Staphylococcus aureus*.[10]

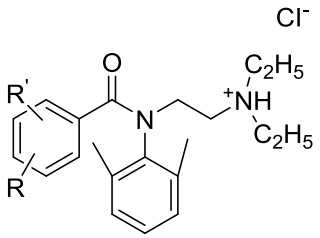

11

R=R'= diffrent alkyl groups

Benzamide derivatives (12)were created by M. L. Carmellino *et al*., and they demonstrated antifungal efficacy.[11]

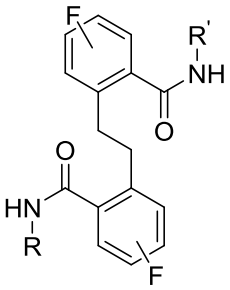

12

R=R'= diffrent alkyl groups

D. Raffa *et al*. produced 2-iodobenzamide derivatives (13) which demonstrated antifungal efficacy against species of *Alternaria*, *B.cinerea*, *R.solani*, and *P. citopathogenicum* .[10]

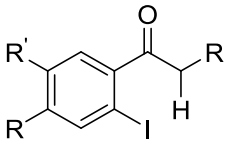

13

R=R'=H, alkyl group

H. Li and colleagues developed and synthesized benzamides containing diketoacids (14) and assessed their HIV-related properties. Through an increase in the carbon chain between the amide group and benzene, the structure-activity relationship of these compounds was examined.[12]

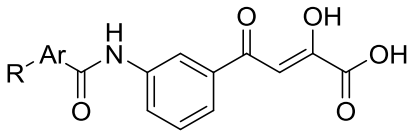

14

R=diffrent alkyl groups
Ar=Ph

N-[substituted phenyl)-5-methyl-4-oxo-1,3-thiazolidin-3-yl]benzamide (15) shows strong anti-HIV properties, according to research by G. Nagalakshmi *et al* .[12]

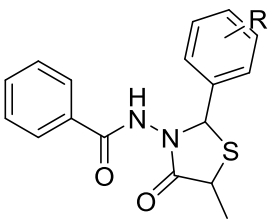

15

R=diffrent alkyl groups

A number of N-phenyl benzamide derivatives are synthesized, and (16) one of those compounds, shows promise as an anti-Enterovirus .[13]

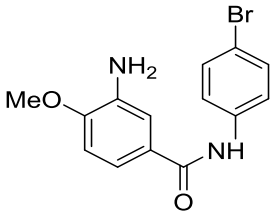

16

Significant reduction of lipid peroxidation was also demonstrated by N-(anilino carbonothioyl)benzamide (17).[14]

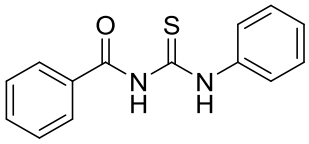

17

The biological activity of a number of benzamide derivatives (18) is studied represented by determining the inhibition diameter zone (IZ), minimum inhibitory concentration (MIC) and minimum bactericidal concentration (MBC) given by these compounds against the test organisms *Staphylococcus aureus* Gr(+) and *Escherichia coli* Gr(-).[15]

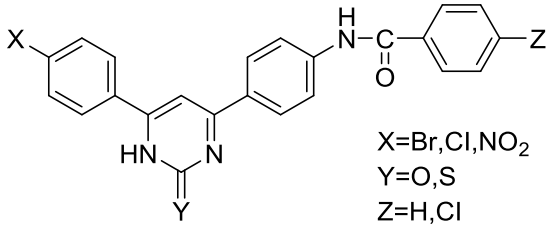

18

1.2.2. Synthesis of benzamides

Tetrabutoxytitanium is previously discovered to be an efficient catalyst for the synthesis of benzanilide through aniline acylation with benzoic acid **Equation 1.6** [16] .

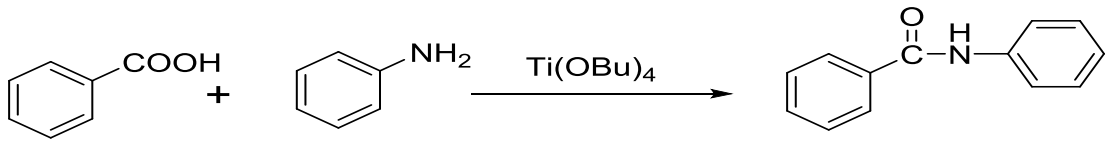

Equation 1.6: Synthesis of benzanilide by acylation process.

A considerable advance over existing processes for the straightforward, scalable, and highly effective amide production process using a heterogeneous Pd-modified clay catalyst in solvent-free conditions **Equation 1.7** [17] .

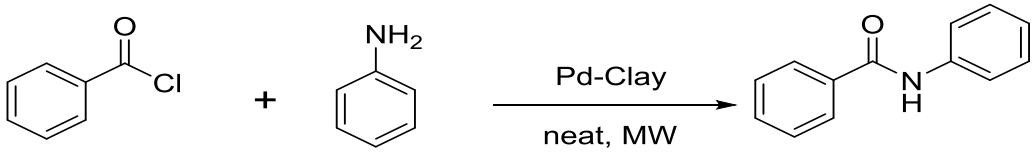

Equation 1.7: Synthesis of benzanilide by using pd-clay catalyst.

N,N-Dialkylformamides are used as the amine source in a straightforward, metal-free process for the direct synthesis of dialkylamides from carboxylic acids. Propylphosphonic acide anhydride (T_3P) in the presence of 0.5 equivalents of HCl facilitates the one-pot process **Equation 1.8** [18].

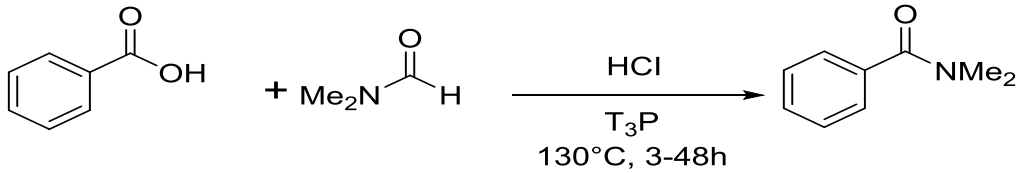

Equation 1.8: Preparation of N,N-Dialkyl benzamide by using T_3P .

The benzamide was produced by a reaction between 3-bromopropylamine and 4-chlorophenylacyl chloride in DCM **Equation 1.9** [19]

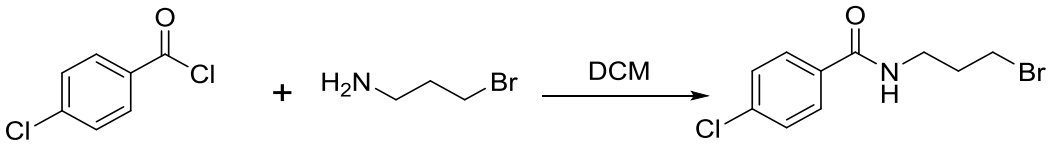

Equation 1.9: Preparation of benzamide from 3-bromopropylamine.

In the absence of transition metals and under unusually mild reaction conditions, a general, mild, and highly chemo-selective method is presented for transamidation of unactivated tertiary amides by a direct acyl(N-C) bond cleavage with non-nucleophilic amines. Through acyl(CO) bond cleavage, amide bonds can be produced with exceptional selectivity through the direct amidation of numerous alkyl esters **Equation 1.10** [20].

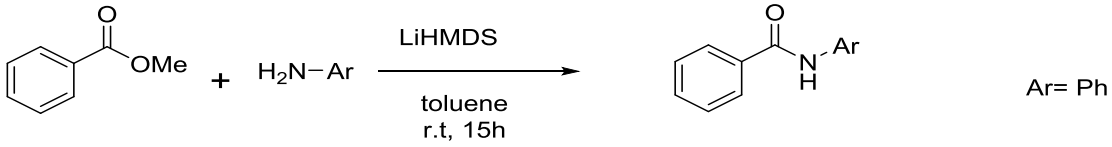

Equation 1.10: Preparation of benzamide from ester.

A chromium-catalyzed activation of acyl (C-O) bonds with magnesium enables an amidation from esters with nitroarenes in the presence of TMSCI as additive. The reaction provides a step-economic strategy to the synthesis of important amide motifs using inexpensive and air-stable nitroarenes as amino sources **Equation 1.11** [21].

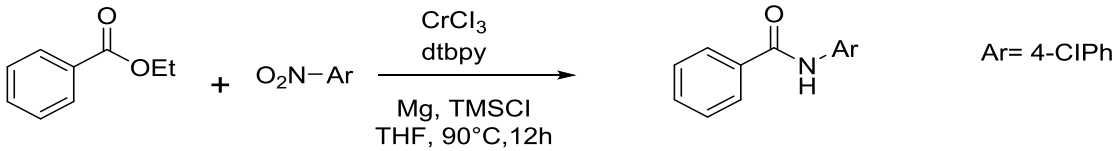

Equation 1.11: Preparation of benzamide by using a chromium catalyst.

A dehydrative amide bond production process involving various combinations of aromatic carboxylic acids and amines is made possible by a degradable 1,3,5-triazo-2,4,6-triphosphorine (TAP) motif **Equation 1.12** [22].

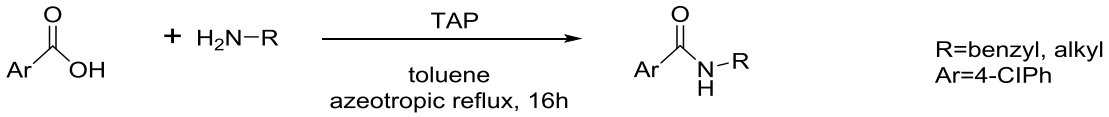

Equation 1.12: Preparation of benzamide by TAP.

N-acylation of primary and secondary amines with *α*-diketones in high yield is induced by ultraviolet UV light at room temperature. This system can also be applied to the synthesis of several amino acid derivatives **Equation 1.13**[6].

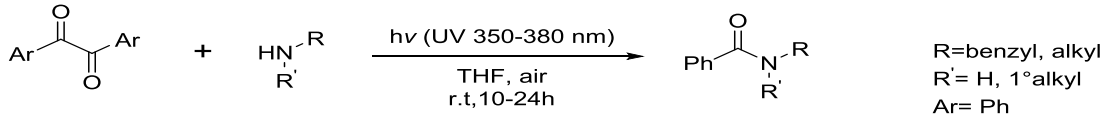

Equation 1.13: Synthesis of benzamide derivatives by α-diketones.

An effective precatalyst for the direct amidation of aromatic and aliphatic carboxylic acids is ammonia-borane **Equation 1.14** [23].

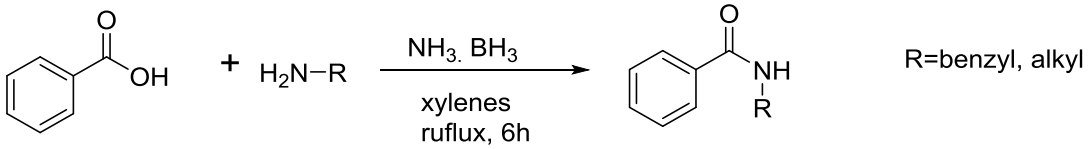

Equation 1.14: Synthesis of benzamide derivatives in the presence of ammonia-borane.

$B_2(OH)_4$ mediates a reductive transamination reaction between N-acyl benzotriazoles and organic nitro compounds or $NaNO_2$ under mild conditions in H_2O as solvent. N-Deuterated amides can be synthesized when conducting the reaction in D_2O **Equation 1.15** [24].

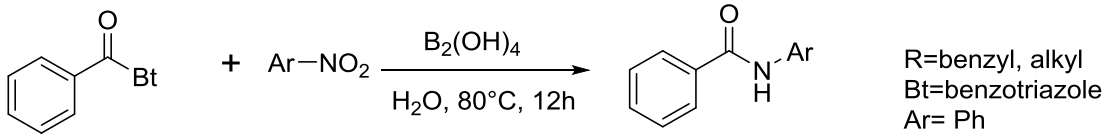

Equation 1.15: Preparation of benzamide derivatives by $B_2(OH)_4$.

Zahraa and Kareem synthesised a number of benzamide derivatives through the benzoylation of some aromatic amines containing a pyrimidine ring in their structure using benzoyl chloride or *p*-chlorobenzoyl chloride in the presence of 1,4-dioxan as solvent **Equation 1.16** [25].

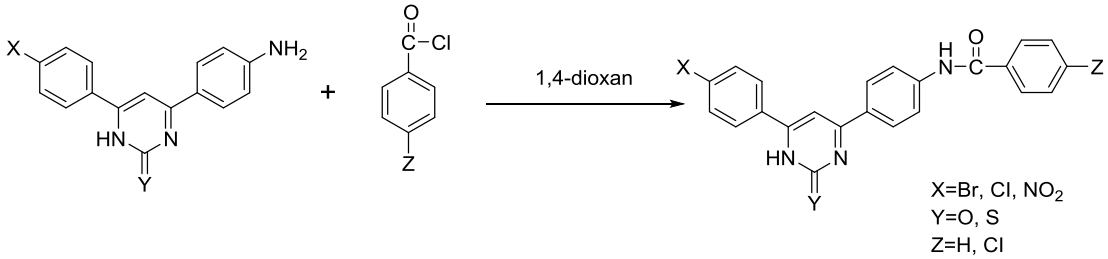

Equation 1.16: Preparation of benzamide derivatives by benzoylation of aromatic amines.

1.3. Sulfonamides

Sulfonamides are an important class of synthetic bacteriostatic antibiotics that still used today for the treatment of bacterial infections and those caused by other microorganisms. They are also known as sulfa drugs and are the main source of therapy against bacterial infections before the introduction of penicillin in 1941. Although sulfonamides have for the most part been replaced by other agents, they still maintain considerable action in certain types of infection, for example in the urinary tract, eye and ear, and bronchitis.[26] Sulfonamides are compounds, which have a general structure represented by **Figure 1.3** [27] .

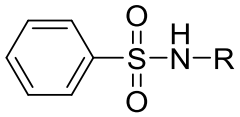

R=H, alkyl, aryl

Figure 1.3: Chemical structure of sulfonamides

In 1908, while researching azo dyes, Gelmo *et al.* [28] Produced sulfonamides for the first time. Hoerlien *et al*.[29] found dyes with the sulfanyl group that have an affinity for wool and silk proteins immediately. After this study, Eisenberg discovered in 1913 as a result of this that chrysolidine, one of the azo dyes under investigation, exhibited a strong bactericidal effect in vitro[29]. Nevertheless, the medicinal benefits of sulfonamides were not understood until 1932. Domagk *et al*.[30] German scientists, discovered that prontosil exhibited strong antibacterial activity in vivo. They have been noticed that prontosil could treat mice suffering from *streptococcal* septicemia. Additionally, Domagk found that prontosil was quickly converted to sulphanilamide in the cell **Equation 1.17** [31].

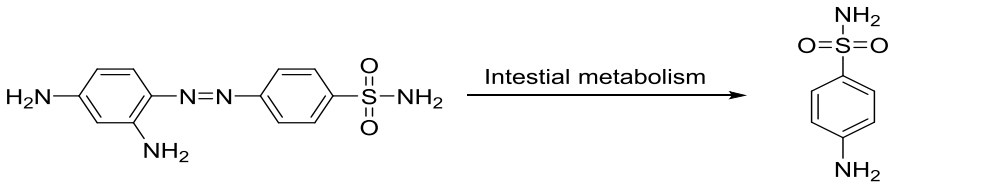

Prontosil Sulfanilamide

Equation 1.17: Synthesis of sulfanilamide in the cell.

This advancement led to many new sulfonamides being synthesized. Today there are over 5000 sulfa drugs in existence but only 33 of those have been introduced for general medical use .[32] The use of sulphonamides as drugs dates back to the beginning of the twentieth

century, when the discovery of the medicinal use of sulphonamides and their derivatives is a milestone in the history of chemotherapy [33].

1.3.1. Biological activity of sulfonamides

The biological activity of typical examples of structures containing a sulfonamide moiety is covered in the text that follows. With over 100 FDA-approved chemicals, many of these substances have been on the pharmaceutical market for many years and hold a unique position. Their broad spectrum of biological activity includes antiviral and anti-retroviral as well as antibacterial and diuretic qualities.[34]

Celecoxib (19), as an example of primary sulfonamide, is a nonsteroidal anti-inflammatory drug (COX-2 inhibitor), and it is used for the treatment of rheumatoid arthritis and acute pain.[35-36]

Furosemide (20) is another primary sulfonamide used in a treatment of edema.[37]

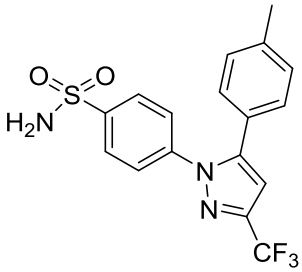

19
Celexoib

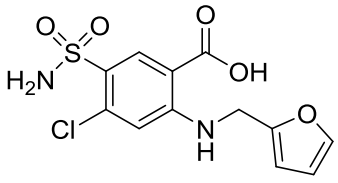

20
Furosemide

Sulfomethaxole (21) as an example of secondary sulfonamide used to treat urinary tract infections, also It is used to treat and prevent toxoplasmosis and pneumocystis pneumonia. Similar to other sulfonamide antibiotics, it works by inhibiting the enzyme dihydripteroate synthase (DHPS).[38]

Sulfasalazine (22) is used to treat ulcerative colitis[39] and Crohn ś disease.[40] Carbutamide (23)[41] and Glibencamide (24)[37] have anti-diabetic properties Glibencamide acts as inhibitor of the ATP- sensitive potassium channels in pancreating beta cells.[42]

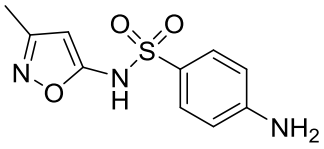

21
Sulfomethaxole

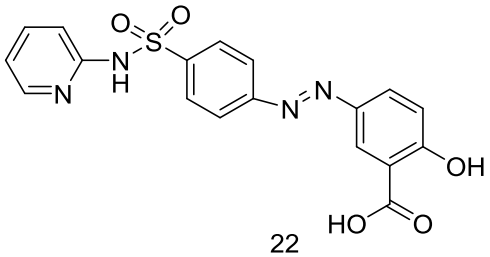

22
Sulasalazine

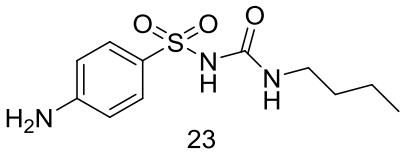

23
Cabutamide

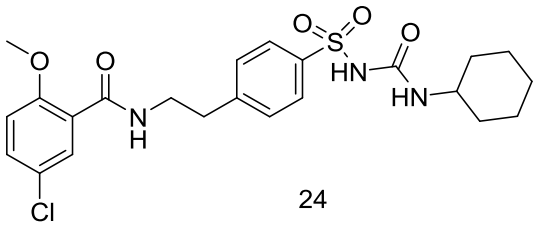

24
Glibencamide

An example of the tertiary sulfonamide is a compound called Darunavir (25). It is an anti-retroviral compound that is used to treat HIV/AIDS.[43] N,N-dipropyl sulfonamide(26), is primarily developed for a treatment of gout and hyperuricemia. In addition, it is sometimes used in a combination with other antibiotics to protect the kidneys.[44]

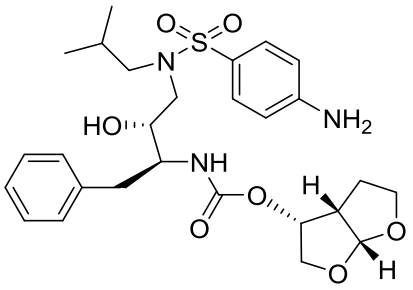

25
Darunavir

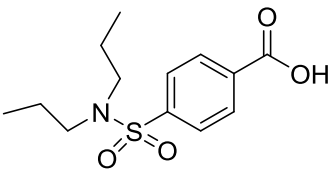

26
Probenecid

1.3.2. Synthesis of sulfonamides

A variety of sulfonamides can be synthesized in great yields by a simple and effective amine-to-Sulfonylation process mediated by indium. **Equation 1.18** [45]

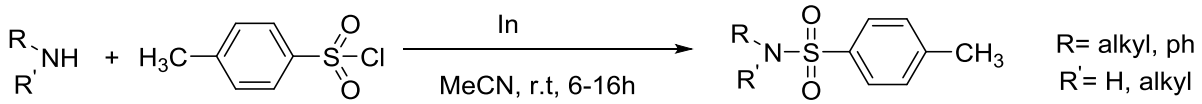

Equation 1.18: Sulfonylation of alkylamine.

Sulfonamides can be easily and conveniently synthesized from sulfonic acids or their sodium salts using microwave irradiation. This process has high yields **Equation 1.19** [46]

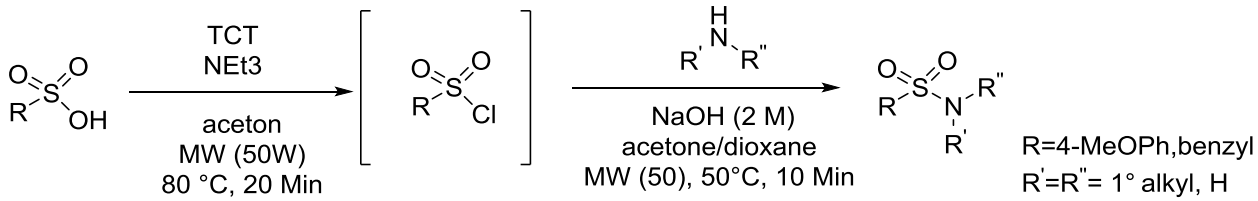

Equation 1.19: Sulfonamides synthesis using microwave irradiation.

For the direct oxidative conversion of thiol derivatives to the corresponding sulfonyl chlorides through oxidative chlorination, H_2O_2 and $SOCl_2$ together constitute a highly reactive reagent. The corresponding sulfonamides are produced in excellent yields in very short reaction times upon reaction with amines **Equation 1.20** [47].

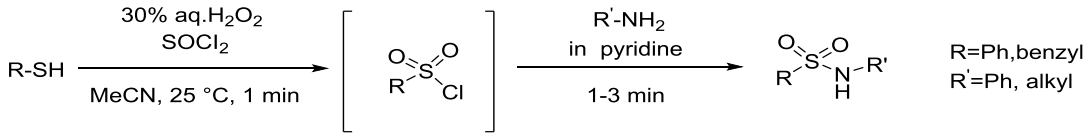

Equation 1.20: Synthesis of sulfonamides from thiol derivatives.

A range of sulfones and sulfonamides have been produced using simple and high-yielding techniques based on the synthesis of thiosulfonates by copper-catalyzed aerobic dimerization. Thiosulfinates are stable, nontoxic

substitutes for metal sulfinate salts formed from hazardous SO_2 **Equation 1.21** [48].

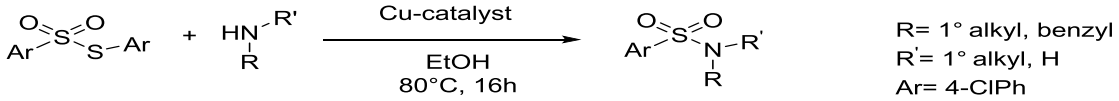

Equation 1.21: Synthesis of the sulfonamide derivatives by copper-catalyst.

In the presence of N-bromosuccinimide, primary and secondary amines underwent sulfonamide formation with vinyl sulfones **Equation 1.22** [49] .

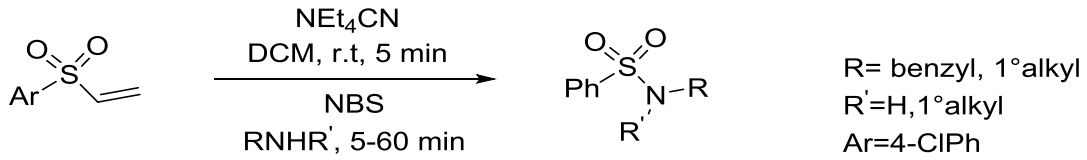

Equation 1.22: Sulfonamides formation in the presence of NBS.

Through successive (C-S) and (S-N) coupling, nitroarenes, (hetero) arylboronic acids, and potassium pyrosulfite have been combined to produce a wide variety of sulfonamides with various reactive functional groups in highly good yields **Equation 1.23** [50].

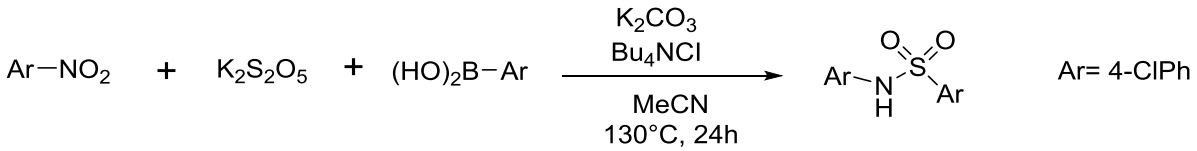

Equation 1.23: Production of sulfonamides from nitroarenes.

A wide variety of sulfonamides have been synthesized at room temperature from a wide range of aliphatic, linear, and cyclic amines, anilines, and N-methylanilines by using 4-nitrophenyl benzylsulfonate as a starting material. This experiment produced yields and reaction times that are either the same as or superior than those previously reported, proving that sulfurphenolate exchange is a workable substitute **Equation 1.24** [51].

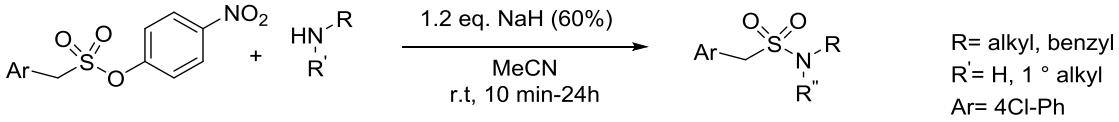

Equation 1.24: Sulfonamides synthesis by using 4-nitrophenylbenzylsulfonate.

Hadeel and Kareem were synthesized some N-aryl sulfonyl derivatives through the reaction of benzene sulfonyl chloride or *p*-toluene sulfonyl chloride with aromatic amines containing a pyrimidine ring in their structure in the presence of pyridine as catalyst at room temperature **Equation 1.24** [52].

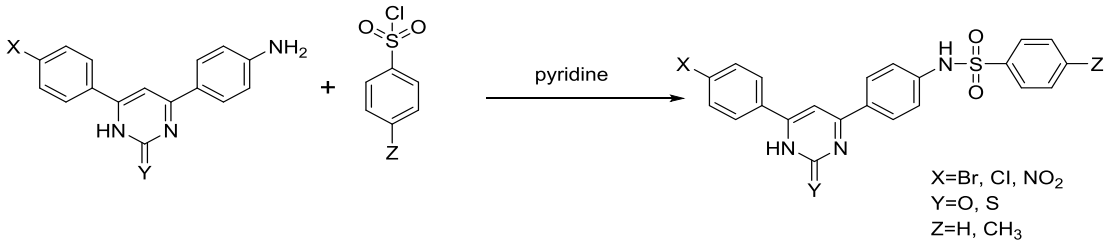

Equation 1.25: Synthesis of some N-arylsulonyl derivatives from aromatic amines.

1.4. N-Alkylation

N-alkylation of aniline derivatives is an important reaction in organic synthesis, which has been widely applied in the preparation of dyes, fluorescence probes, agrochemicals, and pharmaceuticals.[53]The challenge of this reaction is to obtain excellent selectivity for mono- or dialkylation products and to avoid the formation of corresponding quaternary ammonium salts.[54] In order to overcome these problems, noble metal complexes and salts involving [Ru][55], [Ir][56], [Pt][57], as catalysts and alcohols as alkylating agents have been reported extensively **Equation 1.26** .

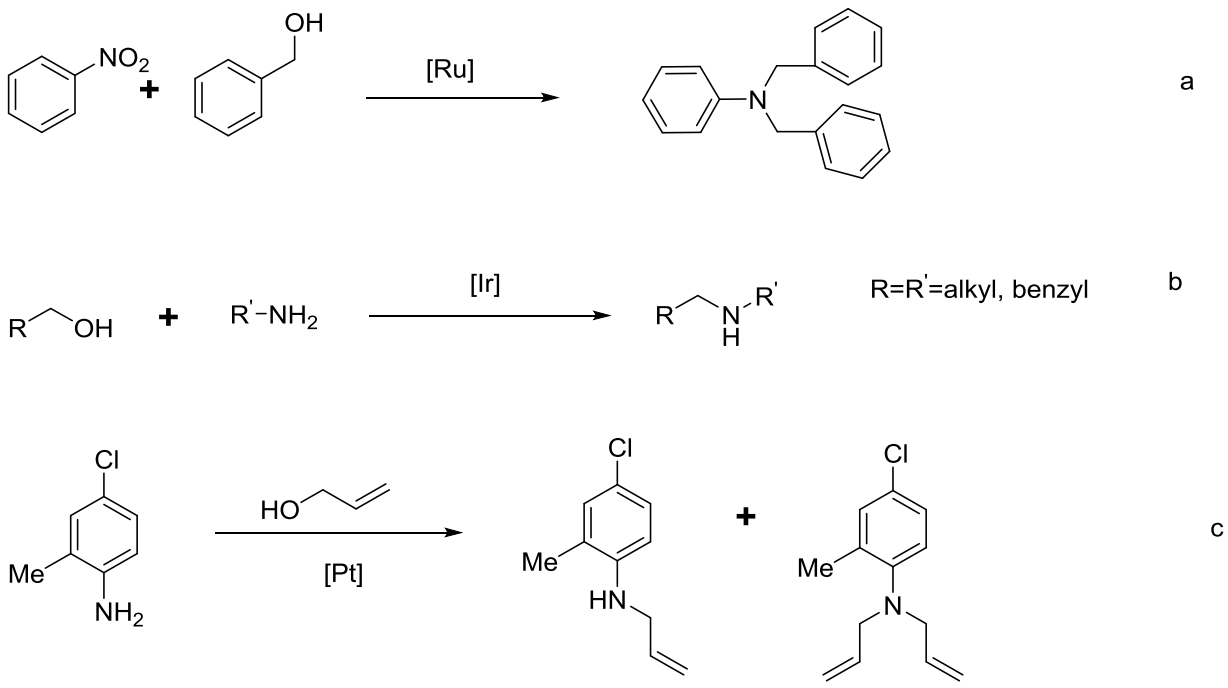

Equation 1.26: Synthesis of aniline derivatives by using [Ru] [Ir] [Pt] as catalysts.

The reaction of cost-effective aniline with allyl bromide in ethanol\H_2O and K_2CO_3 give mix of N, N-diallyl aniline and N-allyl aniline **Equation 1.27**[58].

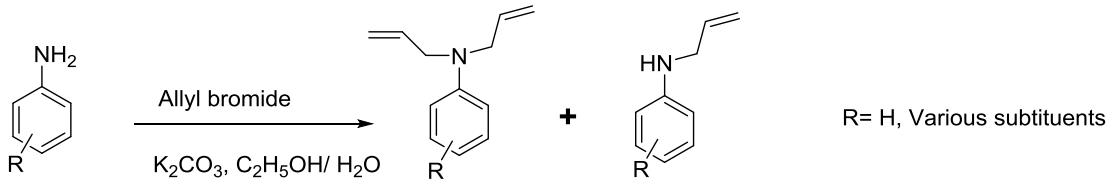

Equation 1.27: Synthesis of N, N-diallyl aniline and N-allyl aniline.

Hadeel and Kareem synthesized of a number of allyl derivatives through the allylation of some aromatic amines containing a pyrimidine ring in their structure using allyl bromide in the presence of DMF as solvent and K_2CO_3 as base **Equation 1.28** [52].

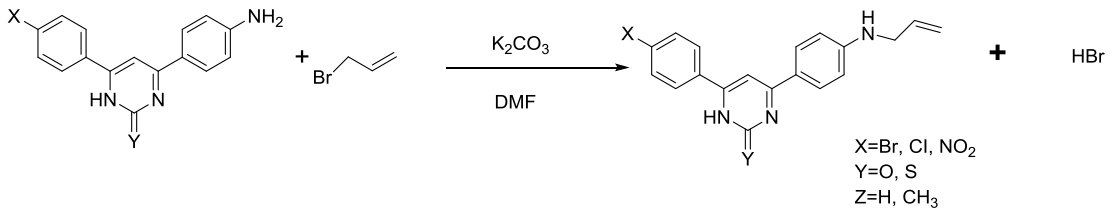

Equation 1.28: Synthesis of allyl derivatives.

An environmentally friendly procedure has been developed to convert activated secondary alcohols to their corresponding carbonyl compounds and to use them as specific mono-alkylating reagents for derivatives of amides **Equation 1.29** .[59]

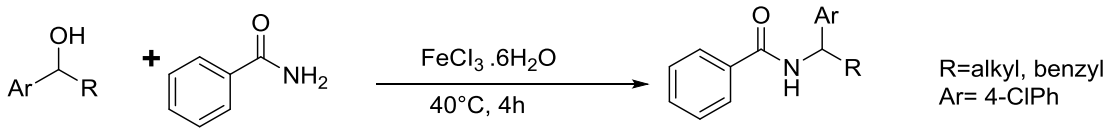

Equation 1.29: Synthesis of benzamide derivatives from secondary alcohol.

Transition metal-free protocols have also been described, although they normally require Harsh reaction conditions, such as high temperatures and pressures, to achieve reasonable yields of products **Equation 1.30** [60].

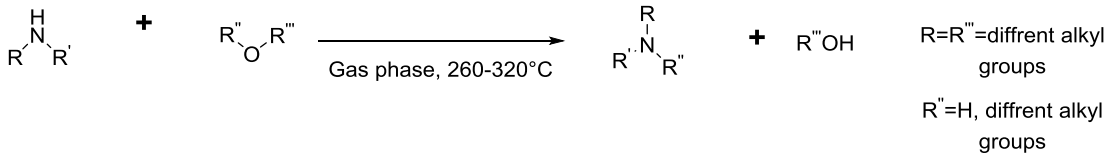

Equation 1.30: Alkylation of secondary amine via Harsh reaction conditions

Recently, microwave irradiation has been proved to be efficient for the syntheses of N-alkyl amine **Equation 1.31** [61]or amide **Equation 1.32** [62].

Equation 1.31: Synthesis of N-alkylamine by microwave irradiation

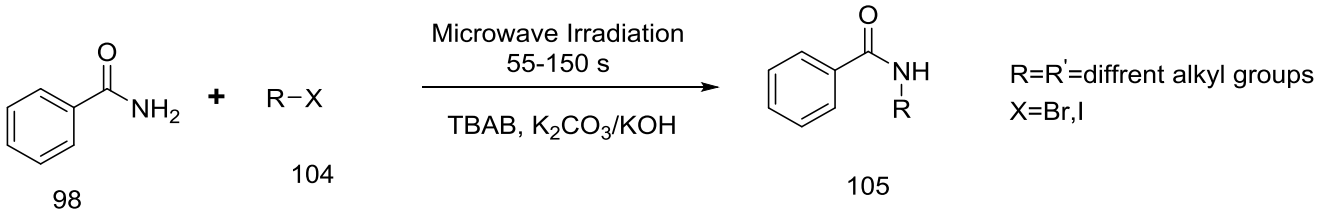

Equation 1.32: Synthesis of N-alkyl amide by microwave irradiation.

With respect to alkylated amides, N-alkylated sulfonamides constitute an important class of compounds because the sulfonamide moiety is found in a large number of agrochemicals and pharmaceuticals **Equation 1.33** [63].

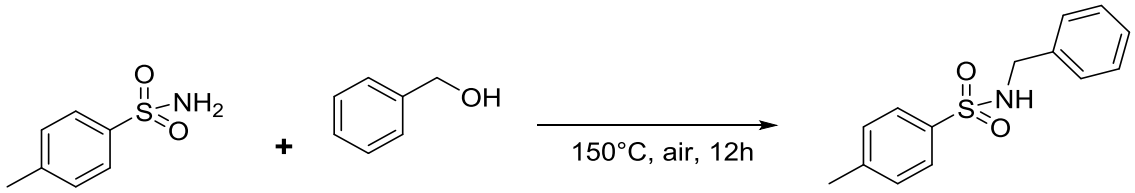

Equation 1.33: Alkylation of sulfonamides by benzyl alcohol.

There is a report on the intermolecular alkylation of sulfonamides with trichloroacetimidates. There is no need for an external acid, base, or transition metal catalyst for this reaction **Equation 1.34** [64].

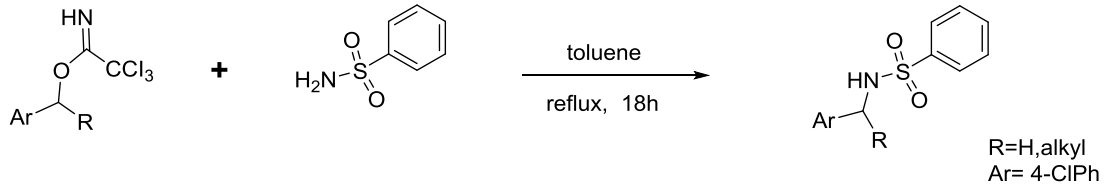

Equation 1.34: Intermolecular alkylation of sulfonamides with trichloroactimidates.

Also, alkylating of sulfonamide by using secondary alcohols **Equation 1.35** [59].

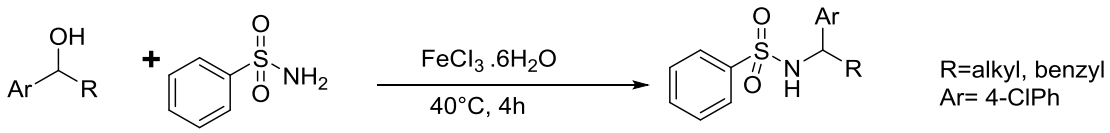

Equation 1.35: Synthesis of alkyl or benzyl sulfonamide.

Other literatures of N- alkylated compounds have been reported in the reviews.[65- 68]

1.5. Molecular Docking

Molecular docking stands as a cornerstone in the modern drug discovery process, providing a computational lens through which the interaction between small molecule ligands and their macro- molecular targets can be scrutinized. At its core, molecular docking simulates the "lock-and-key" mechanism that underlies molecular recognition, which is pivotal for the identification and optimization of compounds with therapeutic potential [69, 70] . The technique's allure lies in its ability to predict how a ligand binds to a protein, thereby offering insights into the binding affinity and biological activity of the ligand, which are crucial for the rational design of drugs[71] .

In addition, Molecular Docking a computational implement that assesses and defenses diverse ligand-receptor conformations based on their binding energies. An exact recording function is imperative for distinguishing high-affinity ligands from low-affinity ones, so makes it likely to identify potential medication candidates for justification in experiments. Molecular docking discoveries application in various domains of Drug Progress, comprising structure-based medication development, virtual screening, lead optimization[72].

1.5.1. Docking types[73]

a) Solid-state docking, where the acceptor and the small molecule are considered solid materials.

b) In elastic docking, the receiver remains rigid while the bonding is elastic.

c) Flexible docking, where the flexibility of both the receptor and ligand is taken into account.

1.6. Breast Cancer

According to GLOBOCAN 2020 statistics, breast cancer is a very prevalent form of cancer and ranks as the sixth most common cause of cancer- related deaths. It is anticipated that there will be around 2.3 million new cases of breast cancer globally. It is a cancerous tumor that develops in the breast cells in both females and males. Breast cancer damages various components of the breast, including ducts, lobules, adipose tissue, connective tissue, lymph nodes, and blood vessels[74].

The incidence of breast cancer in women may be influenced by a number of other factors in addition to genetic susceptibility, such as demographic traits and clinical, reproductive, and environmental factors. Breast cancer risk factors include advanced age, positive family history, socioeconomic status, diet, endogenous or exogenous hormones, benign tumors, oncogenic viruses. Breast cancer is the predominant malignant tumor in Iraq, representing 19.5% of all cases (4996 cases) and 34.3% of female malignancies (4922 cases)[75]. The fact that anti-cancer drugs do not eradicate the population of breast cancer stem cells (BCSCs), leading to disease recurrence, is a major obstacle in the treatment of breast cancer[76].

The scarcity of anti-cancer drugs that target BCSCs may be attributed to the dearth of in vitro screening models that can mimic the tumor microenvironment of BCSCs and preserve the three-dimensional (3D) architecture of in vivo tumors. Antineoplastic chemotherapy is the use of chemotherapy drugs that target cancer cells, either singly or in combination. One of the main targets of antitumor medications is the cell cycle, which stops cancer cells from growing. Targeting cancer cells and quickly growing normal cells, each class of drug acts at a certain stage of the cell cycle. As a result, many drugs are hazardous to users and have negative side effects[77].

1.7. Antioxidant

Antioxidants are substances that inhibit the oxidation of an oxidizing agent, and oxidizing agents include types of free radicals which are types of reactive oxygen species ROS, and reactive nitrogen species (RNS) and others[78]. where these free radicals play an important role in the development of diseases such as arthritis, diabetes, cancer, sclerosis, arteries and vascular diseases and others. Antioxidants have gained significant attention due to their protective role in neutralizing free radicals and repairing damage caused by ROS. Antioxidants include two types: enzymatic and non-enzymatic. Non-enzymatic antioxidants include: vitamins E, C, glutathione, trace elements. Enzymatic antioxidants include: catalase (CAT), superoxide dismutase (SOD), and glutathione peroxidase (GSHpx)[79].

1.8. Aim of the study

The aim of our study firstly includes the synthesis of some benzamide and sulfonamide compounds derived from the aniline amino group and then introducing other groups represented by benzoyl, sulfonyl, and allyl instead of the proton of the amide group.

The molecular docking is an important part of the aim to identify the inhibitory activity of the prepared compounds.

Finally, these modifications may help us to produce derivatives possess effective biological and therapeutic properties.

2.Experimental

2.1. Chemical Materials

The chemicals used in this study were supplied from the companies showing in **Table 2.1**.

Table 2.1: The chemicals used in the study.

No.	Chemicals	Phase	Purity %	Company
1	Allyl bromide	Liquid	99	Fluorochem
2	Aniline	Liquid	99.5	SDFCL
3	Anhydrous magnesium sulfate	Solid	98	Scharlau
4	4-Bromoaniline	Solid	90	Hopkin & Williams
5	4-Chlorobenzoyl chloride	Liquid	96	Fluorochem
6	Dichloromethan	Liquid	99.9	Sigma aldrich
7	1,4-Dioxane	Liquid	99.5	ROMIL
8	Ethyl acetate	Liquid	99.5	SRL
9	n-Hexane	Liquid	99	Sigma aldrich
10	4-Hydroxy aniline	Solid	98	Sigma aldrich
11	4-Methoxy aniline	Solid	98	SRL
12	Petroleum ether	Liquid	40-60	SRL
13	4-Toluene sulphonyl chloride	Solid	97	Fluorochem
14	o-Tolidine	Solid	98	SRL
15	Sodium chloride	Solid	99.5	Fisher chemical

2.2 .Instruments

2.2.1 .Melting Points

All melting points are uncorrected and expressed in degree (°C). They are measured at the Department of Chemistry, College of Science, University of Misan, by using Stuart SMP11 melting point apparatus.

2.2.2 .Thin Layer Chromatography

TLC is performed using silica gel 60 F254 on Merck precoated aluminum sheet (0.2 mm thickness), with visualization by UV light.

2.2.3 .Column Chromatography

All synthesized compounds are purified using flash column chromatography on silica gel (60-120 mesh).

2.2.4 .Fourier Transform Infrared Spectrophotometer

FTIR spactra of all synthesized compounds were measured as KBr disc for solid samples for the region between (400-4000) cm^{-1} using SHIMADZU IR Affinity-1 (Japan) at photon-Anlysis Center in Baghdad, Iraq and Medicine College, Misan University-Iraq (Shimadzo (Ir prestige – 21)). Only principal absorption bands of interest were reported and expressed in $cm^{-1.}$

2.2.5 .Nuclear Magnetic Resonance Spectrometer

^{1}H-NMR and ^{13}C-NMR spectra are recorded at the, College of Education for pure sciences, University of Basrah, Iraq using Bruker DRX-400 spectrometer (Germany) and chemical shifts are reported in ppm (δ). DMSO-d_6 is used as a solvent, while TMS was used as an internal standard.

2.2.6. Mass spectrometer

Mass spectra of the prepared compounds were recorded by Agilent Technology (HP) Model 5973 with (EI) technology at (70 ev) electron energy at the University of Tehran Faculty of Science in the Islamic Republic of Iran.

2.2.7. Molecular Docking

The docking investigations are carried out on a Windows 7 computer with ChemBioDraw Ultra 14.0. The molecular operating environment MOE 2015.10 Molecular docking is used better to understand the effectiveness of the ligand and complexes[69]. MOE 2015.10 is the software used to predict the binding affinity of chemicals. The crystal structures of enzymes were acquired from the Royal Collaboratory for Structural Bioinformatics, RCSB Protein Data Bank (http://www.rcsb.org/pdb/) for molecular docking calculations[80]. The PDB file is stripped of water molecules[81].

2.3. Synthetic Methods

2.3.1. Synthesis benzamide derivatives (A1- A6)[15].

P-Substituted aniline (1 mmol) or o-Tolidine (0.5 mmol) and 4-chlorobenzoyl chloride (1 mmol, 2mmol(A6)), are added to round bottom flask (25ml) containing 1,4-dioxane (6 mL). The reaction mixture was stirred at 90 °C for 12 h and monitored by TLC (EtOAc: Petroleum ether; 1:2) until the reaction was completed. The reaction is poured over an ice bath and the resulting precipitate was filtered and purified using column chromatography (EtOAc: Petroleum ether; 1:4), show in **Table 2-2**.

Table 2-2: Physical properties of benzamide derivatives (A1- A6).

Comp. No.	Structural formula	Molecular Formula	Yield (%)	M.P (°C)	Molecular weight
A1	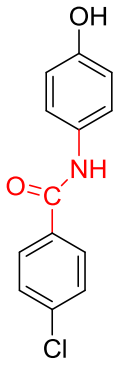	$C_{13}H_{10}O_2ClN$	48	235-237	247.04
A2	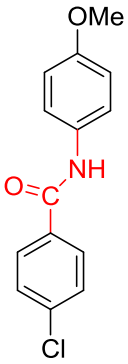	$C_{14}H_{12}O_2ClN$	52	212-214	261.06
A3	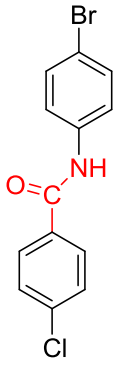	$C_{13}H_9OBrClN$	33	222	310.96
A4	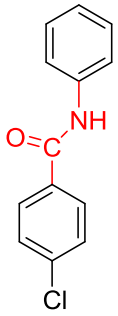	$C_{13}H_{10}OClN$	71	200	231.05

Comp. No.	Structural formula	Molecular Formula	Yield (%)	M.P (°C)	Molecular weight
A5	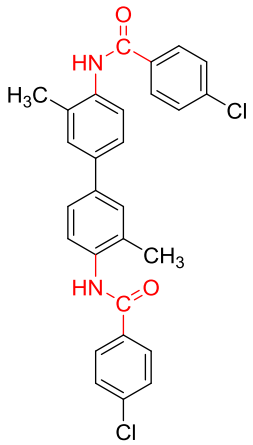	$C_{28}H_{22}O_2Cl_2N_2$	50	325	489.40
A6	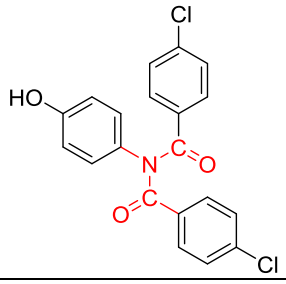	$C_{20}H_{13}O_3Cl_2N$	75	246-248	386.23

Note: The color of all derivatives is Brown

2.3.2. Synthesis of sulfonamides derivatives (B1-B5)[82].

P-Toluene sulfonyl chloride (1.1 mmol, 2.2mmol(B4, B5)) is added to a stirred solution of the p-substituted aniline (1 mmol) or o-Tolidine (0.5 mmol) in CH_2Cl_2 at room temperature. The resulting mixture is cooled down to 0 °C before Et_3N (2.17 mmol) was slowly added. The reaction mixture was stirred for 24 hours and monitored by TLC (EtOAc: hexane; 1:1) until the reaction is completed. The reaction mixture was diluted with DCM (20 mL), washed with brine (3 × 10 mL), dried over $MgSO_4$ and concentrated in vacuo. The remaining residue purified via column chromatography over silica gel using gradient elution with EtOAc and hexane (1:4) to yield sulfonamides **Table 2-3**.

Table 2-3: Physical properties of sulfonamide derivatives (B1-B5).

Comp. No.	Structural formula	Molecular formula	Yield (%)	M.P (°C)	Molecular weight
B1	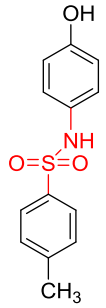	$C_{13}H_{13}O_3NS$	55	129-130	263.31
B2	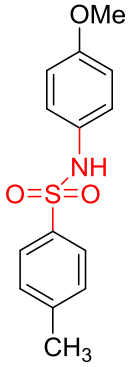	$C_{14}H_{15}O_3NS$	65	107-109	277.34
B3	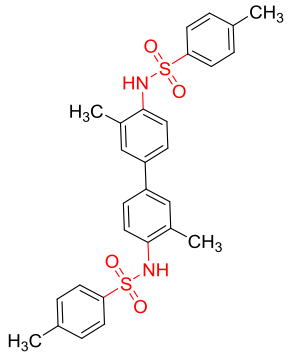	$C_{28}H_{28}O_4N_2S_2$	40	133	520.66
B4	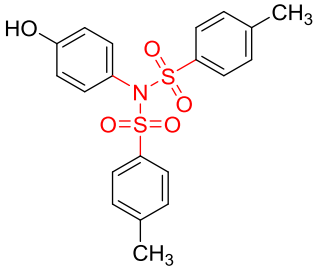	$C_{20}H_{19}O_5NS_2$	75	175	417.07

Comp. No.	Structural formula	Molecular formula	Yield (%)	M.P (°C)	Molecular weight
B5	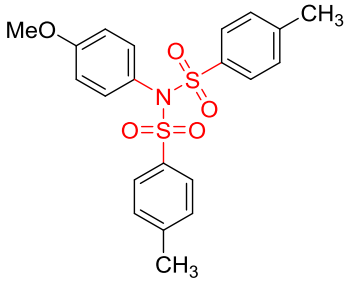	$C_{21}H_{21}O_5NS_2$	**27**	164	431.52

Note: The color of all derivatives is white

2.3.3. Synthesis N- allyl derivatives (C1-C3)[83].

A mixture of (A1, B2 (2.1 mmol)) or o-Tolidine (1.05 mmol), Allyl bromide (2.4 mmol) and K_2CO_3 (4.4 mmol) in acetone (20 mL) and H_2O (3 mL) were stirred for 6 hours at room temperature. The reaction progress was monitored by TLC (EtOAc: Petroleum ether; 1:3) until the reaction was completed. The reaction mixture was diluted with EtOAc (50 mL), washed with brine (3 × 10 mL), dried over $MgSO_4$, evaporated under reduced pressure by rotary evaporator and the product was purified via silica gel chromatography using (EtOAc: Petroleum ether; 1:9) as eluent to give the product as a solid in excellent purity **Table 2-4**.

Table 2-4: Physical properties N-allylamide derivatives (C1-C3).

Comp. No.	Structural formula	Molecular formula	Yield (%)	M.P (°C)	Molecular weight
C1	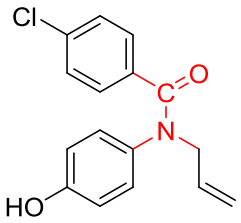	$C_{16}H_{14}O_2ClN$	75	177-179	387.74

Comp. No.	Structural formula	Molecular formula	Yield (%)	M.P (°C)	Molecular weight
C2	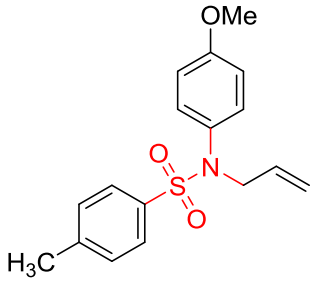	$C_{17}H_{19}O_3NS$	60		317.40
C3	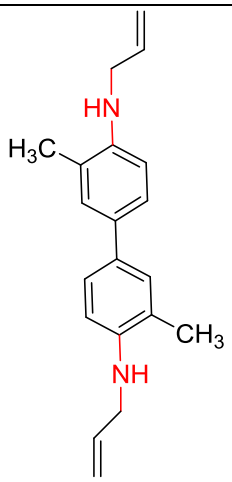	$C_{20}H_{24}N_2$	30	—	292.43

Note: The color of all derivatives is Light yellow

2.4. Biological activity

2.4.1.Measurement of In Vitro Anticancer Activity

2.4.1.1. Cell lines and culture

MCF-7 (a human breast cancer cell line) was purchased from National Cell Bank of Iran (Pasteur Institute, Iran). Cells were grown in RPMI-1640 medium (Gibco) with 10% FBS (Gibco) supplemented with antibiotics (100 U/ml penicillin and 100 µg/ml streptomycin), respectively. Cells were maintained at 37 °C under humidified air containing 5% CO_2 and were passaged using trypsin/EDTA (Gibco) and phosphate- buffered saline (PBS) solution[88].

2.4.1.2. MTT cell viability assay in MCF7 Cells

Cell growth and cell viability were quantified using the MTT [3-(4, 5-dimethylthiazol-2-yl)-2, 5-diphenyltetrazolium Bromide] (Sigma-Aldrich) assay. In brief, cells were digested with trypsin, harvested, adjusted to a density of 1.4 × 104 cells/well and seeded to 96-well plates filled with 200 µl fresh medium per well for 24 h. When cells formed a monolayer, they were treated with 600-7.4 µg/ml of each compounds for h at 37 °C in 5% CO_2. At the end of the treatment (24 h), while the monolayer culture was left untouched in the original plate, the supernatant was removed and 200 µl/well of MTT solution (0.5 mg/ml in phosphate-buffered saline [PBS]) was added and the plate was incubated at 37 °C for an additional 4 h. MTT solution (the supernatant of cells was removed and dimethyl sulfoxide was added (100 µl per well). Cells were incubated on a shaker at 37 °C until crystals were completely dissolved. Cell viability were quantified by measuring absorbance at 570 nm using an ELISA reader (Model wave xs2, BioTek, USA). The concentration of the compounds that resulted in 50% of cell death (IC_{50}) was determined from respective dose-response curves.

2.4.2. Antioxidant activity

2.4.2.1. DPPH assay

This is an assay for scavenging activity against free radicals. The scavenging activity of Natural or synthetic products can be assayed by measuring the decrease in absorbance at 515 nm of the stable free radical DPPH. The purple-colored free radical reacts with scavenger to yield the colorless product 1, 1-diphenyl-2-picrylhydrazine.

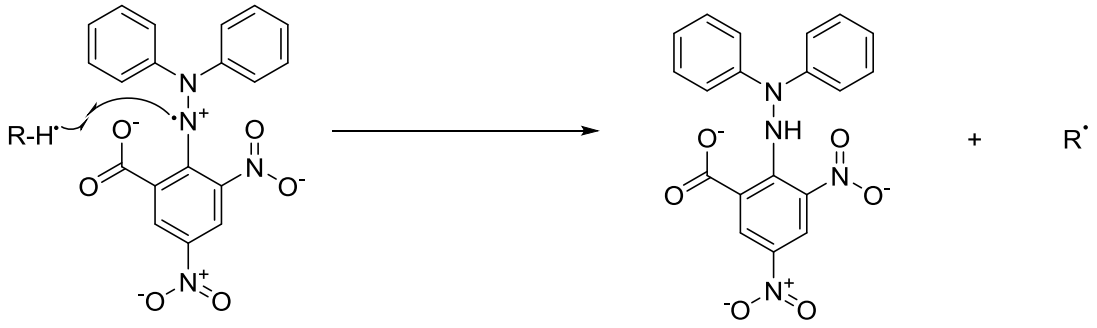

In brief, to perform this assay 9 sample dilutions were first prepared in 100 µl of methanol at a final concentration ranging from 800-6.25 µg/ml. Subsequently, Samples were added to a 96 well plate wells in duplicates and 100 µl of 0.2 mM DPPH solution in methanol was added to each well. Plates were incubated for 30 min in the dark and the absorbance was recorded at 515 nm by micro plate reader spectrophotometer (Model wave xs2, BioTek, USA). Then, for each sample the concentration that showed 50% DPPH scavenging activity (IC_{50}) was calculated by plotting compounds concentration against DPPH scavenging activity (anti-oxidant activity). Ascorbic acid was used as positive control[89, 90].

2.5. Docking studies for synthetic compounds

The selection of these individuals was made via a rigorous process of virtual screening and extensive literature investigation. The protein structures were acquired from the RCSB Protein Data Bank using X-ray crystallography. The use of molecular docking facilitated a deeper comprehension of the efficacy of the ligands and complexes[84]. The program MOE 2015.10 was used for predicting the binding affinity of compounds. The enzyme's crystal structures were obtained from the Royal Collaboratory for Structural Bioinformatics[85]. RCSB Protein Data Bank (https://www.rcsb.org/pdb) For the purpose of conducting molecular docking calculations[86]. Co-crystallized ligands and water molecules were removed from the PDB file. To design and improve the

synthetic compounds' structures, MOE 2015.10 was used[87]. Some of the stages involved in docking are as follows:

Step 1: Selection from PDB

Target proteins for docking studies were downloaded from the RCSB Protein Data Bank.

Step 2: Protein structure refinement

It is not possible to employ proteins from the Protein Data Bank directly in the docking process. Before docking, it has to be refined. The process of refining downloaded proteins includes the removal of water and any bound ligand, if any. The following are the steps to follow:

- Open MOE 2015.10
- File ⟶ Open ⟶ Protein (downloaded from PDB).
- Click water molecule.
- Ctrl + Shift and click the last water molecule (select all the water molecules).
- Give right click and cut.
- Compute ⟶ Prepare ⟶ Structure preparation
- Compute ⟶ Site finder
- Compute ⟶ Surface and maps

Step 3: Ligand file format conversion:

The synthesized compounds under study, known as ligands, were drawn using the ChemBioDraw Ultra (3D)14.0.

- Open MOE 2015.10
- Compute ⟶ Energy ⟶ Minimize (Force field MMFF94x, Gradient 0.05) ⟶ Ok
- File ⟶ New ⟶ Database

- Database ⟶ Edit ⟶ New ⟶ Entry

Step 4: Docking

The docking process was carried out using MOE 2015.10 software, necessitating a refined protein and ligand, both of which must be in PDB file format. The docking procedure is conducted using MOE 2015.10. The process includes the following steps:

- Open MOE 2015
- File ⟶ Open ⟶ Select protein
- Compute ⟶ dock ⟶ Select ligand ⟶ Run

3. Reactions and mechanisms

3.1. Synthesis of benzamide derivatives A1-A6

The protocol involves treatment of (1 mmol) *p*-substituted aniline with (1mmol) 4-chlorobenzoyl chloride (except o-tolidine 0.5 mmol) in R.B flask containing (6 mL) 1,4-dioxane. The reaction mixture was stirred at 90°C until the reaction completed **Equation 3.1**.

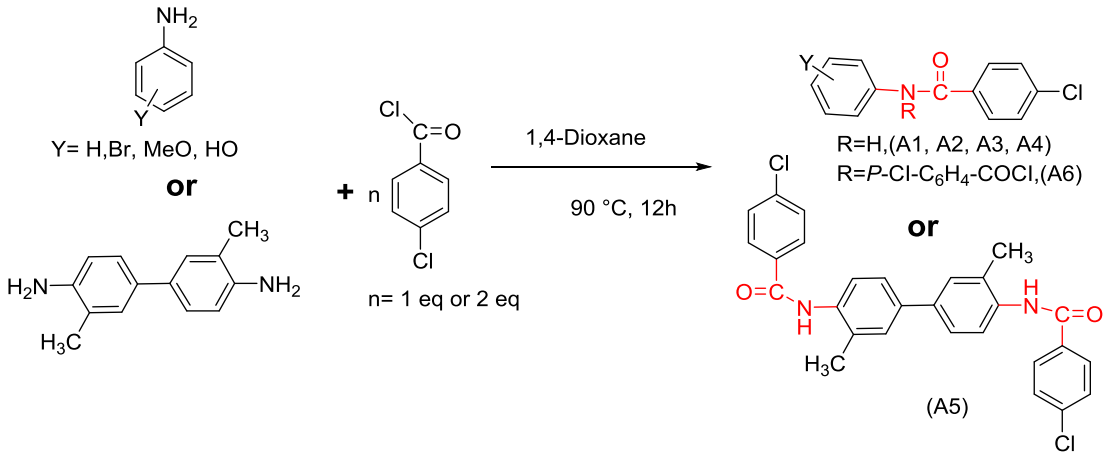

Equation 3.1: Synthesis of benzamide derivatives A1-A6.

3.1.1. The mechanism

The first stage of the reaction involves the attack of the nitrogen atom on the carbonyl carbon atom of the benzoyl chloride. Nitrogen in primary amine curries alone pair of electrons and the carbonyl carbon is highly electrophilic. As a result, carbon-nitrogen is formed and the chloride ion lose. Next, the nitrogen loses hydrogen ion. Nitrogen being more electronegative attracts the pair and an amide is formed a result **Scheme 3.1** .

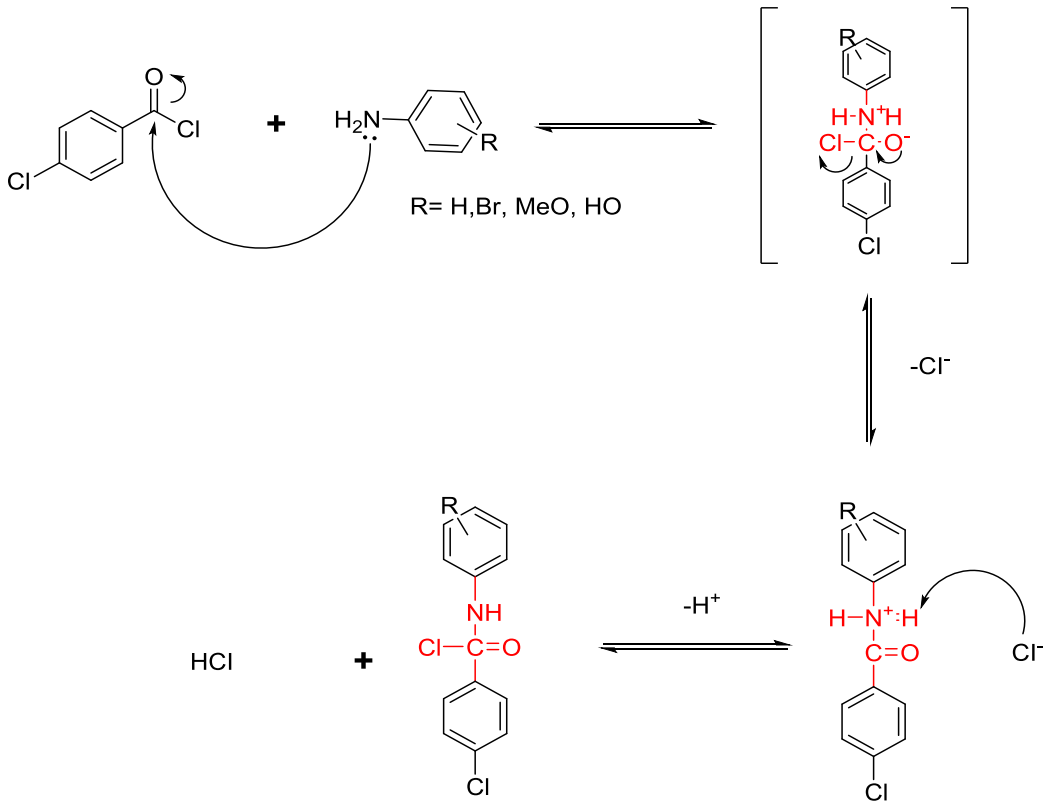

Scheme 3.1: Mechanism of synthesis of benzamide derivatives A1- A6.

3.1.2. Characterization of the A1-A6

All the synthesized derivatives were characterized by some physical measurements, such as melting point besides the spectroscopic techniques, IR, ^{1}H-NMR, ^{13}C-NMR and Mass spectroscopy.

The IR spectra of the derivatives A1-A6 are appeared in **Table 3.1** and **Figures 3.1-3.6** .

The derivatives (A1-A5) are characterized by nine bands corresponding to the stretching vibrations of the -OH, -NH, aromatic C-H, Aliphatic C-H, C=O, C=C, C-O, C-N and C-X groups, which occur within the ranges (3438.55-3435.43), (3435.64-3273.68), (3134.00-2852.72), (2923.72-2853.04), (1683.16-1644.99), (1595.39-1514.93), (1344.00-1097.50), (1296.00-1014.56), (842.44-750.00) cm^{-1} respectively. While the derivative (A6) is characterized by seven bands corresponding to the stretching vibrations of the -OH, aromatic C-H, C=O, C=C, C-O, C-N

and C-X groups, which occur within the ranges 3438.55, (3095.34-3052.08), 1682.85, 1592.46, 1322.24, 1092.50, 762.55 cm^{-1} respectively.

We also notice that the absorption band of a group NH- of A6 is disappearance and this indicates that the reaction between A1 and 4-chlorobenzoyl chloride is di-substitution.

Table 3.1:FT-IR Spectral data of the stretching vibrations of A1-A6 cm^{-1}

Symbol	-OH (w)	-NH	CH Aromatic (w)	CH Aliphatic (w)	C=O (vs)	C=C (s)	C-O	C-N	C-X
A1	3435.43	3348.41 (s)	3082.37-2852.86	___	1649.09	1514.93	1233.59 (s)	1092.04 (w)	831.92 C-CI (s)
A2	___	3435.64 (br.)	3052.00-3095.22	2923.72	1683.16	1592.41	1295.60 (s)	1092.53 (s)	762.86 C-CI (s)
A3	___	3344.57 (s)	3101.54-2852.72	___	1653.00	1595.13	1097.50 (w)	1014.56 (s)	823.60 C-CI (s) 758.02 C-Br (s)
A4	___	3378.00 (s)	3134.00-3036.00	___	1668.00	1546.00	1344.00 (s)	1296.00 (s)	750.00 C-CI (s)
A5	___	3273.68 (w)	2963.03-2923.03	2853.04	1644.99	1595.39	1288.94 (w)	1091.88 (w)	842.44 (w)
A6	3438.55		3095.34 3052.08		1682.85	1592.46	1322.24 (s)	1092.50 (s)	762.55 C-CI (s)

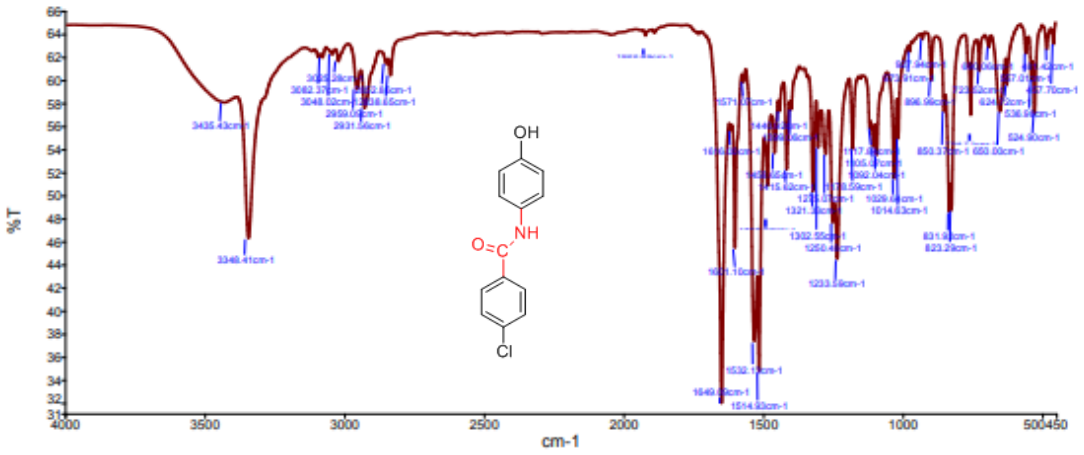

Figure 3.1: FT-IR Spectrum of the compound A1.

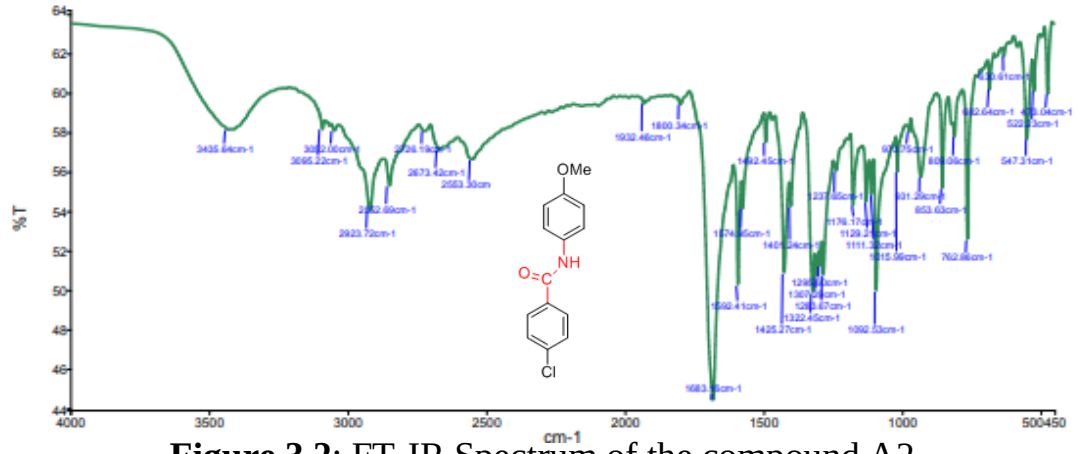

Figure 3.2: FT-IR Spectrum of the compound A2.

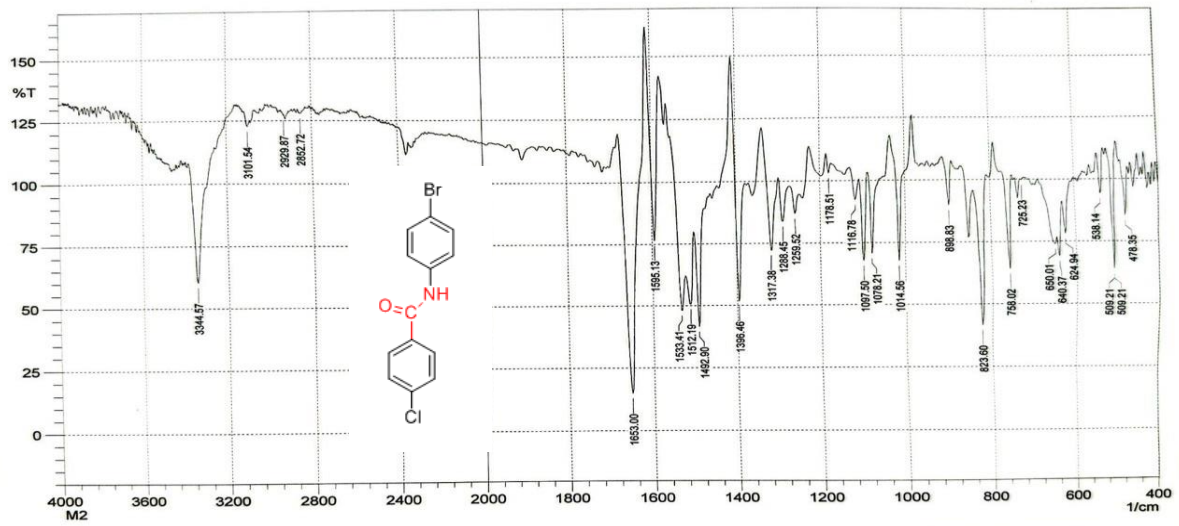

Figure 3.3: FT-IR Spectrum of the compound A3.

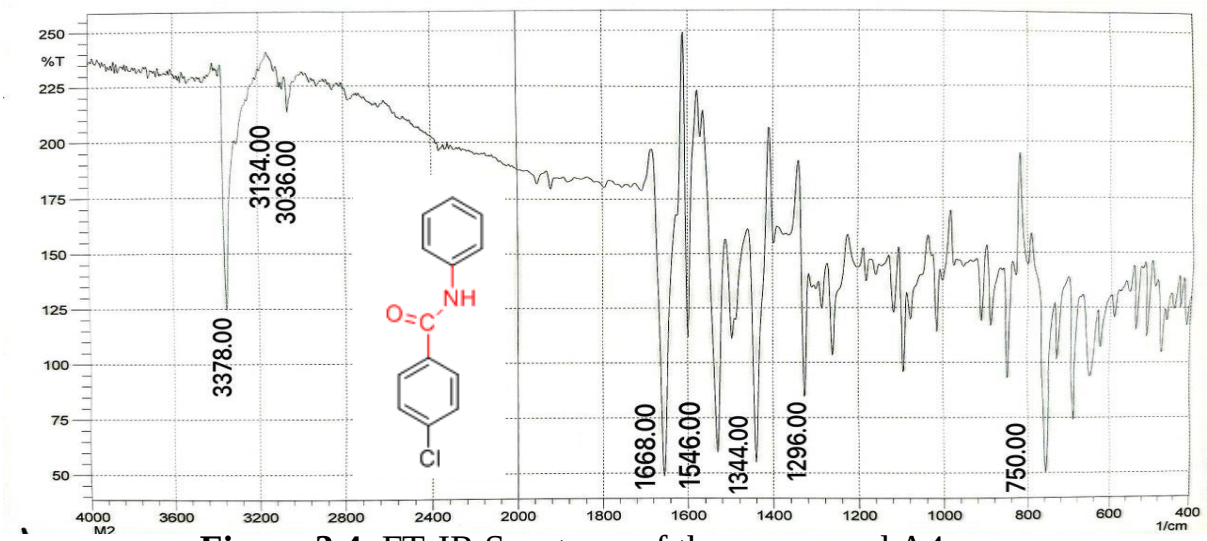

Figure 3.4: FT-IR Spectrum of the compound A4.

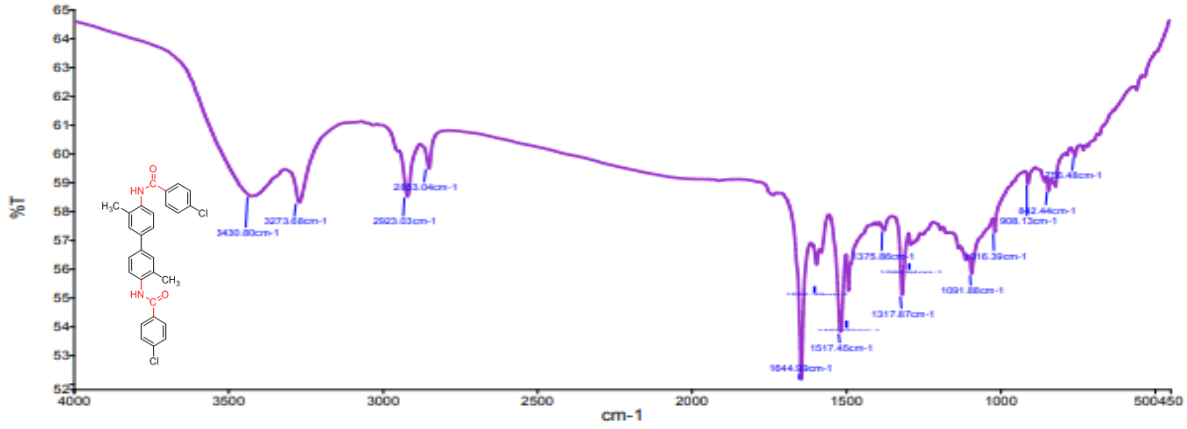

Figure 3.5: FT-IR Spectrum of the compound A5.

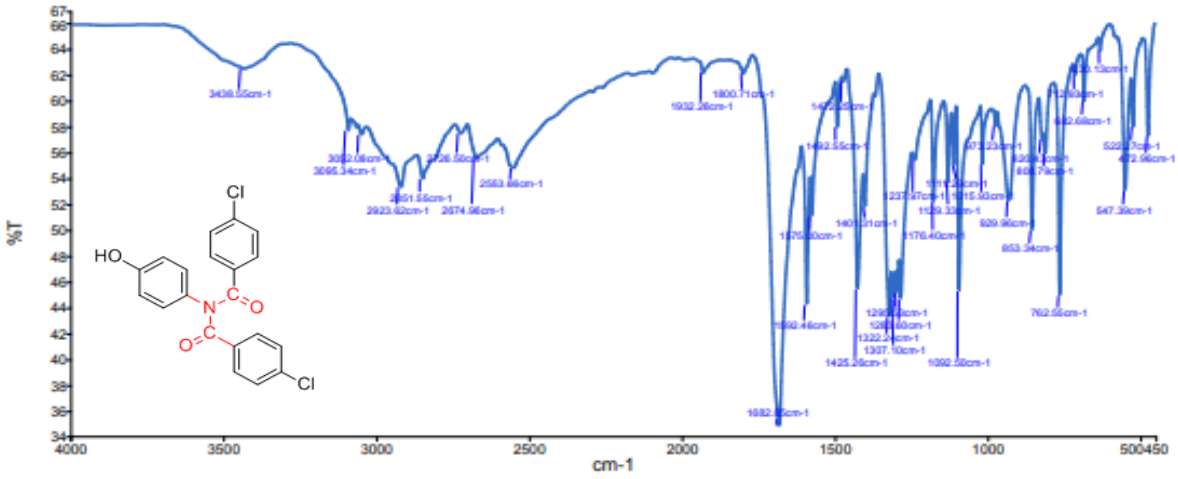

Figure 3.6: FT-IR Spectrum of the compound A6.

Also, the derivatives (A1-A6) were identified by ^{1}H-NMR spectra which appeared five signals shown in **Table 3.2** and **Figures 3.7-3.12**.

The ranges (A1-A5) of the signals are 10.12(-OH, s), 10.45-9.32(-NH, s), 8.05-6.75(Aromatic-H, m), 3.43(OCH_3, s) and 2.32(CH_3, s) ppm.

While the signals of the derivative A6 are 13.25(-OH, s), 7.99-7.58 (Aromatic-H, m) ppm.

Table 3.2: ^{1}H-NMR Spectral data of the A1-A6 ppm.

Symbol	-OH (s)	-NH (s)	Ar-H	O-CH_3 (s)	CH_3 (s)
A1	10.12	9.32	7.97(d.2H,J=8) 7.78(d.2H,J=8) 7.54(d.2H,J=8) 6.76(d.2H,J=8)	___	___
A2	___	10.22	7.99(d.2H,J=8) 7.69(d.2H,J=8) 7.58(d.2H,J=8) 6.93(d.2H,J=8)	3.42	___
A3	___	10.45	7.99(d,2H,J=12) 7.77(d.2H,J=8) 7.61(d,2H,J=8) 7,54(d,2H,J=8)	___	___
A4	___	10.35	7.54(d,2H,J=12) 7.80(d,2H,J=8) 7.61(d,2H,J=8) 7.37(t,2H,J=8) 7.12(t,1H,J=8)	___	___

A5	___	10.04	8.03(d,4H,J=8) 7.63(d,4H,J=8) 7.61(s,2H,J=8) 7.54(d,2H,J=8) 7.44(d,2H,J=8)	___	2.32
A6	13.25	___	7.99(d,4H,J=8 7.97(d,4H,J=8) 7.60(d,2H,J=8) 7.58(d,2H,J=8	___	___

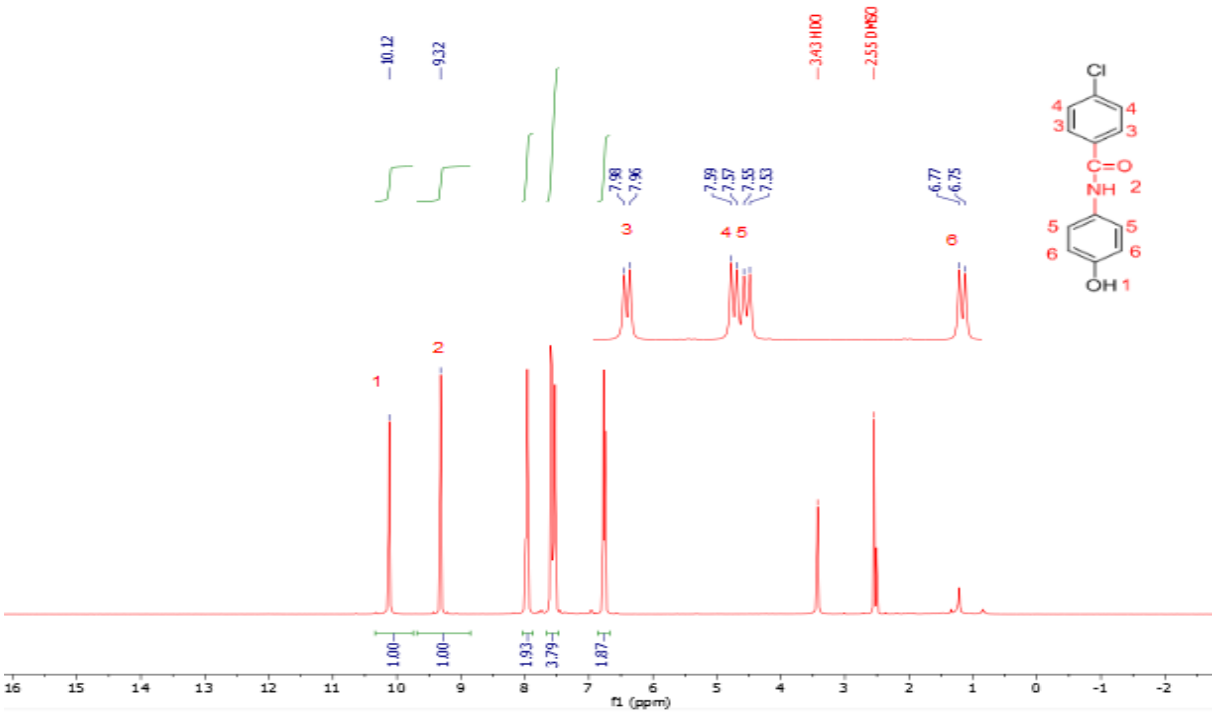

Figure 3.7: ^{1}H-NMR Spectrum of the compound A1.

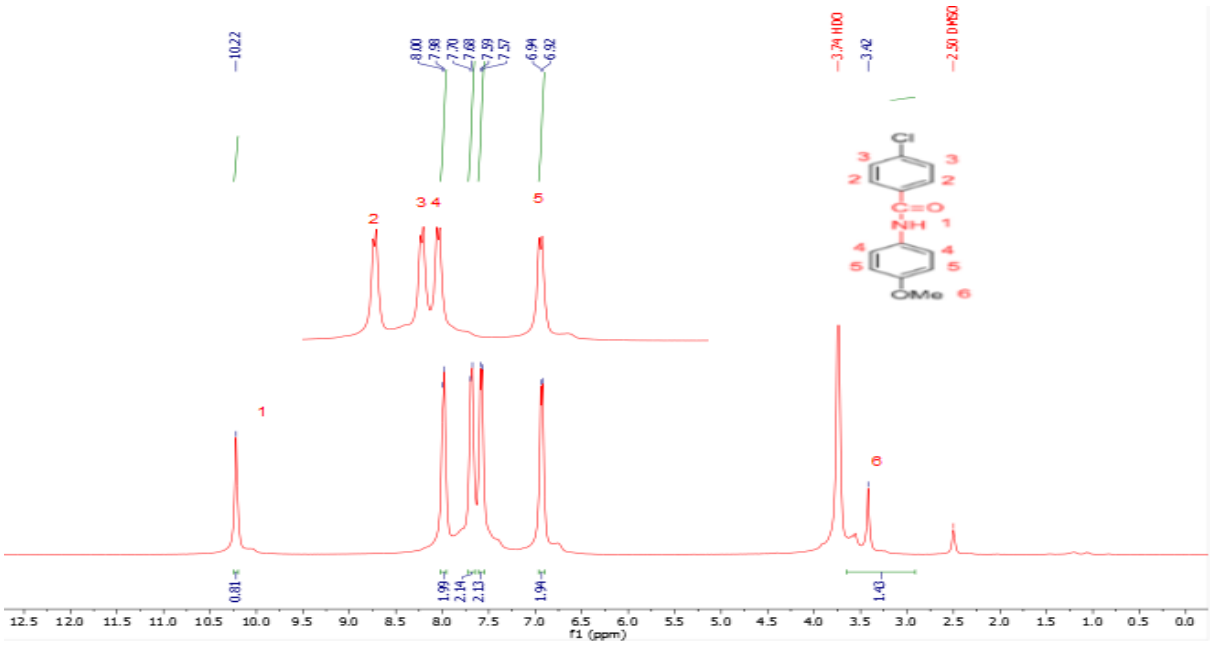

Figure 3.8: ^{1}H-NMR Spectrum of the compound A2.

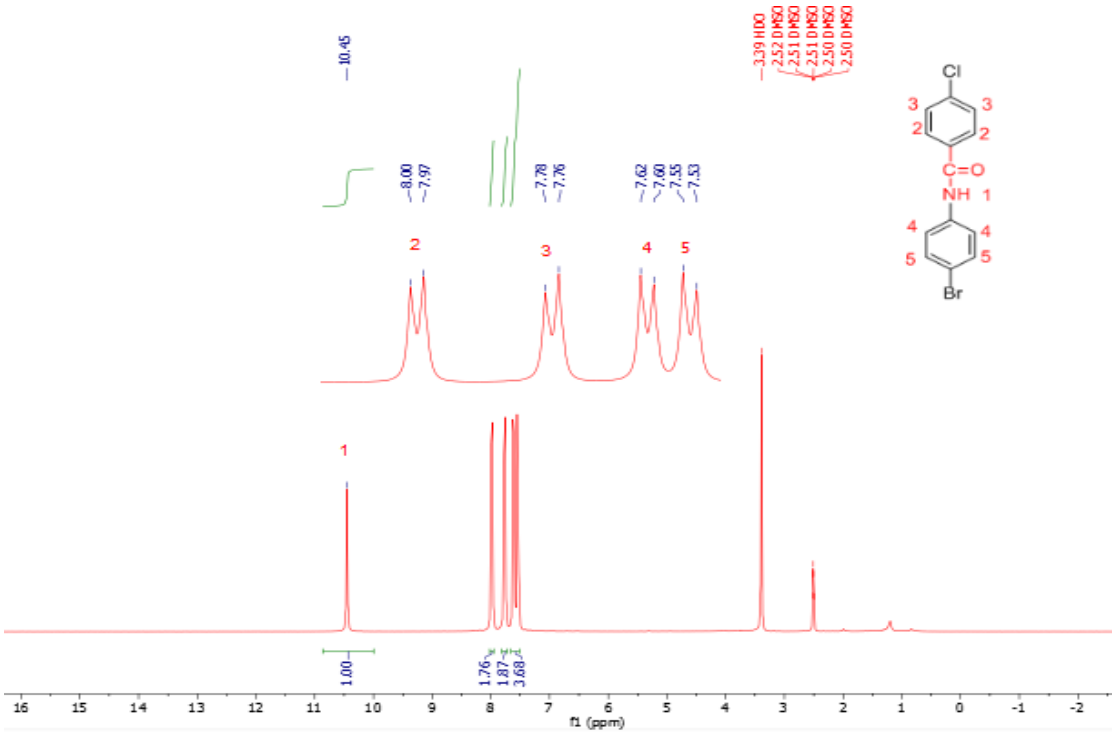

Figure 3.9: ^{1}H-NMR Spectrum of the compound A3.

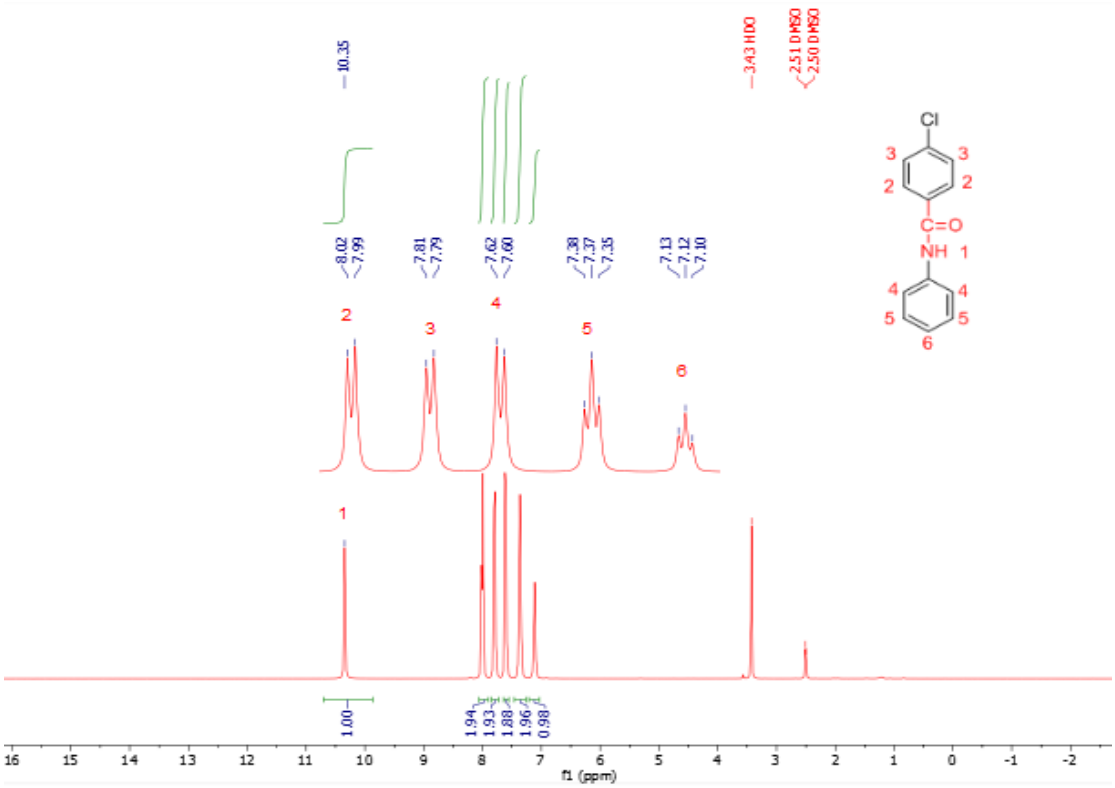

Figure 3.10: ^{1}H-NMR Spectrum of the compound A4.

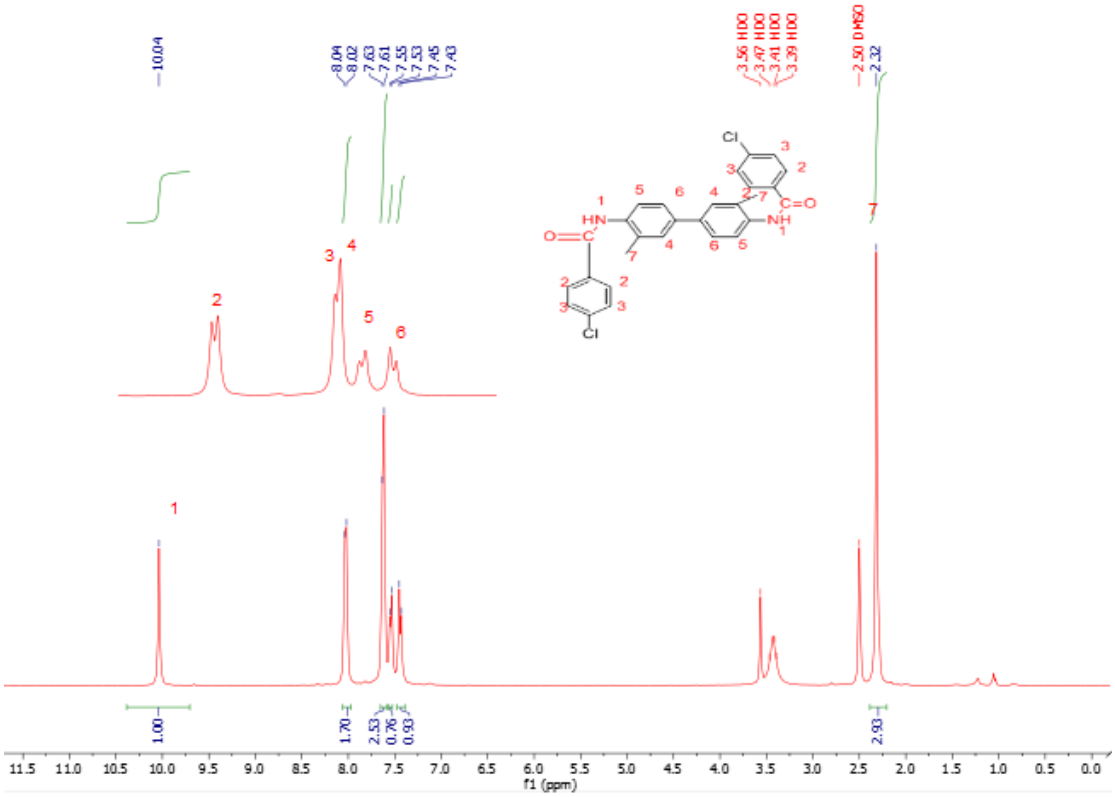

Figure 3.11: ^{1}H-NMR Spectrum of the compound A5.

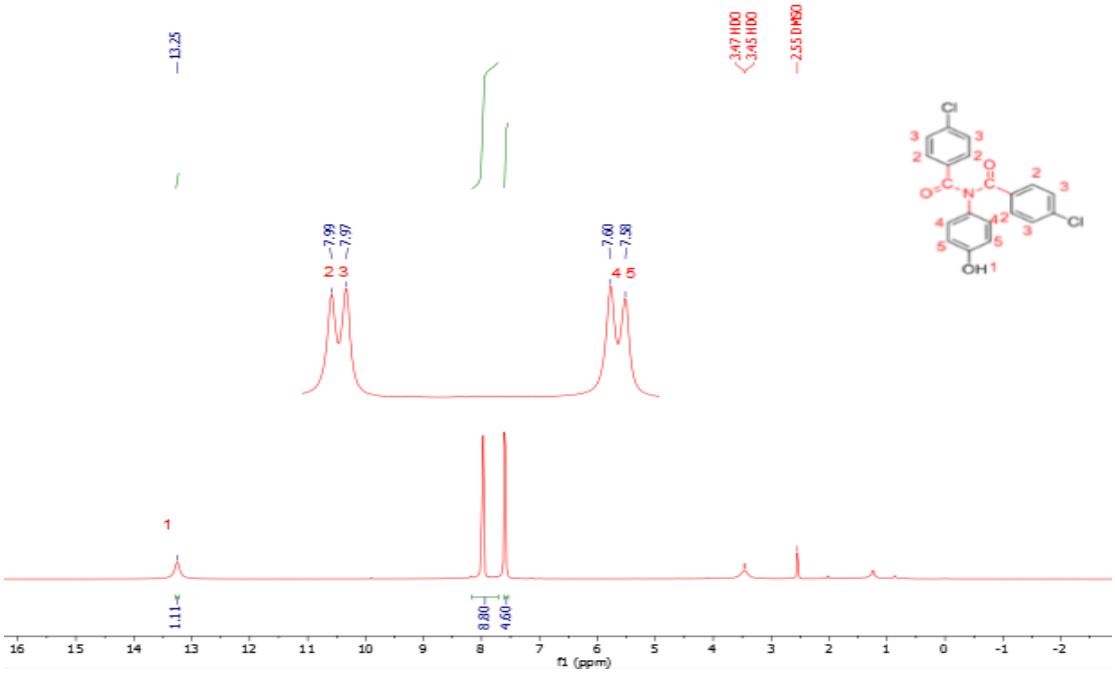

Figure 3.12: ^{1}H-NMR Spectrum of the compound A6.

Whereas the ^{13}C-NMR spectra of derivatives A1-A5 showed signals ascending 164.99-163.99 (C=O), 156.11-139.48(C-O), 137.83- 130.93 (C-N), 139.46-116.00 (C-X), 136.04-114.20(Aromatic ring), 55.61(OCH_3) and 18.56 (CH_3) ppm.

While the signals of the derivative A6 are 166.94 (C=O), 138.27 (C-N), 130.08 (C-X), and 131.60-129.19(Aromatic ring) ppm as shown in **Table 3.3** and **Figures 3.13-3.18**.

Table 3.3: ^{13}C-NMR Spectral data of the A1-A6 ppm.

Symbol	C=O	C-O	C-N	C-X	Ar-C	-OCH_3	-CH_3
A1	164.29	154.32	130.93	136.57 C-Cl	129.94-115.47	___	___
A2	164.43	156.11	132.48	136.69 C-Cl	129.98-114.20	55.61	___
A3	164.99	___	133.82	138.85 C-CI 116.00 C-Br	131.94-122.72	___	___

A4	164.91	___	134.12	139.46 C-Cl	130.10- 120.90	___	___
A5	164.82	___	137.83	136.87 C-Cl	136.04- 124.62	___	18.56
A6	166.94	138.27	___	130.08 C-Cl	131.60- 129.19	___	___

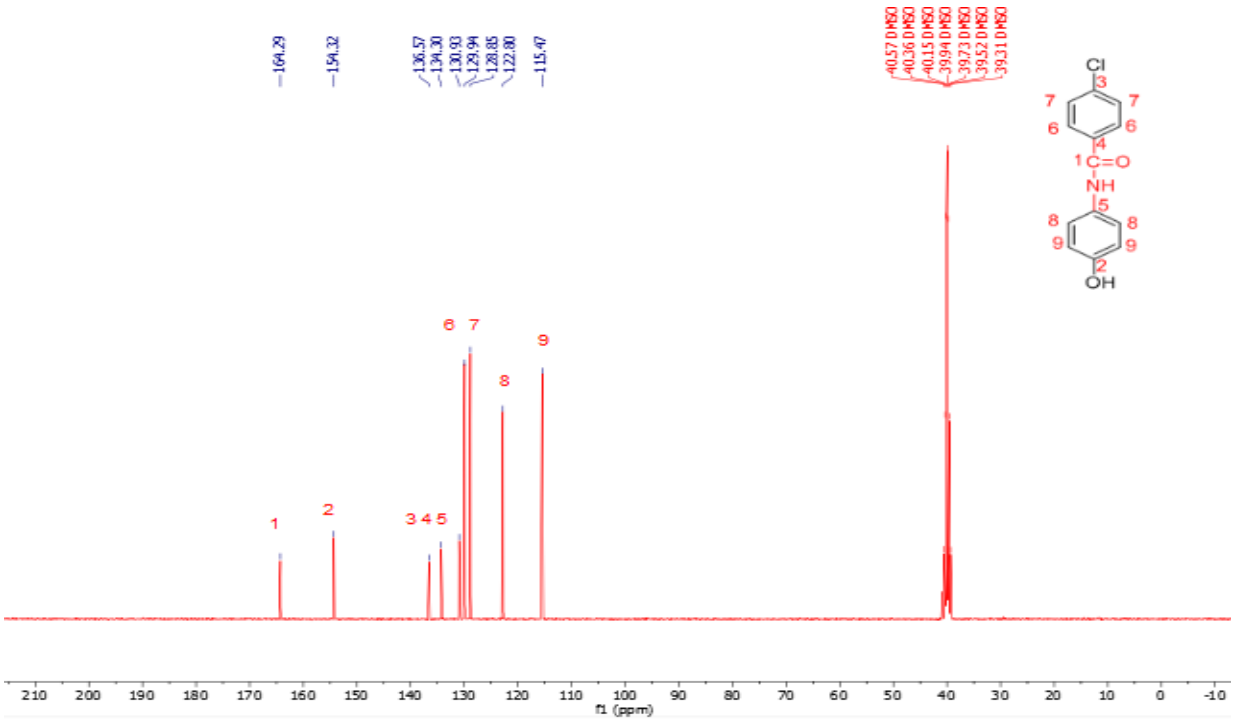

Figure 3.13: ^{13}C-NMR Spectrum of the compound A1.

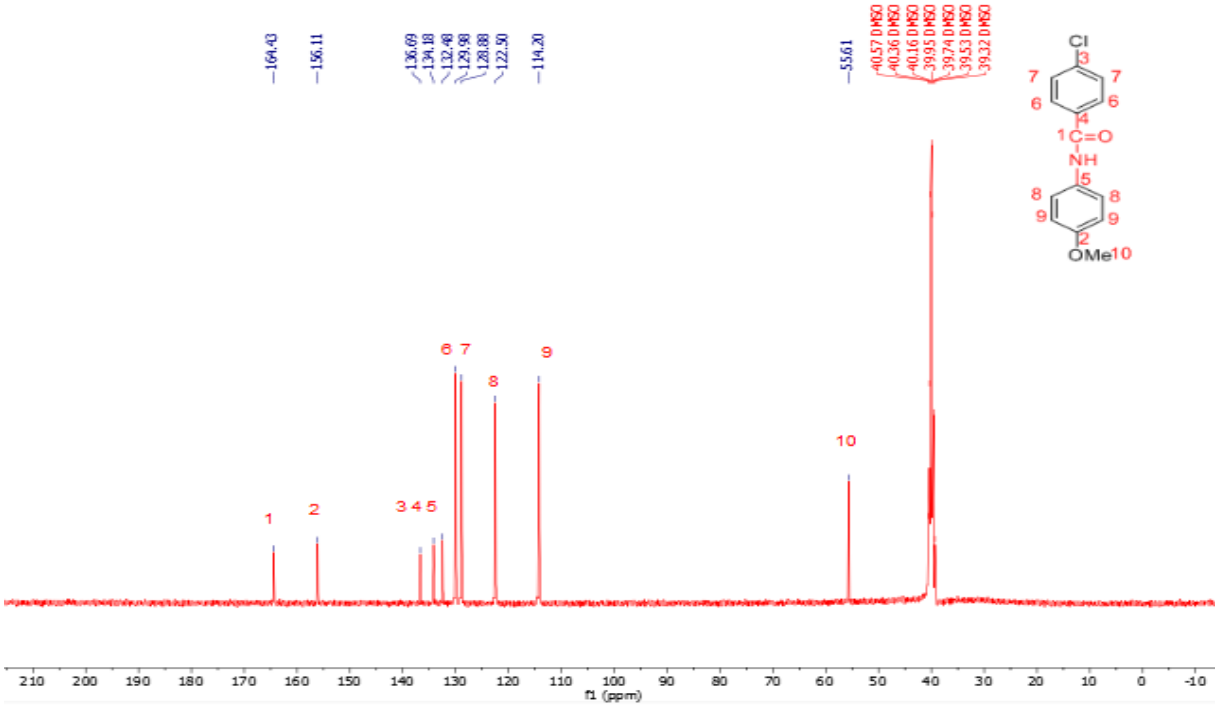

Figure 3.14: ^{13}C-NMR Spectrum of the compound A2.

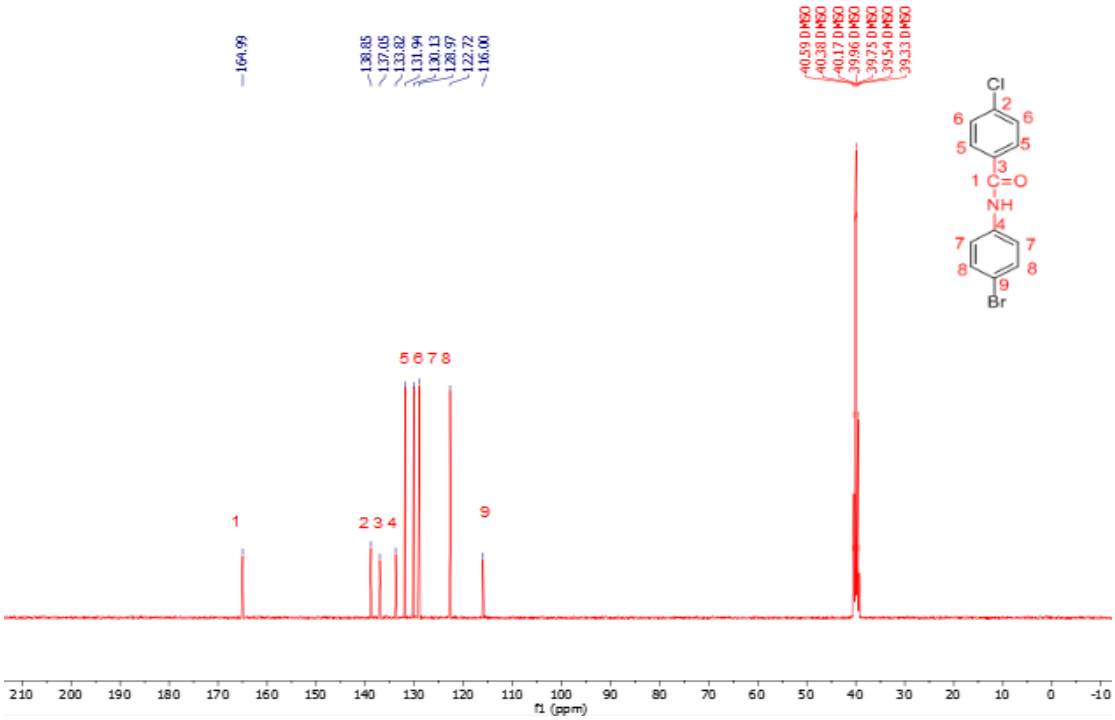

Figure 3.15: ^{13}C-NMR Spectrum of the compound A3.

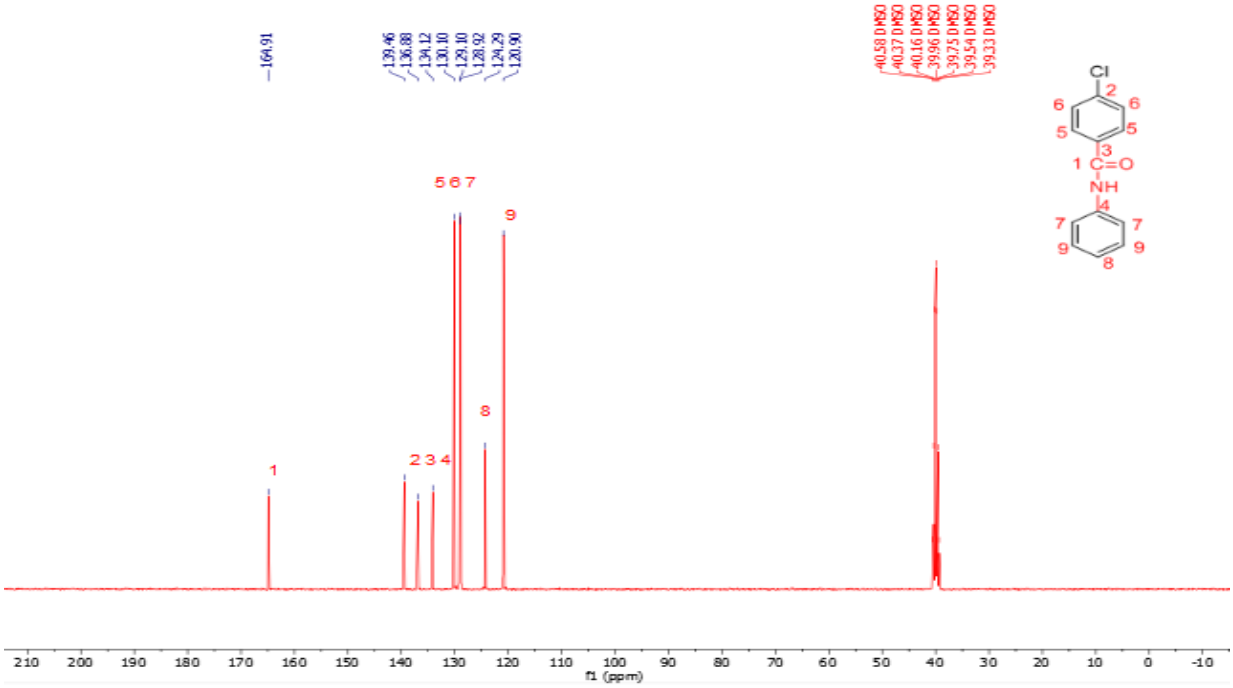

Figure 3.16: ^{13}C-NMR Spectrum of the compound A4.

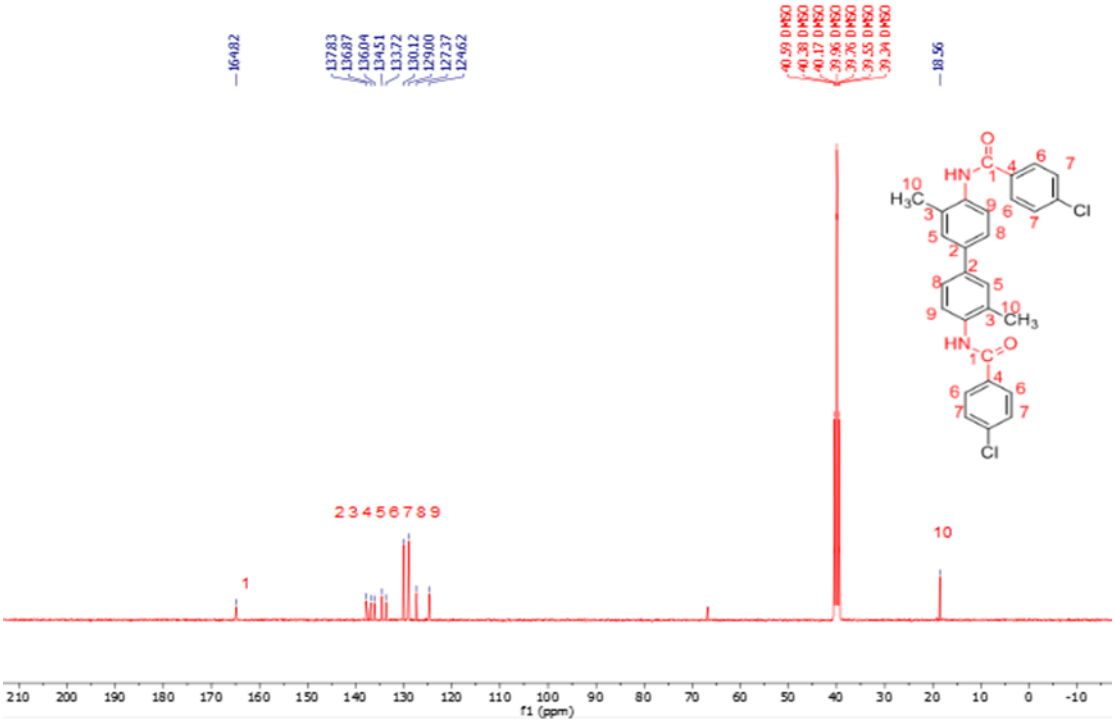

Figure 3.17: ^{13}C-NMR Spectrum of the compound A5.

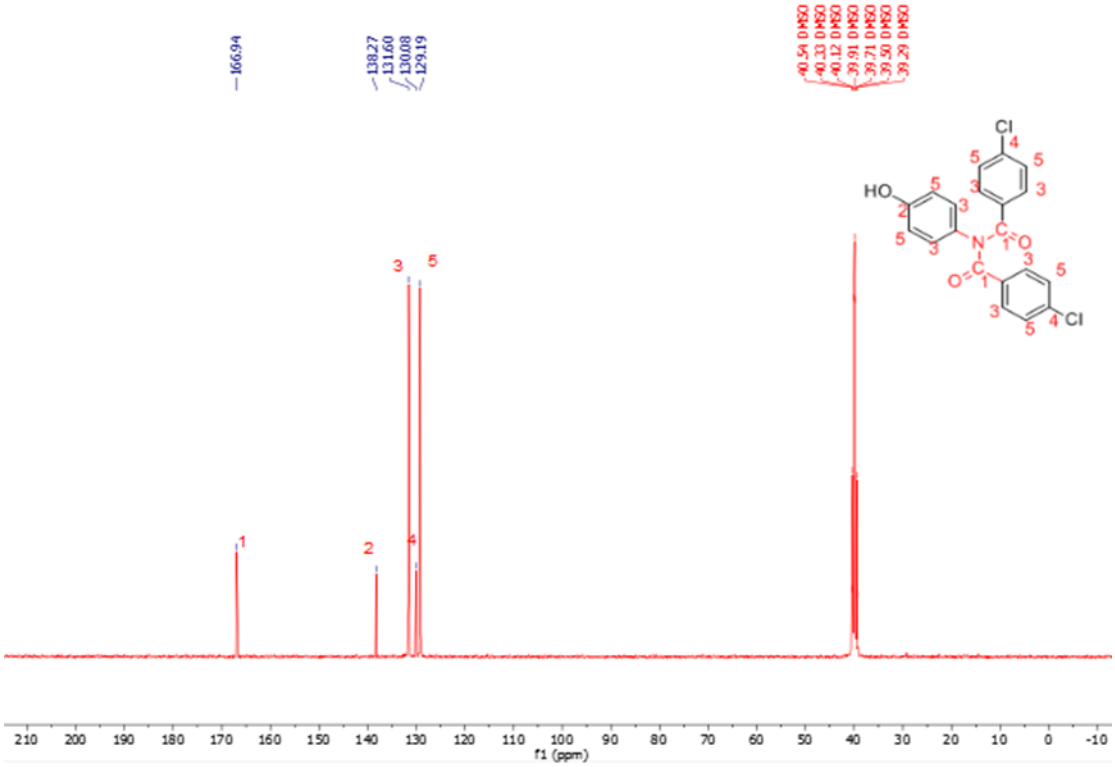

Figure 3.18: ^{13}C-NMR Spectrum of the compound A6.

The mass spectrum of the A5 derivative as shown in **Table 3.4**, **Figure 3.19** and **Scheme 3.2**, is referred that the molecular ion is corresponding with the molecular wight of this derivative.

Table 3.4: Mass spectral data of A5.

Symbol	Molecular ion (M^+) m/z	The peaks m/z
A5	488.11	$[C_{22}H_{17}ClN_2O_2]^{+\cdot}$ = 376.11 $[C_{21}H_{18}ClN_2O]^{+\cdot}$ =350 $[C_{21}H_{17}ClNO]^{+\cdot}$ =335 $[C_{15}H_{14}N_2O]^{+\cdot}$ =238.29 $[C_{15}H_{17}N_2]^{+\cdot}$ =225 $[C_{15}H_{17}N]^{+\cdot}$ =211 $[C13H12N]^{+\cdot}$ =180 $[C_{13}H_9]^{+\cdot}$ =165 $[C_7H_4ClO]^{+\cdot}$ =139 $[C_6H_4Cl]^{+\cdot}$ =111 $[C_6H_4]^{+\cdot}$ =76

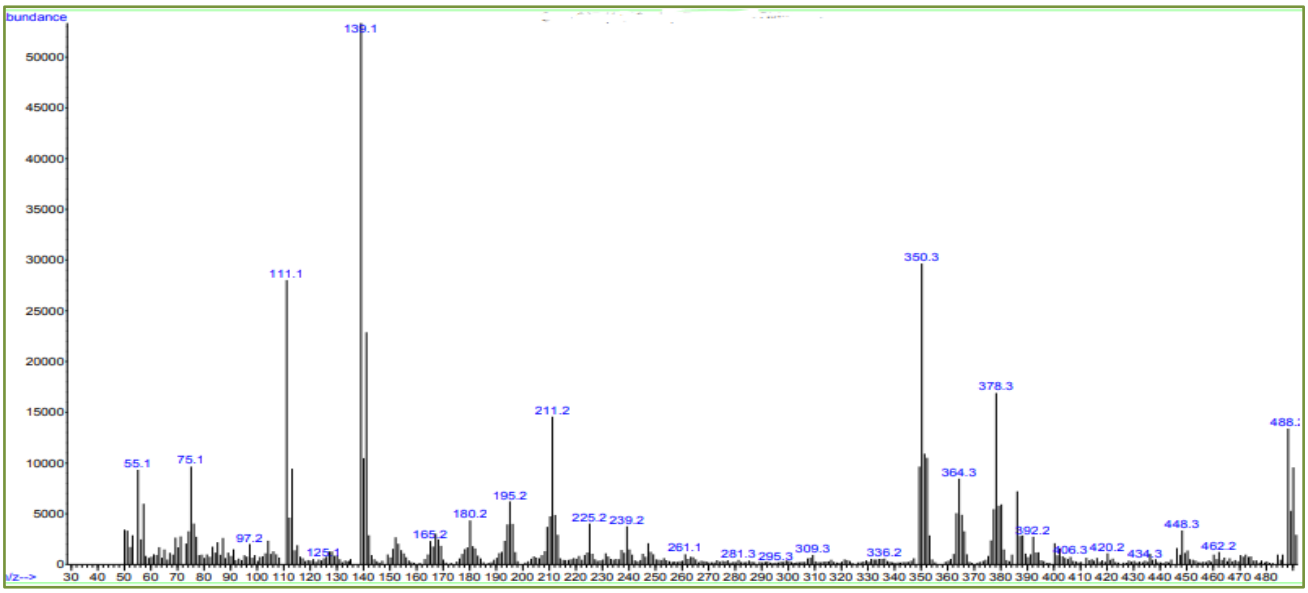

Figure 3.19: Mass Spectrum of A5.

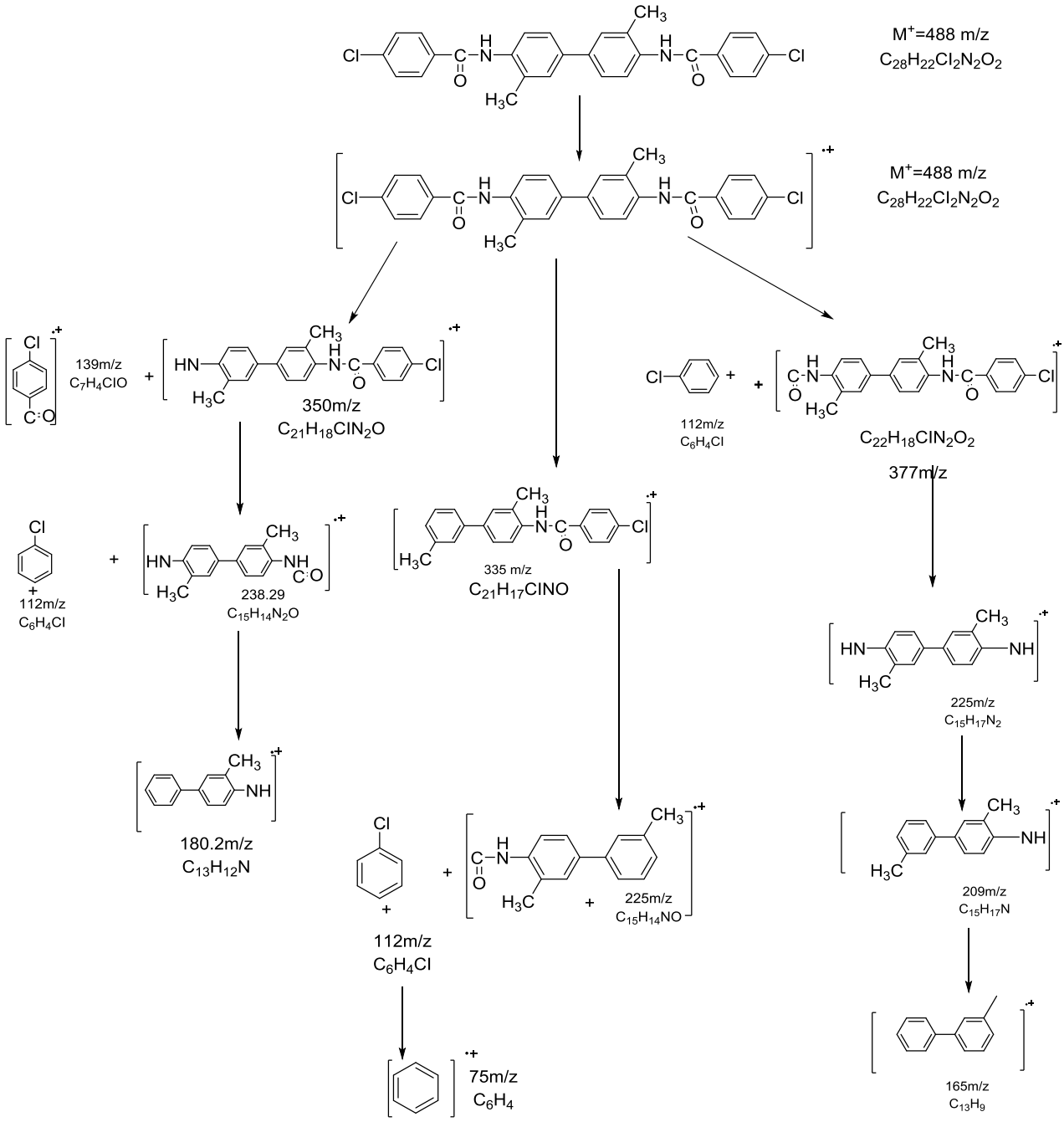

Scheme 3.2: Fragmentation of compound A5.

3.2. Synthesis of sulfonamide derivatives B1-B5

Sulfonamide derivatives (B1-B5) are synthesized by the reaction of *p*-substituted aniline or o-tolidine with *p*-toluene sulfonyl chloride in the presence of DCM as solvent and Et_3N: as catalyst **Equation 3.2** and **Scheme 3.2**.

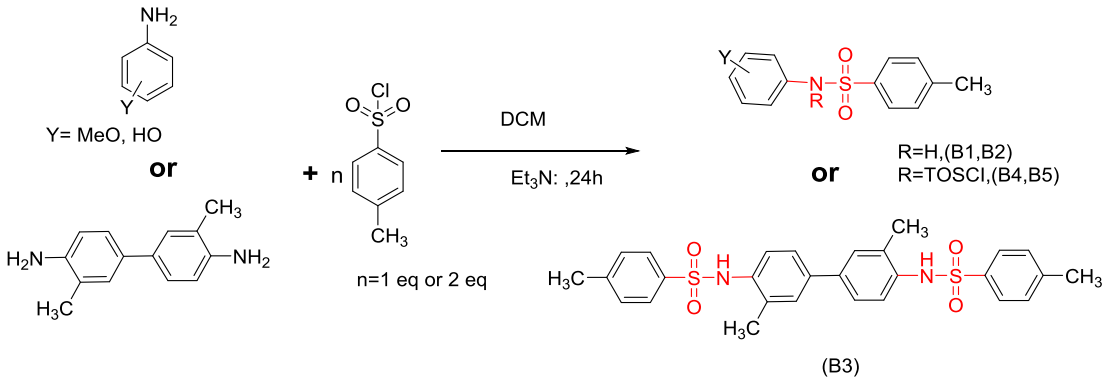

Equation 3.2: Synthesis of sulfonamide derivatives B1-B5.

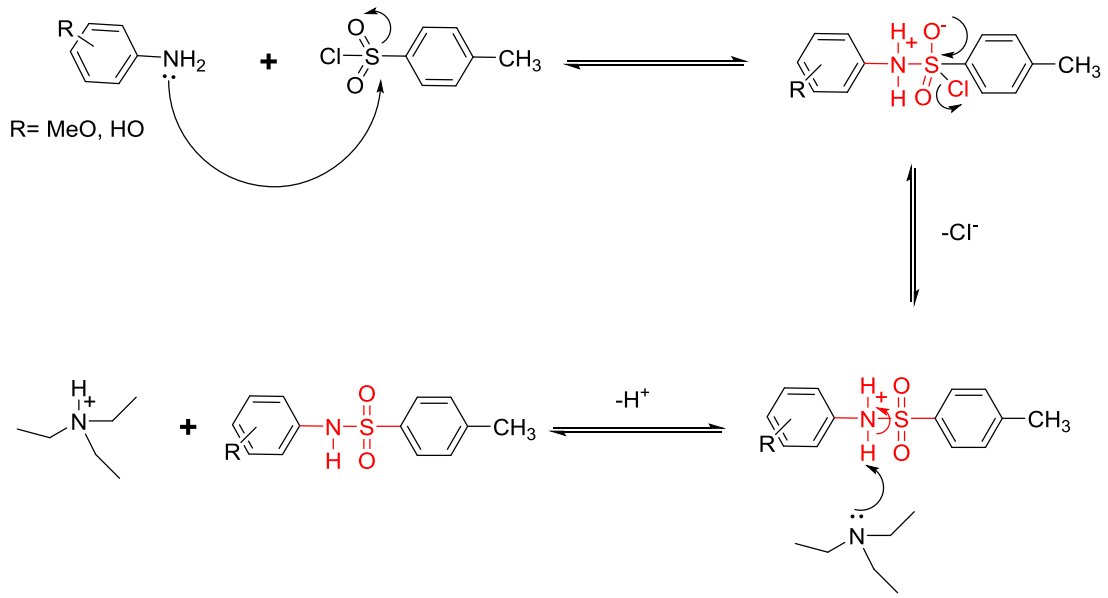

Scheme3.3: Mechanism of synthesis of sulfonamide derivatives B1-B5.

3.2.1. Characterization of the B1-B5

The IR spectra of the derivatives B1-B5 as show in **Table 3.5** and **Figures 3.20-3.24**.

The derivatives (B1-B3) are characterized by eight bands corresponding to the stretching vibrations of the -OH, -NH, aromatic C-H, Aliphatic C-H, C=C, S=O, C-O, and C-N groups, which occur within the ranges 3439.19, (3370.38-3269.68), (3243.21-2923.44), (2921.95-2839.85), (1598.55-1506.66), (1490.94-1330.21), (1183.80-1159.81), (1093.16-1090.93) cm^{-1} respectively.

While the derivatives (B4, B5) are characterized by seven bands corresponding to the stretching vibrations of the -OH, aromatic C-H, Aliphatic C-H, C=C, S=O, C-O, and C-N groups, which occur within the ranges 3242.34, (3107.32-2939.52), (2981.95-2677.20), (1598.99-1510.26), (1465.90-1460.11), (1199.72-1061.15), 1091.71 cm^{-1} respectively.

The disappearance of the band of a group NH- of B4, B5 is confirmed that the reaction is di- substitution.

Table 3.5: FT-IR Spectral data of the stretching vibrations of A1-A6 cm^{-1}.

Symbol	-OH	-NH	CH Aromatic (w)	CH Aliphatic (w)	C=C	S=O	C-O	C-N
B1	3439.19 (s)	3370.38 (s)	3243.21-3065.15	2921.95-2852.11	1506.66 (s)	1330.21 (vs)	1183.80 (s)	1093.16 (s)
B2	___	3269.68 (s)	3011.86-2963.03	2920.25-2839.85	1510.52 (s)	1334.38 (s)	1159.81 (vs)	1090.93 (w)
B3	___	3286.05 (w)	2923.44	2853.01	1598.55 (w)	1490.94 (s)	1163.47 (vs)	1092.45 (w)
B4	3242.34 (vs)	___	3107.32	2981.95-2860.43	1598.99 (s)	1460.11 (s)	1199.72 (s)	1091.71 (s)
B5	___	___	3030.17-2939.52	2839.22-2677.20	1510.26 (vs)	1465.90 (s)	1161.15 (vs)	1091.71 (s)

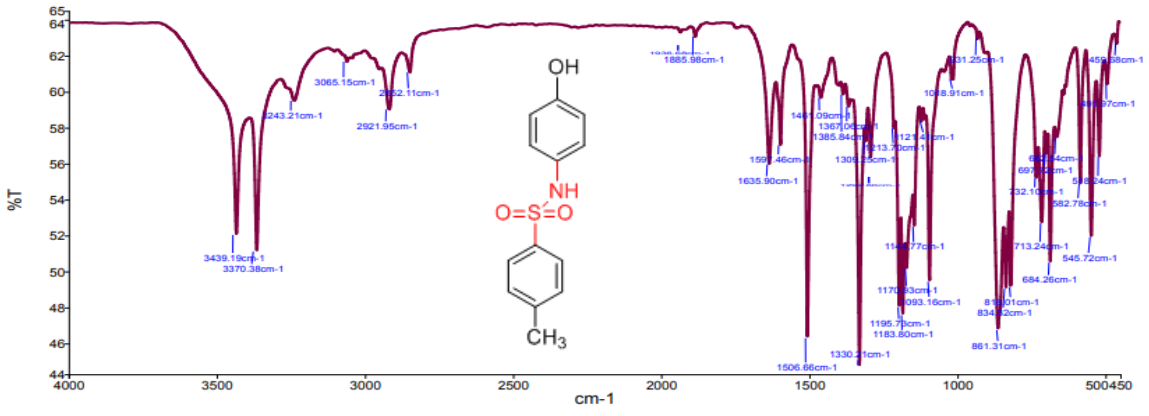

Figure 3.20: FT-IR spectrum of the compound B1.

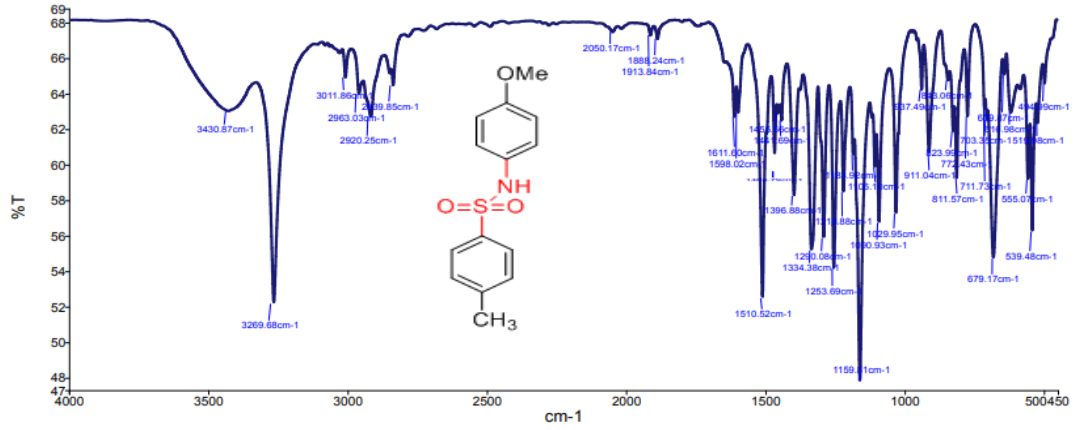

Figure 3.21: FT-IR spectrum of the compound B2.

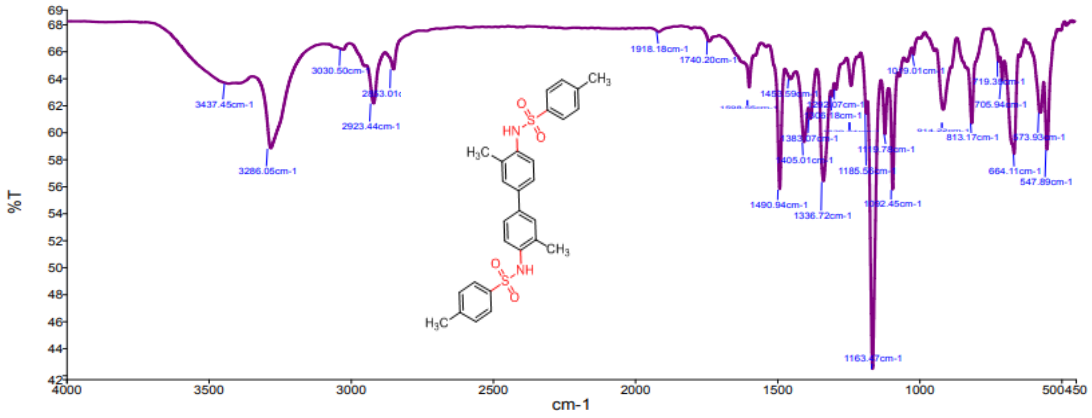

Figure 3.22: FT-IR spectrum of the compound B3.

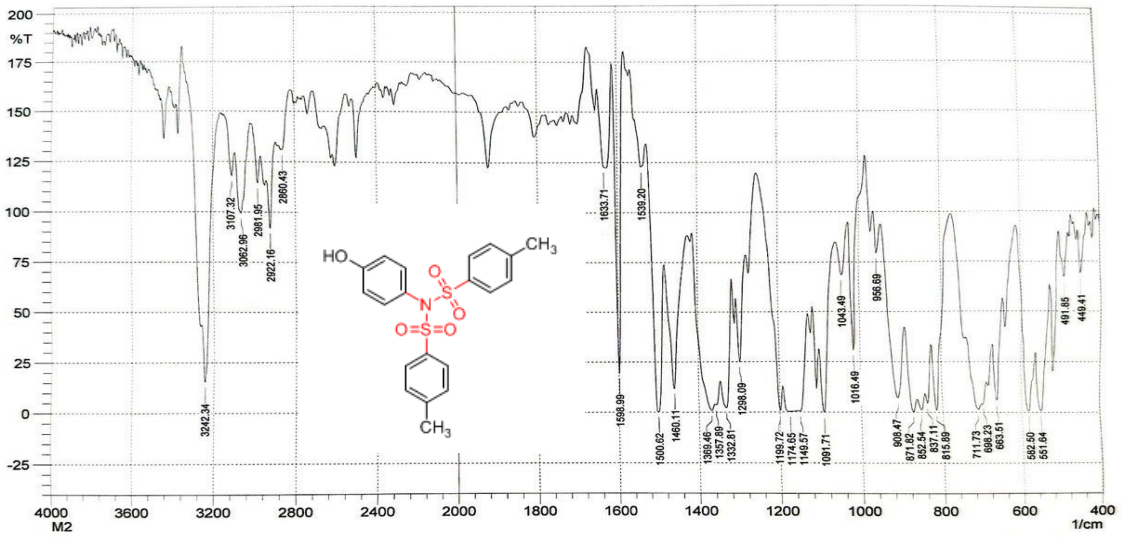

Figure 3.23: FT-IR spectrum of the compound B4.

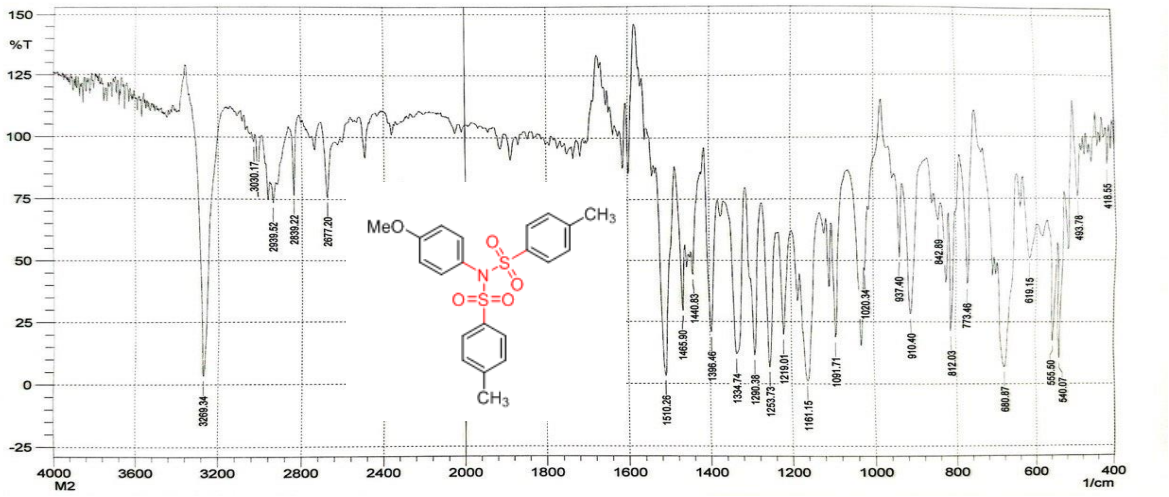

Figure 3.24: FT-IR spectrum of the compound B5.

The ^{1}H-NMR spectra of the mono-substituted derivatives B1-B3 were identified by five signals shown in Table (3.6) and Figures (3.25-3.27).

The range of the signals are 9.67 (-OH, s), 9.87-9.30 (-NH, s), 7.67-6.60 (Aromatic-H, m), 3.66 (OCH_3, s) and 2.36-2.02 (CH_3, s) ppm.

While the signals of the di-substituted derivatives B4, B5 are 14.57 (-OH, s), 7.70-6.88 (Aromatic-H, m), 3.78 (OCH_3, s) and 2.45- 2.35 (CH_3, s) ppm shown in **Table 3.6** and **Figures 3.28, 3.29**.

Table 3.6: ^{1}H-NMR spectral data of the B1-B5 ppm.

Symbol	-OH (s)	-NH (s)	Ar-H	O-CH_3 (s)	CH_3 (s)
B1	9.67	9.30	7.55(d,2H,J=8) 7.31(d,2H,J=8 6.87(d,2H,J=8) 6.61(d,2H,J=8	___	2.32
B2	___	9.87	7.57(d,2H,J=8) 7.32(d,2H,J=8) 6.68(d,2H,J=8)	3.66	2.32

			6.2 3(d,2H,J=12		
B3	___	9.57	7.66(d,4H,J=8) 7.56(d,2H,J=8) 7.48(d,4H,J=8)	___	2.36-2.02
B4	14.57	___	7.59(d,4H,J=8) 7.57(d,4H,J=8) 7.22(d,2H,J=8) 7.20(d,2H,J=8)	___	2.35
B5	___	___	7.69(d,4H,J=8) 7.48(d,4H,J=8) 7.97(d,2H,J=8) 6.89(d,2H,J=12)	3.78	2.45

s=singlet

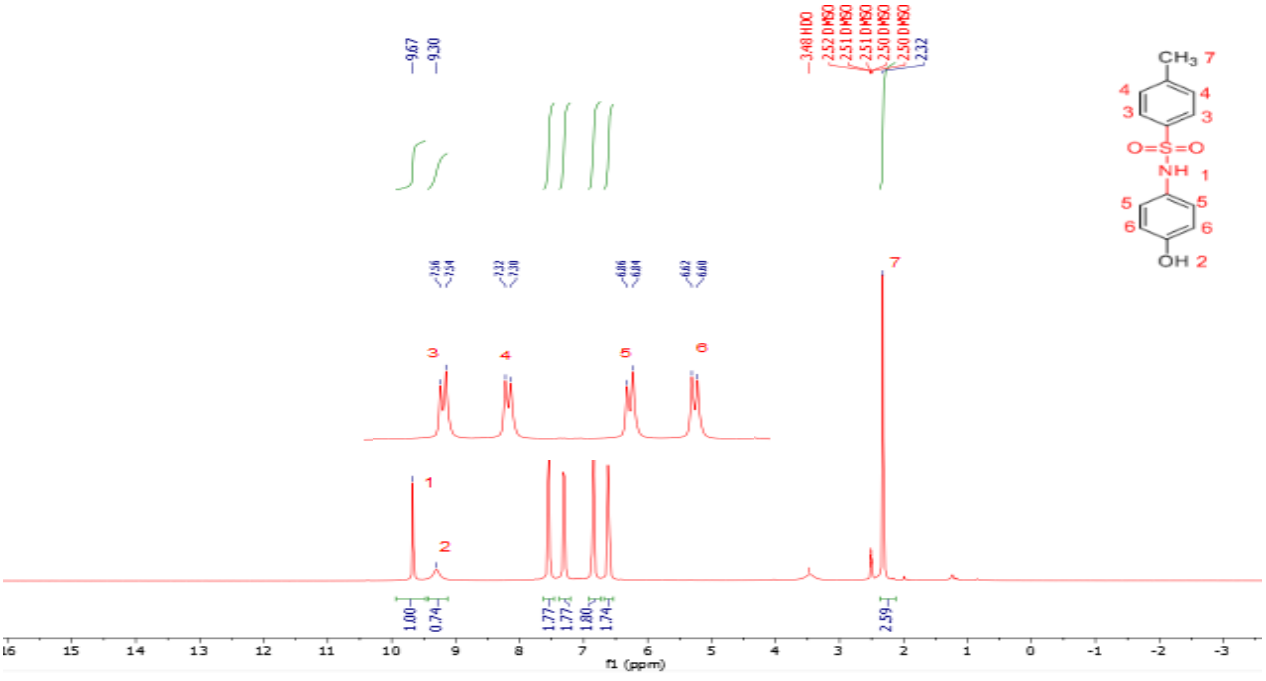

Figure 3.25: ^{1}H-NMR Spectrum of the compound B1.

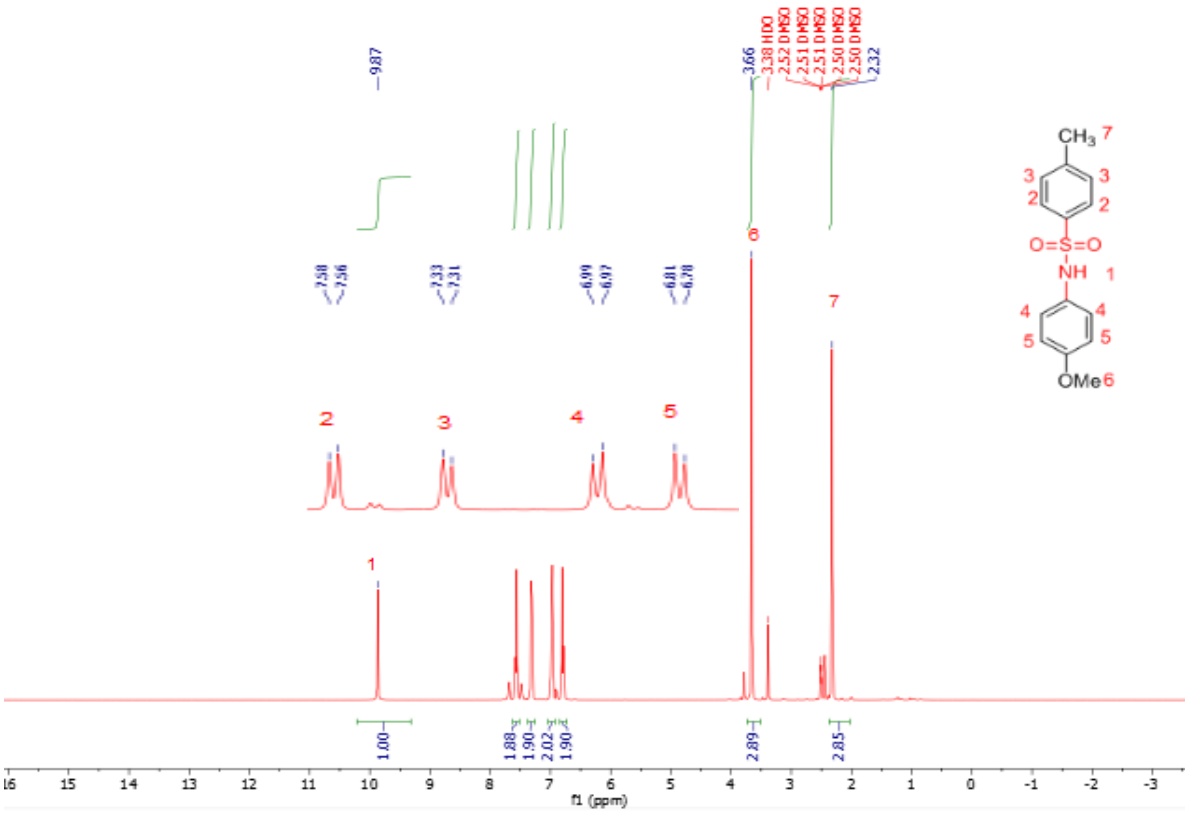

Figure 3.26: ^{1}H-NMR Spectrum of the compound B2.

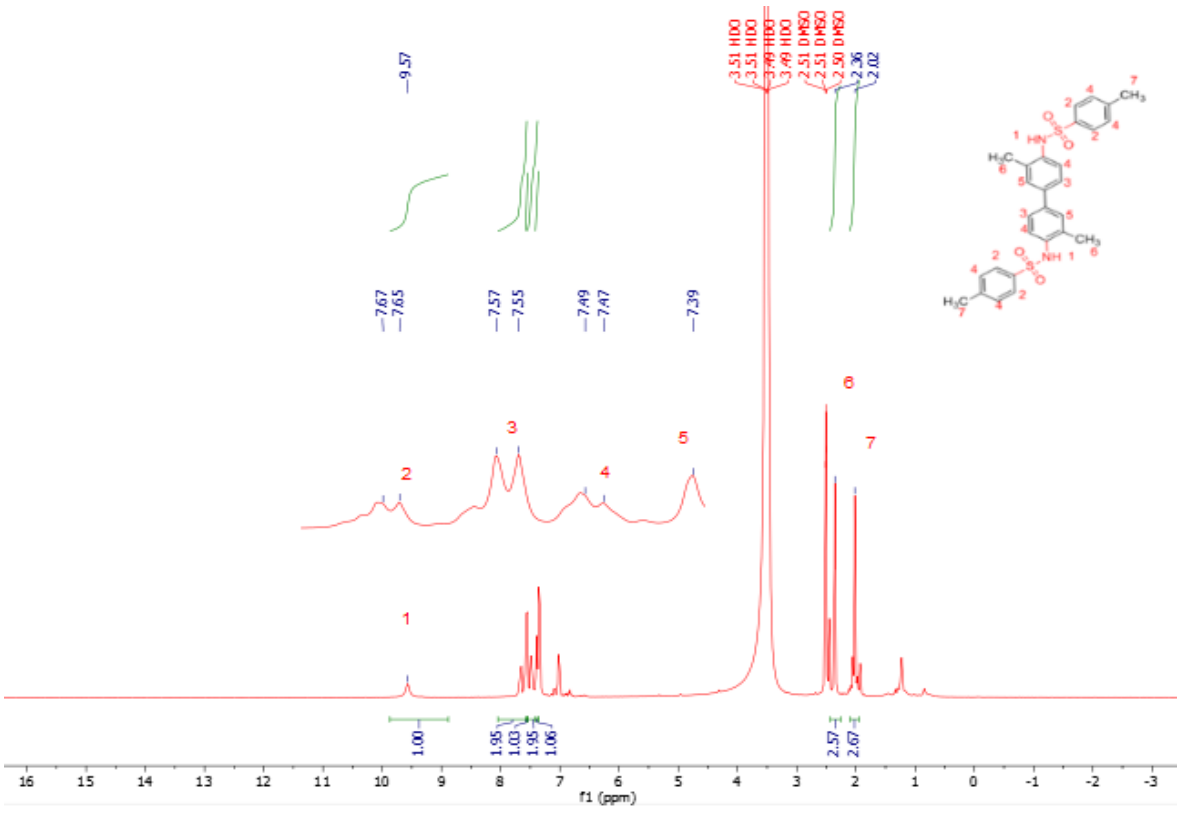

Figure 3.27: ^{1}H-NMR Spectrum of the compound B3.

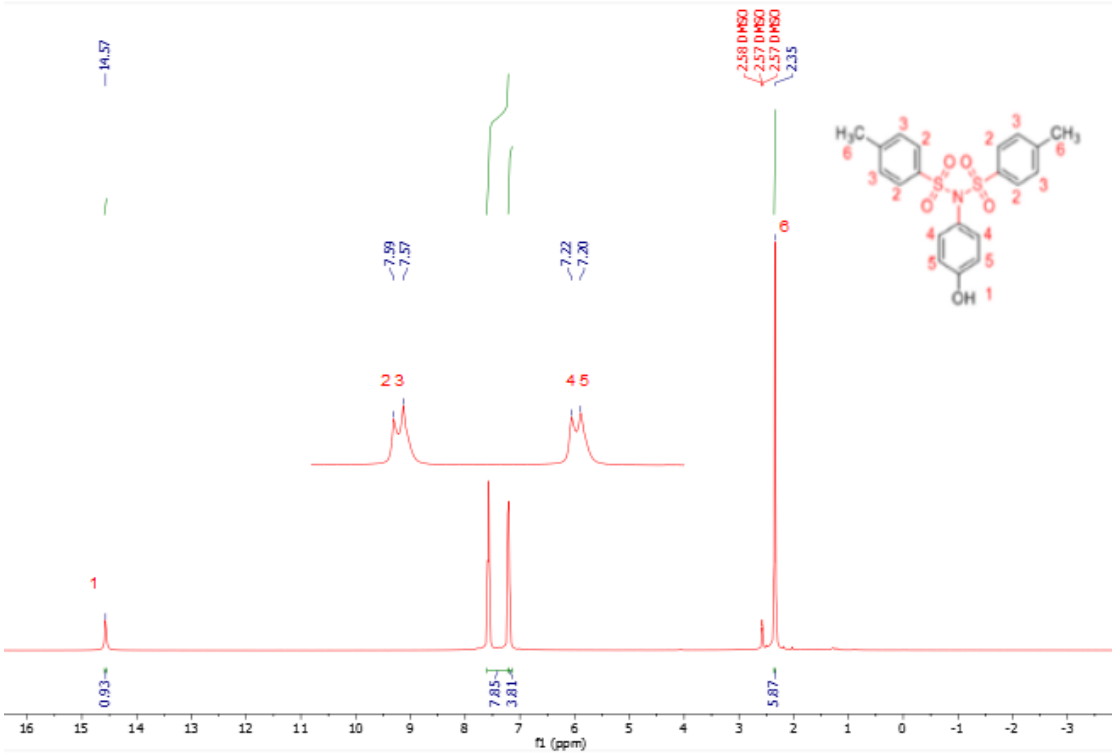

Figure 3.28: ^{1}H-NMR Spectrum of the compound B4.

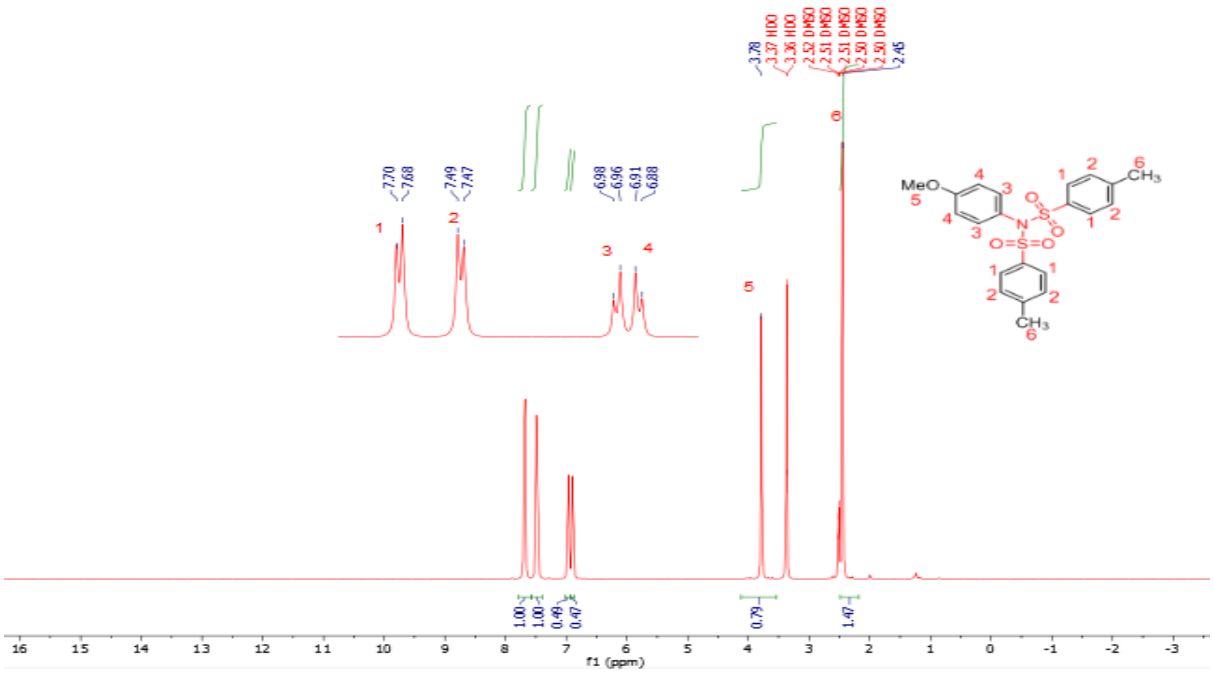

Figure 3.29: ^{1}H-NMR Spectrum of the compound B5.

Whereas the ^{13}C-NMR spectra of the derivatives B1-B3 showed six signals ascending 156.89-155.25(C-O), 137.37-137.08(C-S), 134.76-129.07(C-N), 134.70-114.71(Aromatic ring), 55.56(OCH_3) and 21.65-18.17(CH_3) ppm.

While the signals of the di- substituted derivatives B4, B5 are 160.90-148.37(C-O), 139.41-136.30(C-S), 145.79-145.78(C-N), 133.01-115.10(Aromatic ring) 55.97(OCH_3) and 21.65-21.62(CH_3) ppm. As shown in **Table 3.7** and **Figures 3.30-3.34.**

Table 3.7: ^{13}C-NMR spectral data of the B1-B5 ppm.

Symbol	C-O	C-S	C-N	Ar-C	-OCH_3	-CH_3
B1	155.25	137.20	129.07	129.92-115.98	___	21.40
B2	156.89	137.08	130.70	130.01-114.71	55.56	21.40
B3	___	137.37	134.76	134.70-124.77	___	21.65-18.17
B4	148.37	139.41	145.79	132.14-122.95	___	21.62
B5	160.90	136.30	145.78	133.01-115.10	55.97	21.65

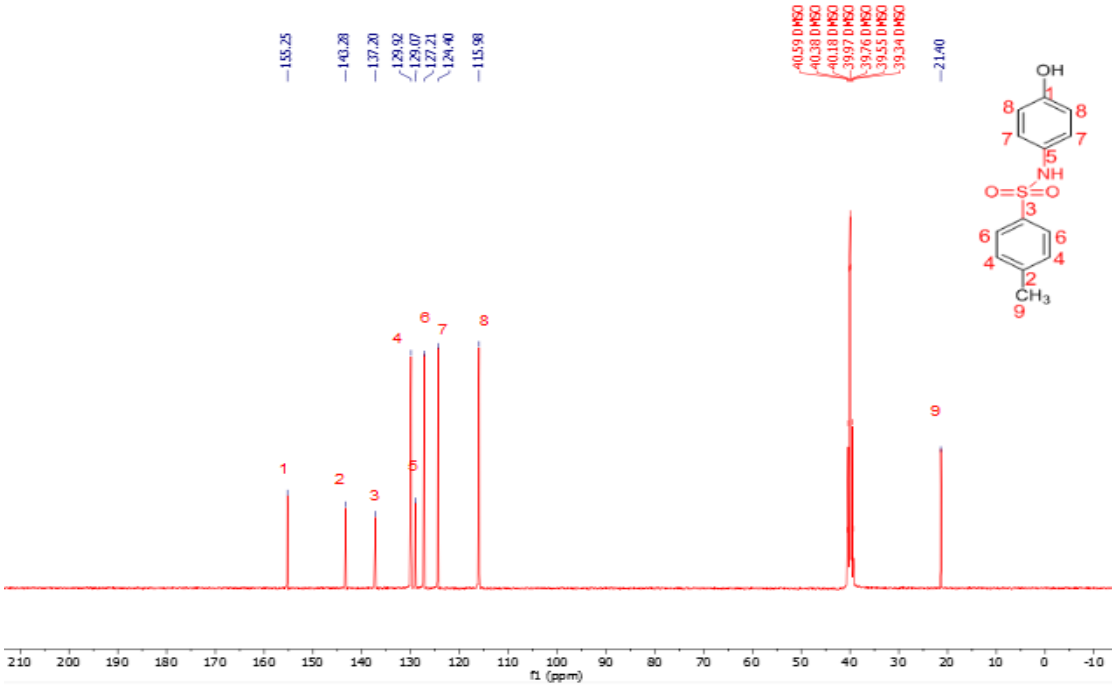

Figure 3.30: ^{13}C-NMR Spectrum of the compound B1.

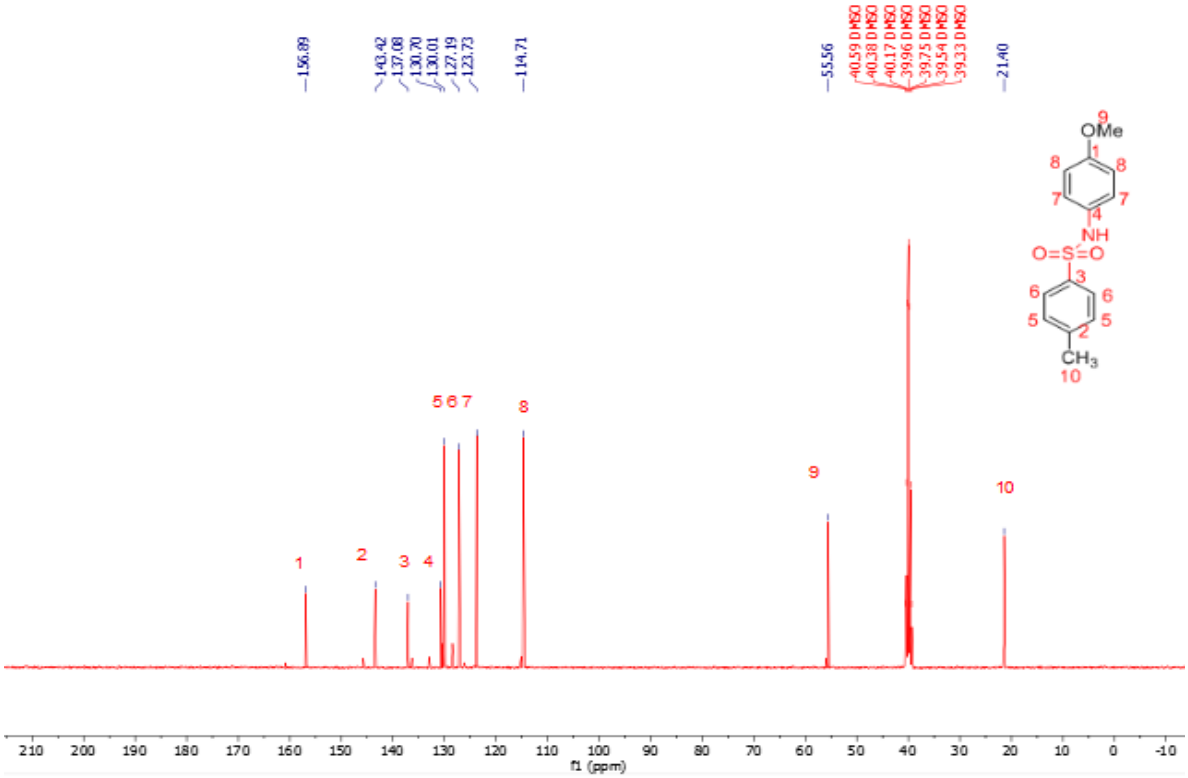

Figure 3.31: ^{13}C-NMR Spectrum of the compound B2.

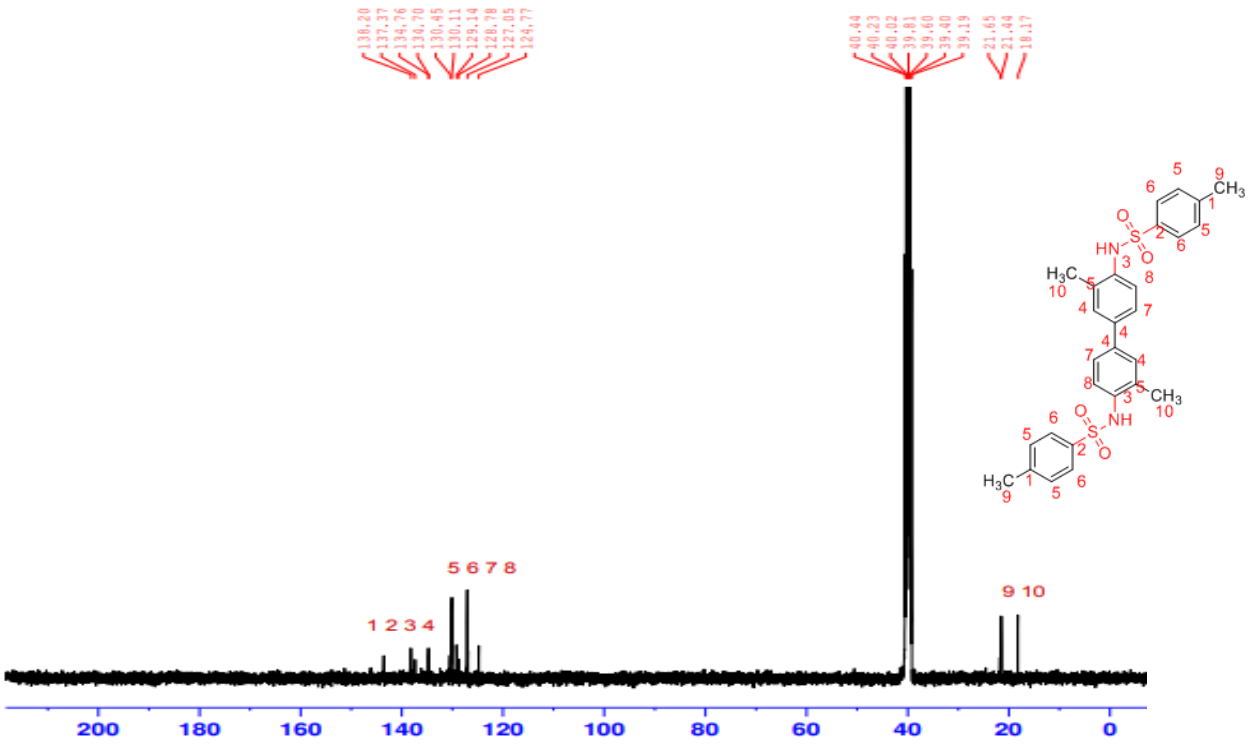

Figure 3.32: ^{13}C-NMR Spectrum of the compound B3.

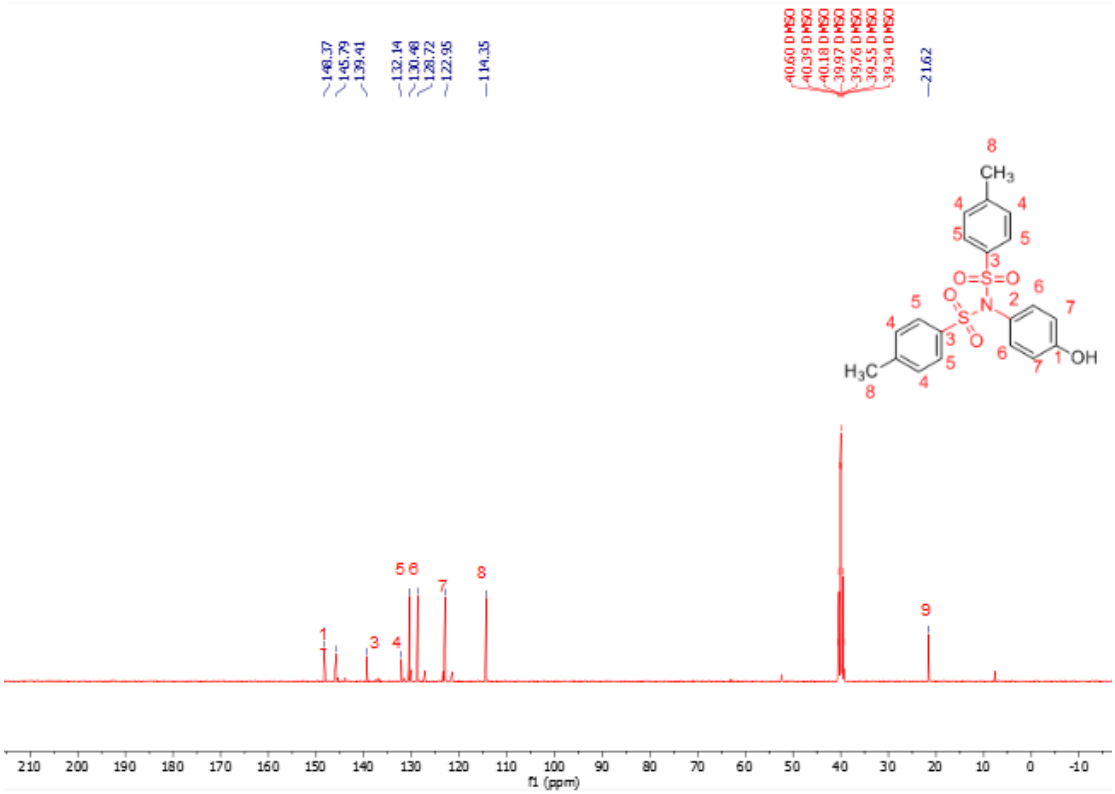

Figure 3.33: ^{13}C-NMR Spectrum of the compound B4.

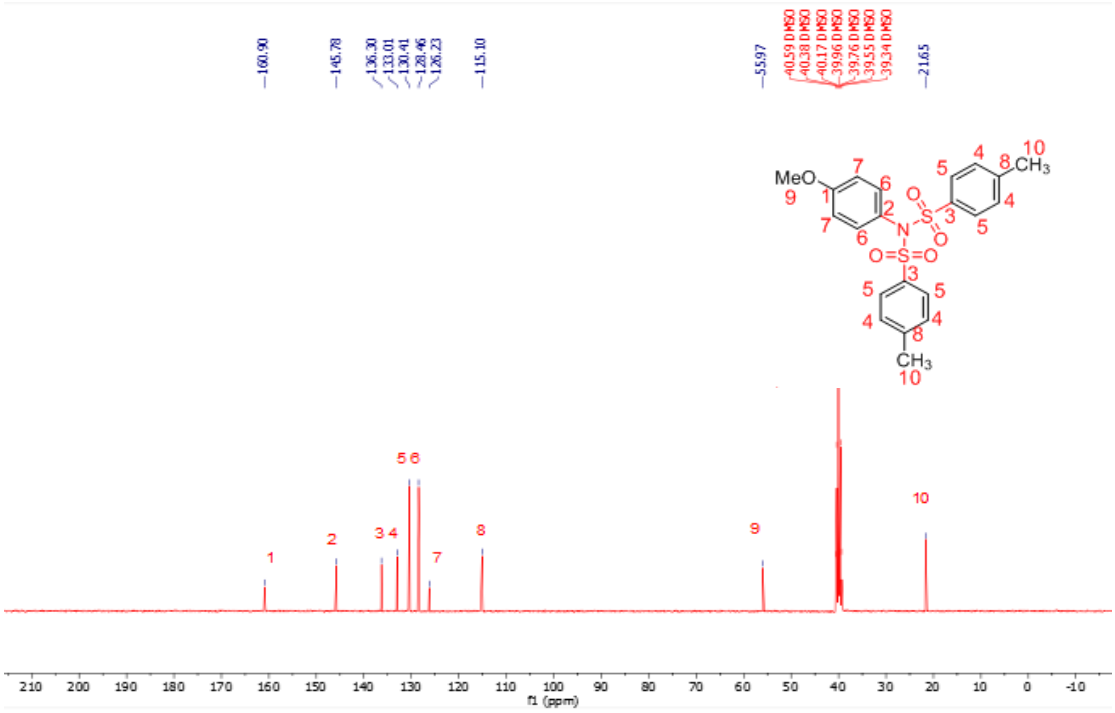

Figure 3.34: ^{13}C-NMR Spectrum of the compound B5.

The mass spectral data of the derivative B3 was referred to the correctness of the suggested structure of the above derivative as shown in **Table 3.8**, **Figure 3.35** and **Scheme 3.4**.

Table 3.8: Mass spectral data of B3.

Symbol	Molecular ion (M^+) m/z	The peaks m/z
B3	520.15	$[C_{21}H_{21}N_2O_2S]^{+\cdot}$ =365.15 $[C_{14}H_{14}N_2]^{+\cdot}$ =210.12 $[C_8H_{10}N]^{+\cdot}$ =120.08 $[C_7H_6]^{+\cdot}$ =90

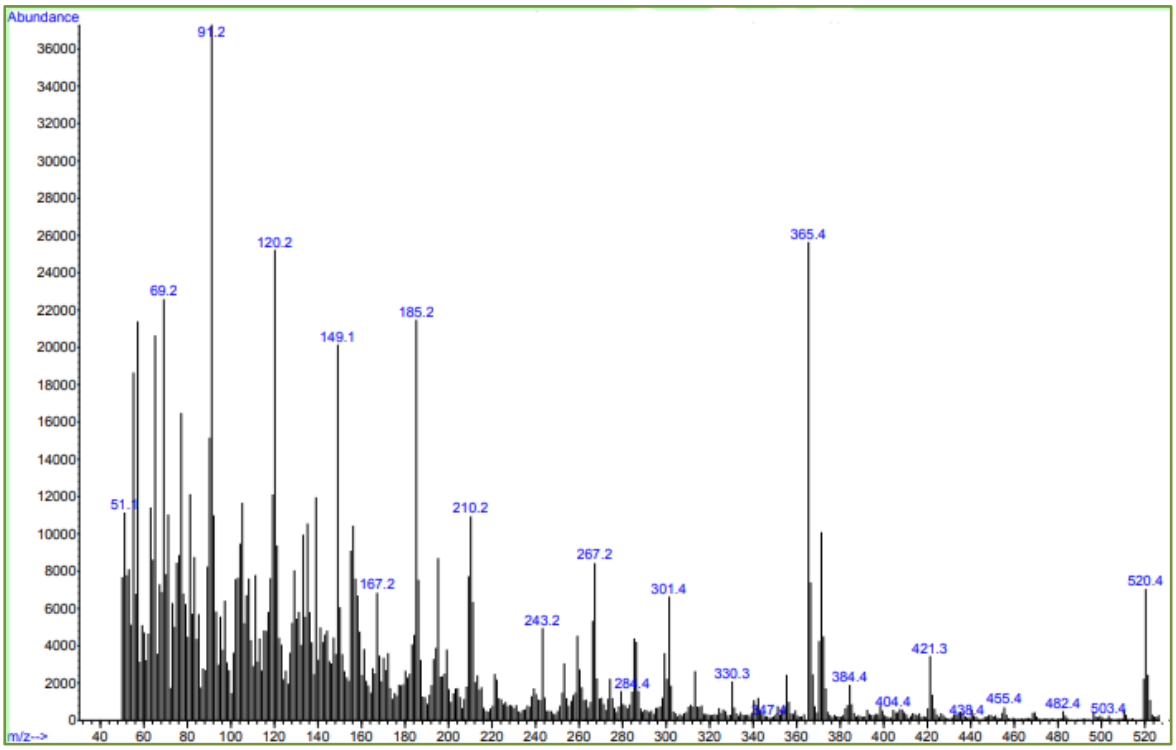

Figure 3.35: Mass Spectrum of B3.

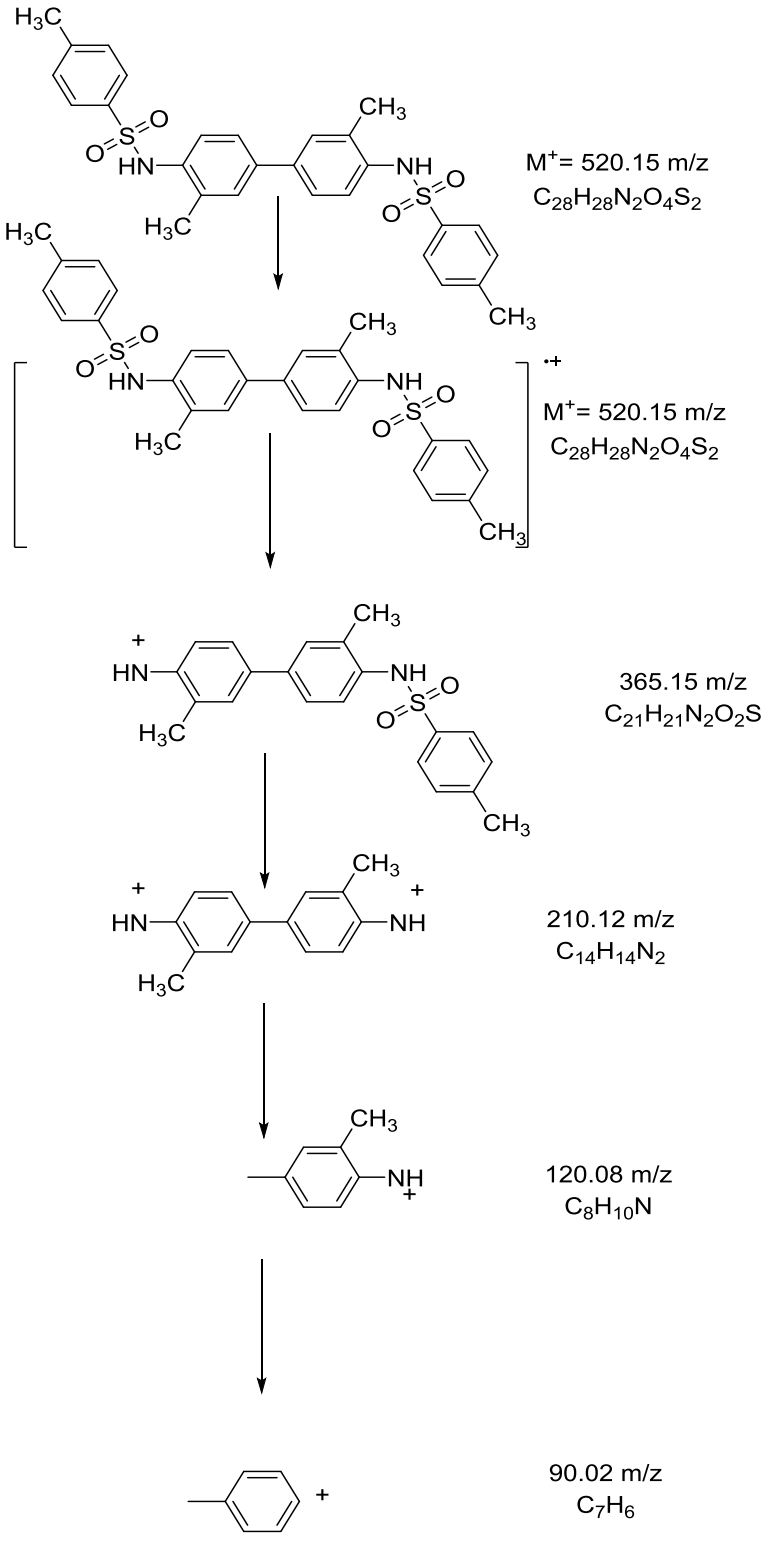

Scheme 3.4: Fragmentation of compound B3.

3.3. Synthesis of allyl derivatives C1-C3

The synthesis of allyl derivatives C1-C3 is achieved by mixing A1, B2, or o-tolidine with allyl bromide and potassium carbonate in acetone/H_2O **Equation 3.3** and **Scheme 3.3**.

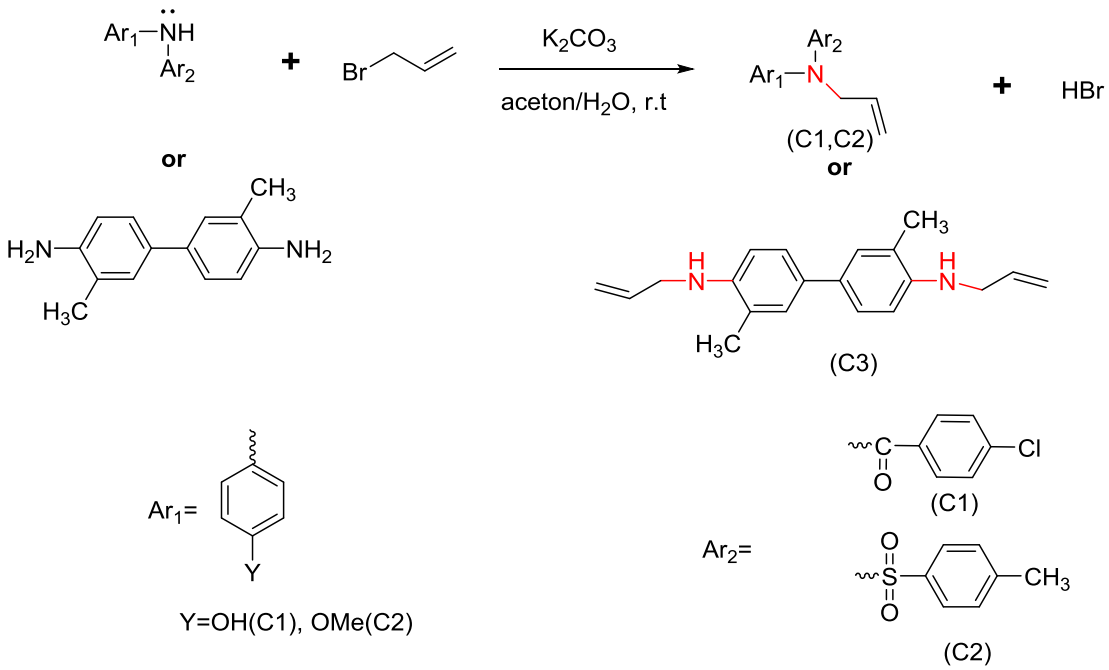

Equation 3.3: Synthesis of allyl derivatives C1-C3.

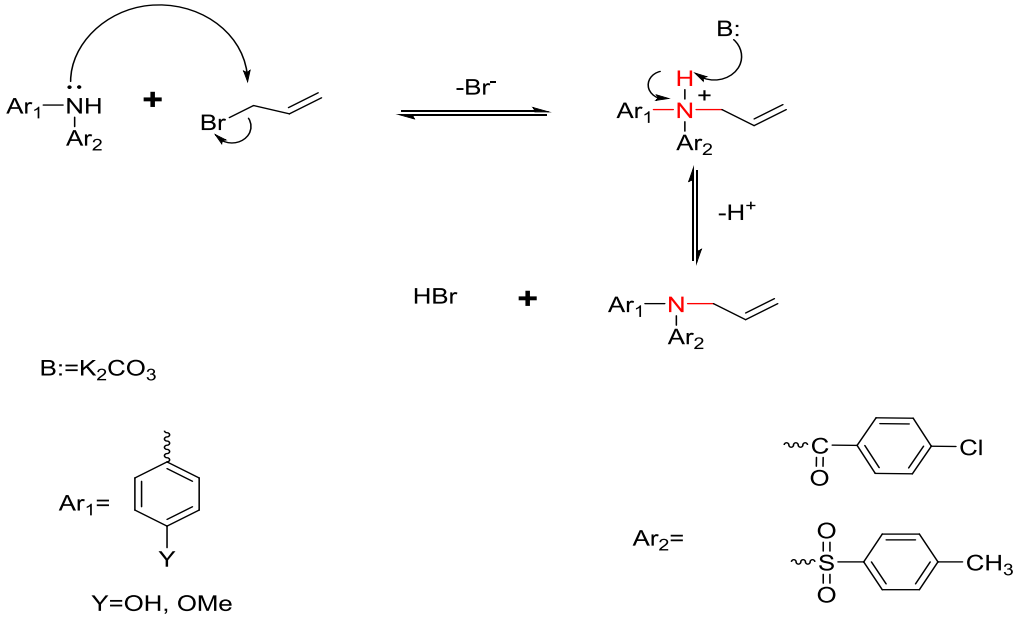

Scheme 3.5: Mechanism of synthesis of allyl derivatives C1-C3.

3.3.1. Characterization of the C1-C3

The derivatives C1-C3 were characterized by some physical measurements, such as melting point besides the spectroscopic techniques, IR, ^{1}H-NMR, ^{13}C-NMR and Mass spectroscopy.

The IR spectra of the derivatives C1-C3 are represented by ten bands which ascribed to the stretching vibrations of the -OH, -NH, aromatic C-H, Aliphatic C-H, C=O, C=C, S=O, C-O, C-N and C-X groups, which occurred within the ranges 3341.48, 3431.36, (3074.53-2921.19), (2920.23-2841.15), (1648.44), (1612.49-1508.33), (1487.32-1460.11), (1253.35-1249.87), (1096.07-1070.49), (822.13) cm^{-1} respectively, as show in Table (3.9) and in Figures (3.36-3.38).

Table 3.9: FT-IR spectral data of the stretching vibrations of C1-C3 cm^{-1}.

Symbol	-OH	-NH	CH Aromatic	CH Aliphatic (w)	C=O	C=C (s)	S=O (w)	C-O	C-N (w)	C-CI (s)
C1	3341.48 (s)	___	2921.19 (s)	2852.16	1648.44 (vs)	1538.81	1487.32	1253.35 (w)	1096.07	822.13
C2	___	___	3066.82-2926.01 (s)	2841.15		1508.33	1460.11	1249.87 (s)	1089.78	___
C3	___	3431.36 (br.)	3074.53-3012.81 (w)	2920.23 - 2852.72	___	1612.49	___	___	1070.49	___

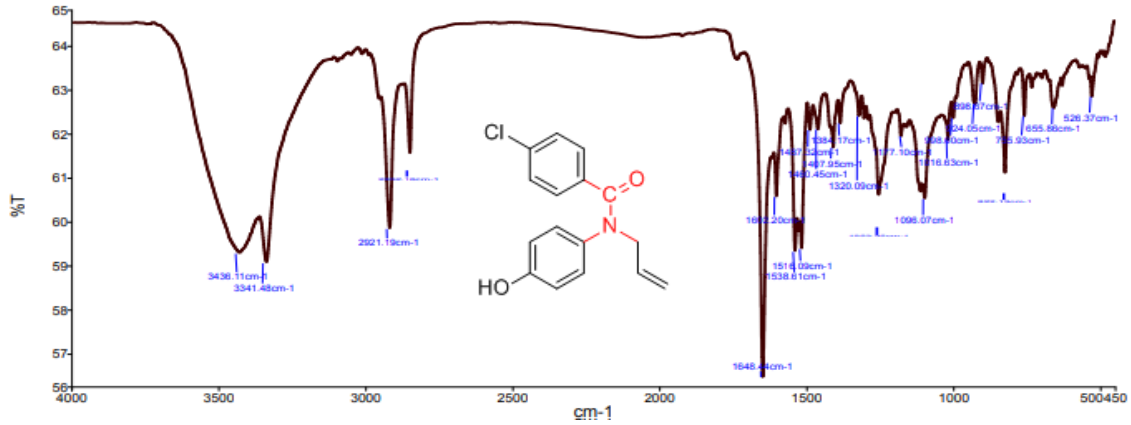

Figure 3.36: FT-IR spectrum of the compound C1.

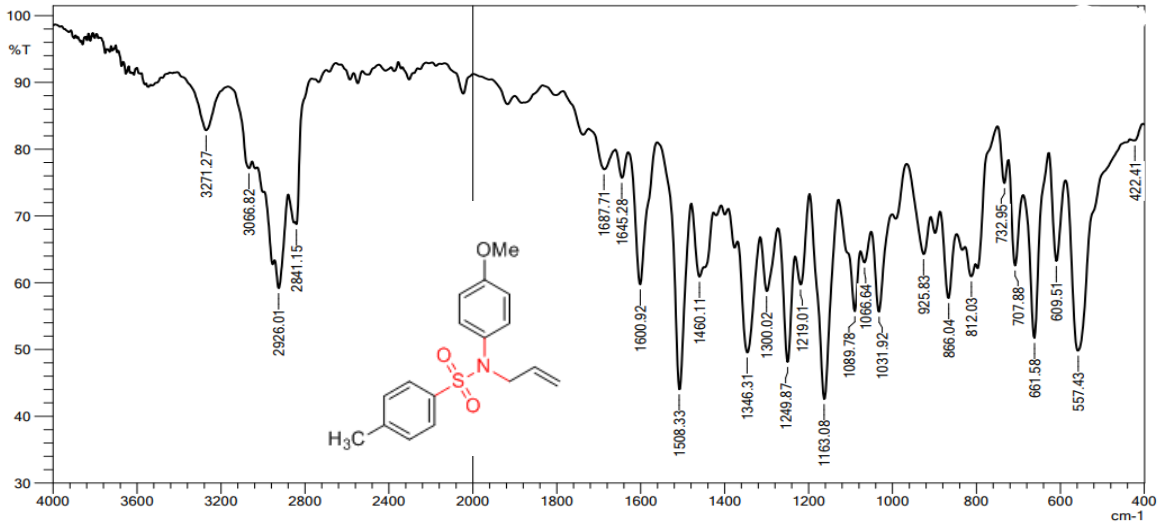

Figure 3.37: FT-IR spectrum of the compound C2.

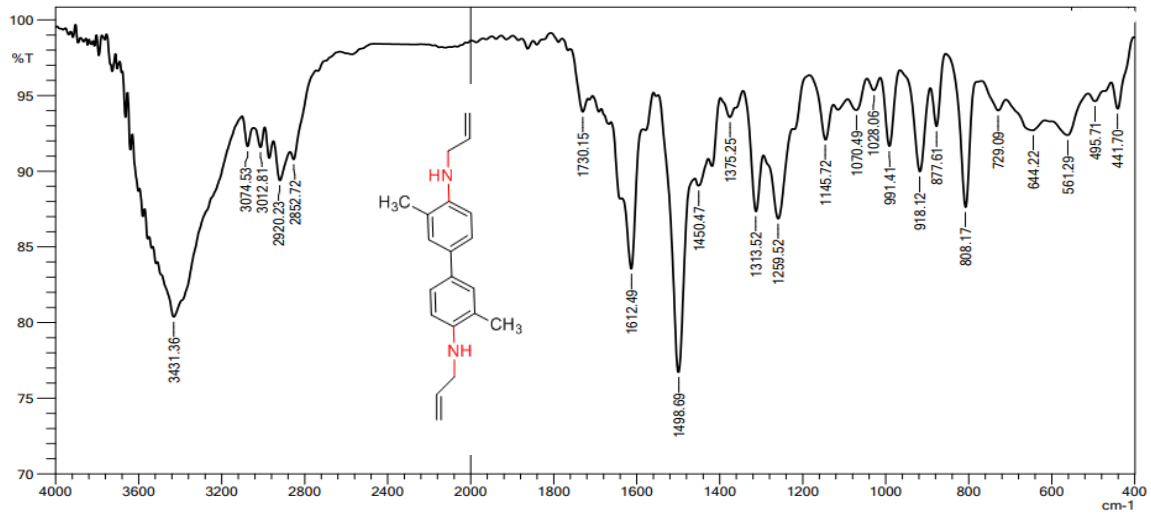

Figure 3.38: FT-IR spectrum of the compound C3.

^{1}H-NMR spectra of the derivatives (C1-C3) were identified by five signals as shown in Table (3.10) and Figures (3.39-3.41).

The range of the signals are 10.22 (-OH, s), 7.26 (-NH, s), 7.99-6.85 (Aromatic-H, m), allyl group showed three resonance signals, the first(a) is multiple in the range δ (6.07-5.65) ppm which belongs to the protons of the = CH group, the second (b) is doublet-doublet at the range δ (5.42-5.02) ppm which returns to the protons of the $=CH_2$ group and the third (c) is doublet in the range δ (4.56-3.57)ppm ascribes to the protons of the $-CH_2$ group which attached to the nitrogen atom, 3.73(OCH_3, s) and 2.51-2.40 (CH_3, s) ppm.

Table 3.10: ^{1}H-NMR spectral data of the C1-C3 ppm.

Symbol	-OH (s)	-NH (s)	Ar-H	$-CH_2-CH=CH_2$ c a b	O-CH_3 (s)	CH_3 (s)
C1	10.22	___	7.98(d,2H,J=8) 7.67(d,2H,J=8) 7.6(d,2H,J=8) 6.95(d,2H,J=8)	6.04 (m,1H,J=8) (a) 5.33(dd,2H,J=8) (b) 4.55(d,2H,J=8) (c)	___	___
C2	___	___	7.46(d,2H,J=8) 7.38(d,2H,J=8) 6.92(d,2H,J=8)	5.65(m,1H,J=8) (a) 5.06(dd,2H,J=8) (b) 4.13(d,2H,J=8) (c)	3.73	2.40
C3	___	7.26	7.41(S,1H) 7.34(d,2H,J=4) 7.07(d,2H,J=8)	5.78(m,1H,J=8)(a) 5.12(dd,2H,J=12 (b) 3.58(d,2H,J=4) (c)	___	2.51

s=singlet

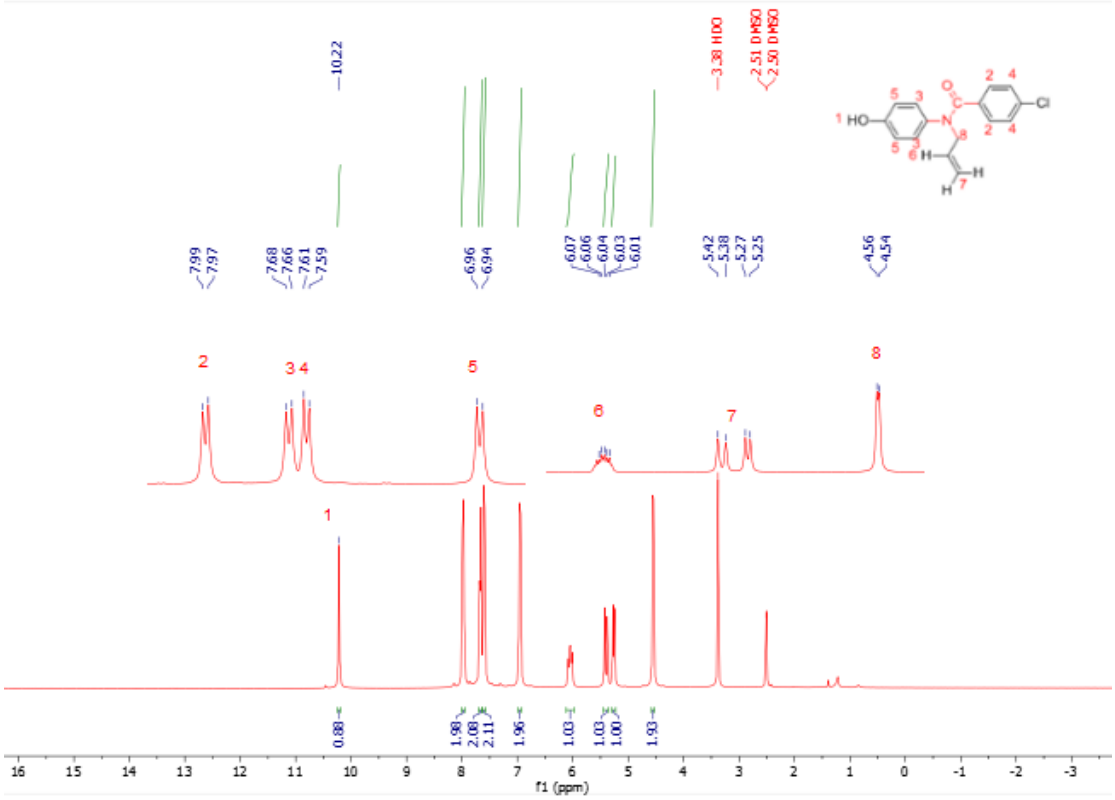

Figure 3.39: ^{1}H-NMR Spectrum of the compound C1.

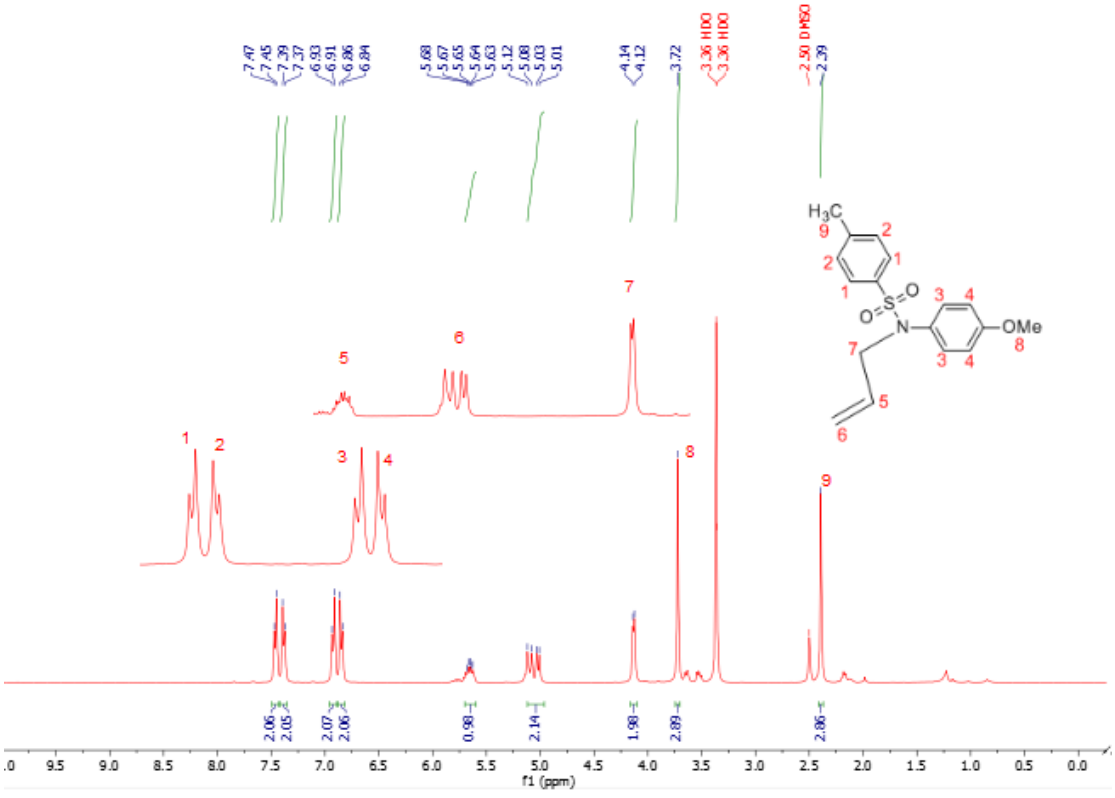

Figure 3.40: ^{1}H-NMR Spectrum of the compound C2.

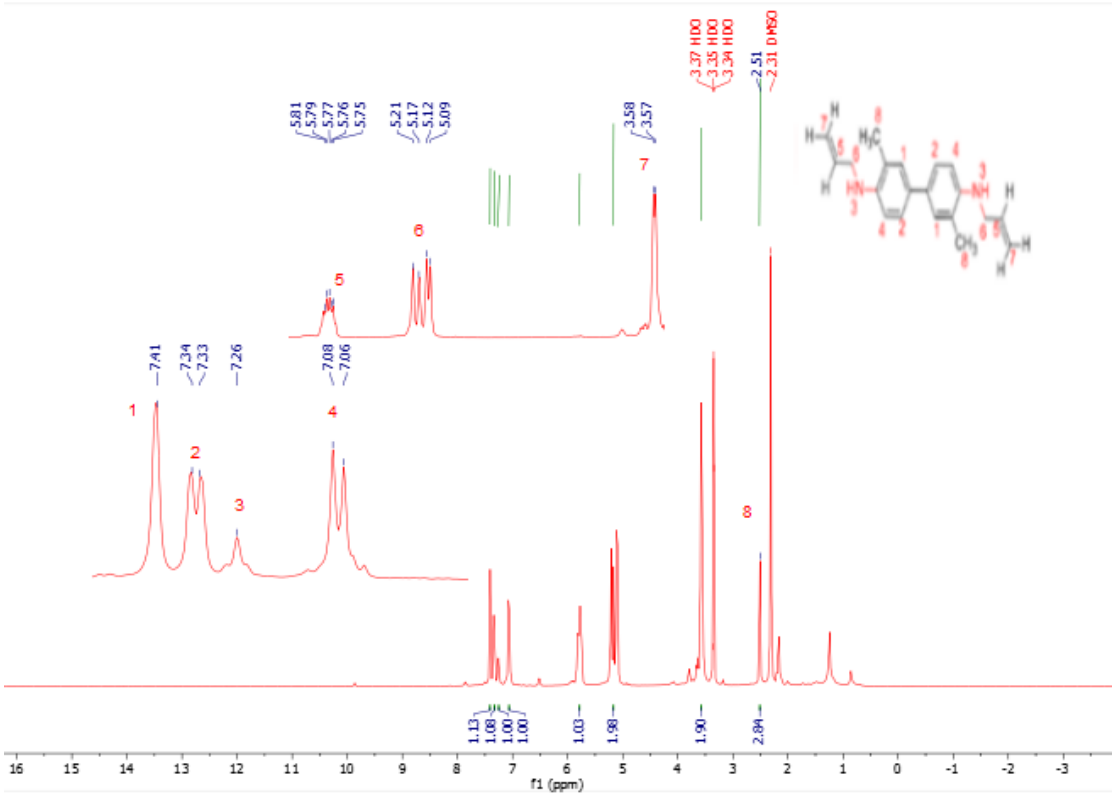

Figure 3.41: ^{1}H-NMR Spectrum of the compound C3.

Whereas the ^{13}C-NMR spectra of derivatives C1-C3 showed eight signals ascending 164.45(C=O), 158.86-155.01(C-O), 136.69(C-CI), 148.82-131.60(C-N), 134.93-114.45(Aromatic ring), 135.79-132.61(-CH), 122.43-117.83(=CH_2), 68.77-53.41(-CH_2), 55.70(OCH_3) and 21.50-18.74(CH_3) ppm as shown in **Table 3.11** and **Figures 3.42-3.44**.

Table 3.11: ^{13}C-NMR spectral data of the C1-C3 ppm.

Symbol	C=O	C-O	C-CI	C-N	Ar-C	-CH_2-CH=CH_2 c a b	-OCH_3	-CH_3
C1	164.45	155.01	136.69	134.18	129.99-115.03	132.61 (a) 117.83 (b) 68.77 (c)	___	___
C2	___	158.86	___	131.60	130.26-114.45	133.62 (a) 119.14 (b) 53.41 (c)	55.70	21.50
C3	___	___	___	148.82	134.93-117.66	135.79 (a) 122.43 (b) 55.58 (c)	___	18.74

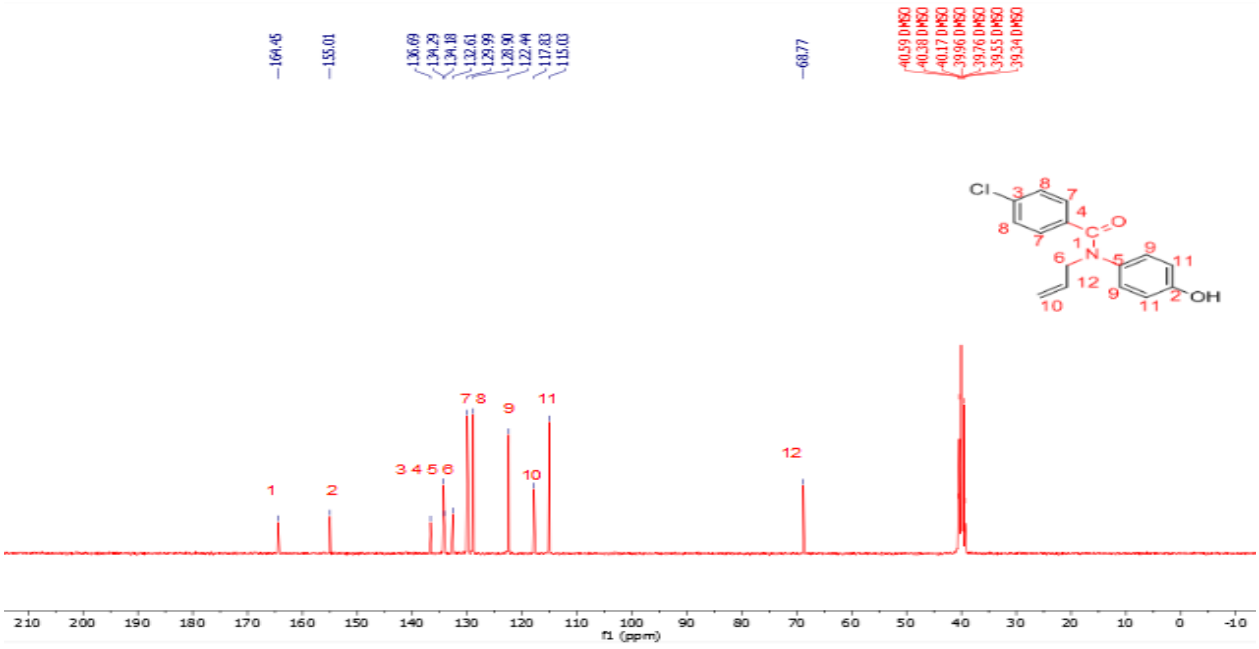

Figure 3.42: ^{13}C-NMR Spectrum of the compound C1.

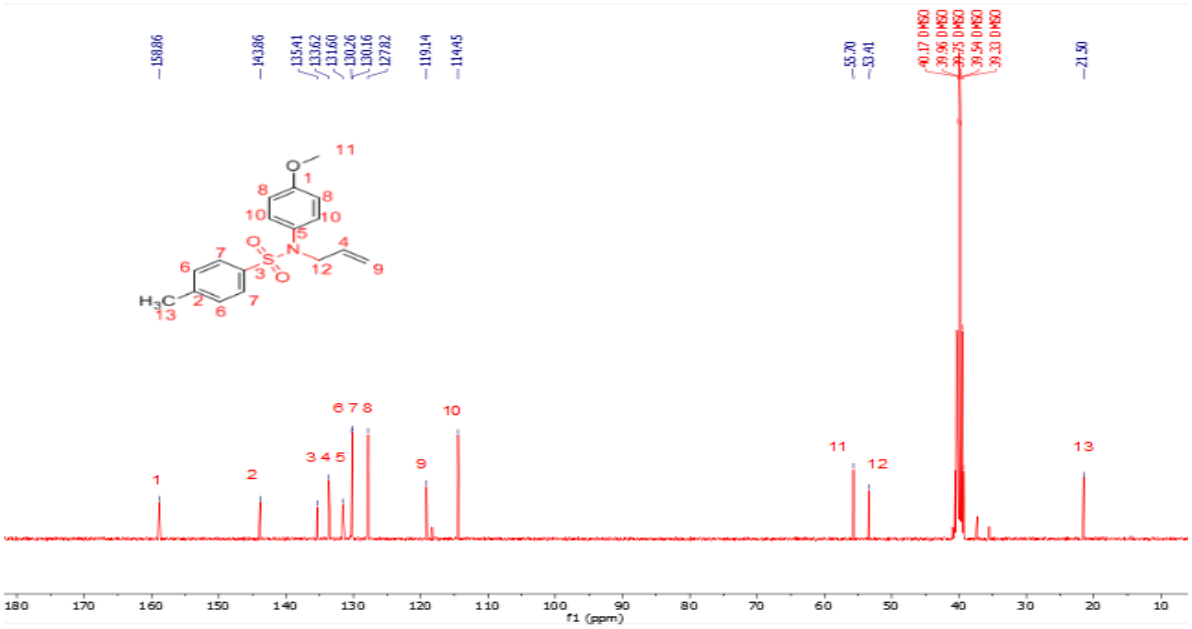

Figure 3.43: ^{13}C-NMR Spectrum of the compound C2.

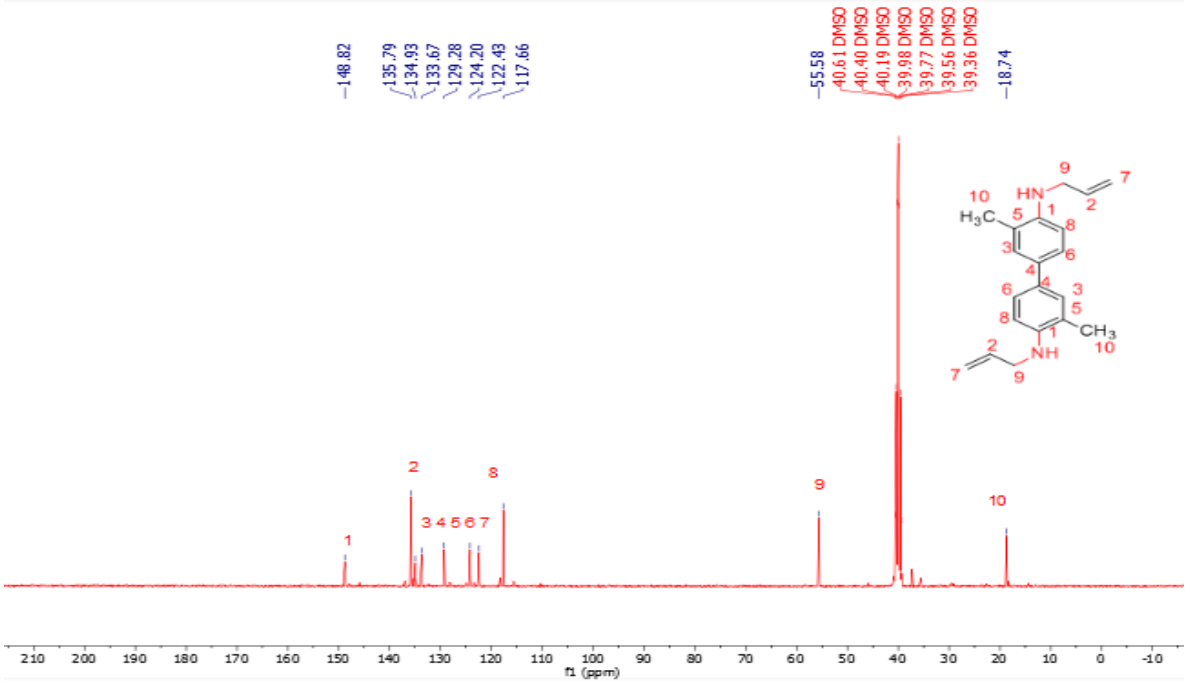

Figure 3.44: ^{13}C-NMR Spectrum of the compound C3.

The mass spectral data of C1 and C2 derivatives are explained in **Table 3.12**, **Figures 3.45, 3.46** and **Schemes 3.6, 3.7**.

Table 3.12: Mass spectral data of C1, C3.

Symbol	Molecular ion (M^+) m/z	The peaks m/z
C1	287.2	$[C_{13}H_9ClNO_2]^{+\cdot}$ = 246.03 $[C_7H_4ClO]^{+\cdot}$ =139 $[C_6H_4CI]^{+\cdot}$ =111 $[C_6H_4]^{+\cdot}$ =76
C3	292.19	$[C_{19}H_{22}N_2]^{+\cdot}$ = 278 $[C_{18}H20N_2]^{+\cdot}$ = 264 $[C_{17}H_{18}N_2]^{+\cdot}$ =250 $[C_{16}H_{17}N_2]^{+\cdot}$ =237 $[C_{15}H_{15}N_2]^{+\cdot}$ =224 $[C_{14}H_{12}N_2]^{+\cdot}$ =208 $[C_{13}H_{10}N_2]^{+\cdot}$ =194 $[C_{13}H_{10}N]^{+\cdot}$ =180 $[C_{12}H_7N]^{+\cdot}$ =165

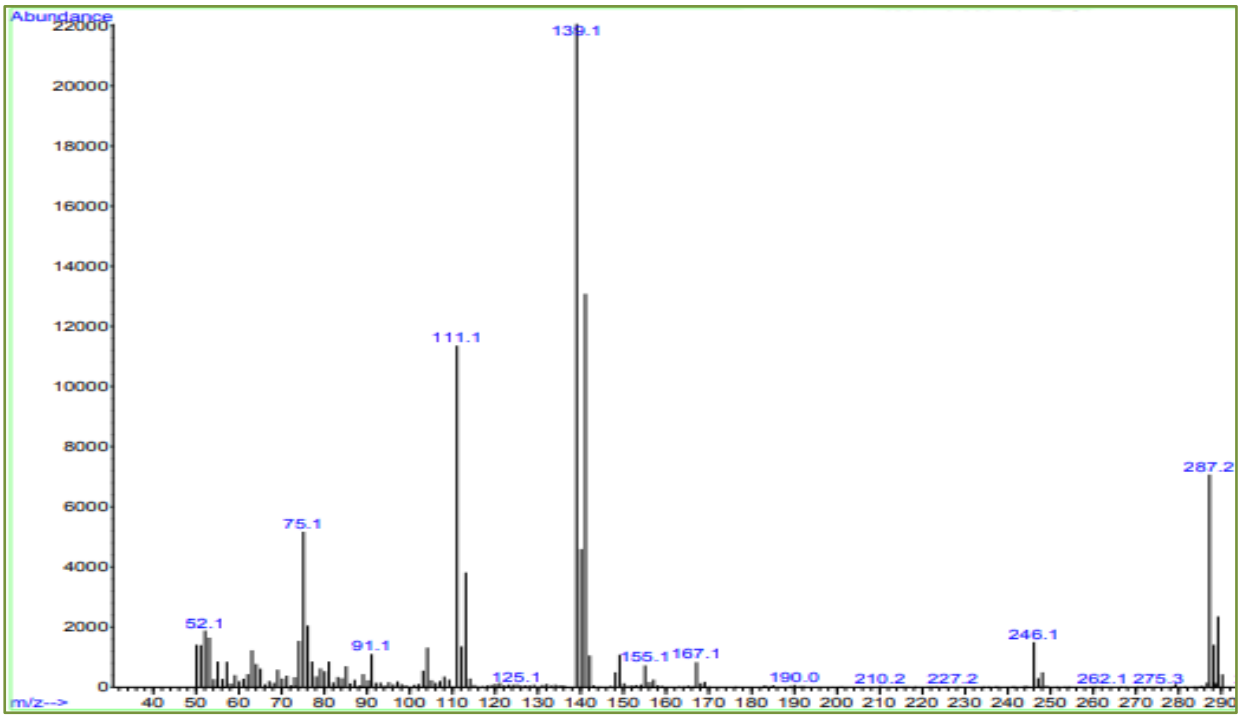

Figure 3.45: Mass spectrum of C1.

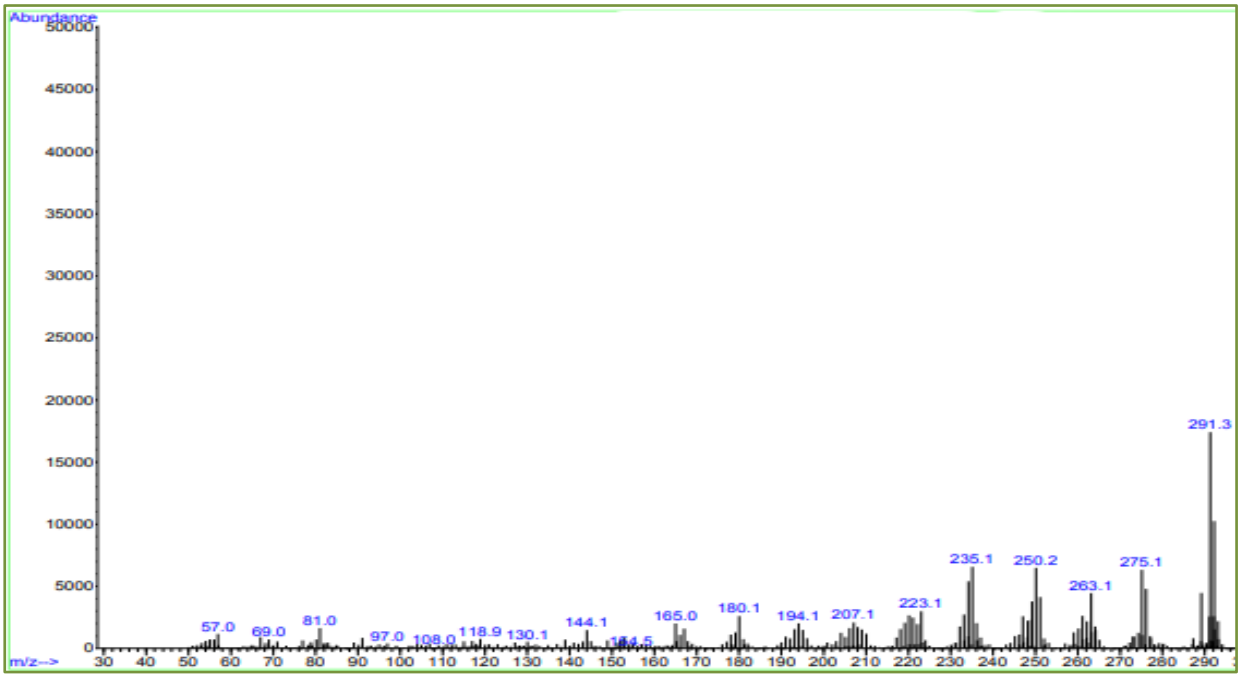

Figure 3.46: Mass spectrum of C3.

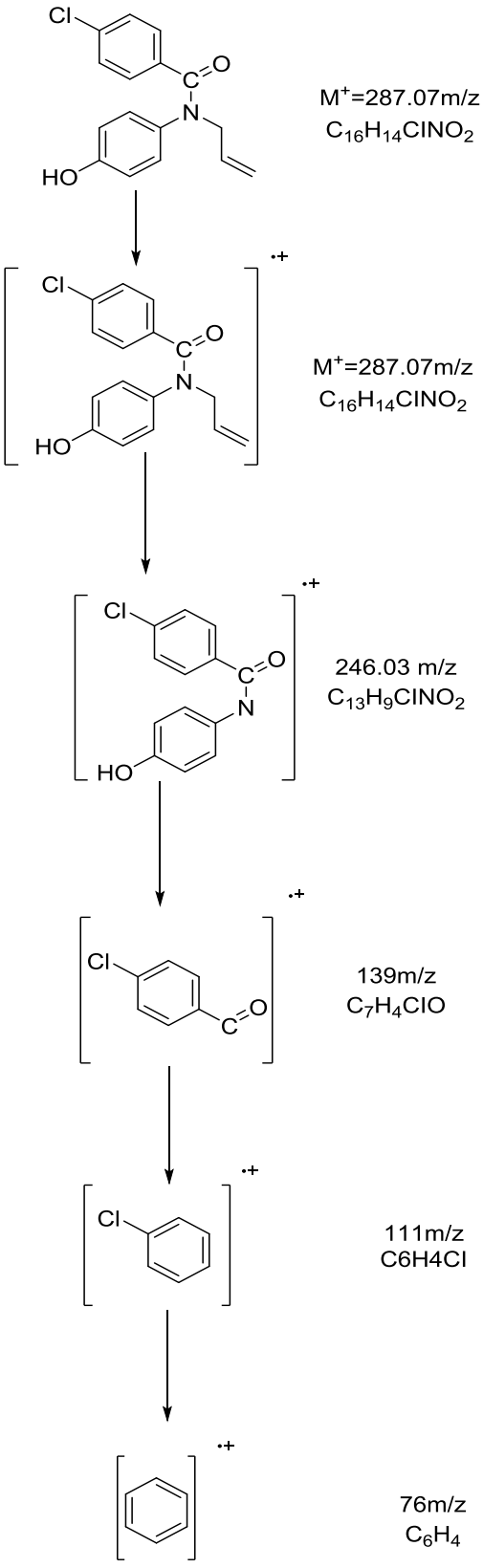

Scheme 3.6: Fragmentation of compound C1.

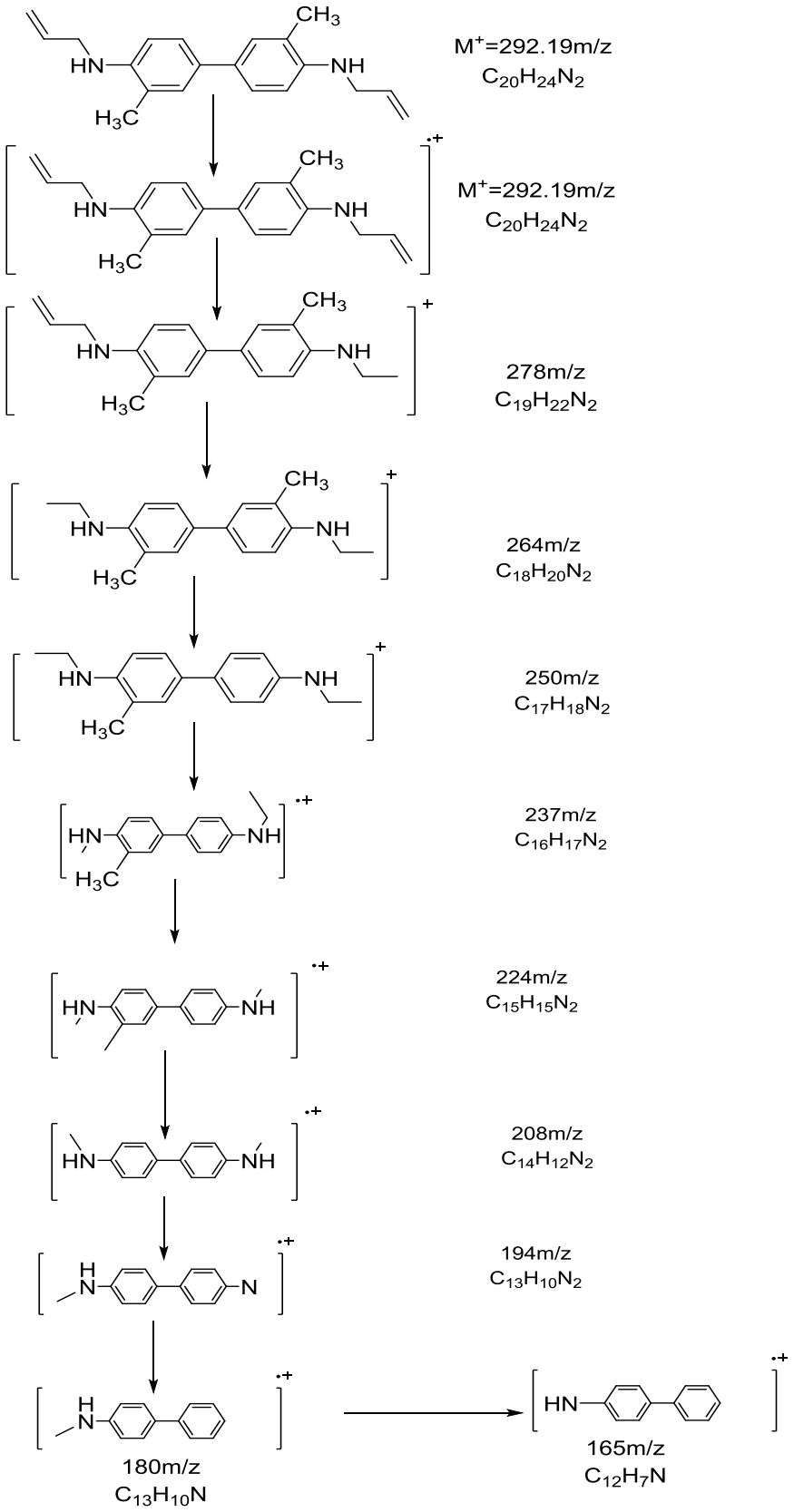

Scheme 3.7: Fragmentation of compound C3.

3.4. Molecular docking

The program (MOE 2015.10) was employed to analyze the capacity of compounds to inhibit breast cancer by coupling them with a single protein (PDB: 3eqm)[91,92] . The compounds (A1, A5, B2, B3, B5, C1) showed good activity via a group of factors[93, 94]:

1 .The correlation energy value.

2 .The binding number between the receptor (protein) and the ligand (compound).

3 .The correlation type and the (RMSD) value where less than 2 is better.

4 .How well the prepared ligand binds to the protein at its binding sites compared to the original ligand accessible to the protein?

3.4.1. Identification of protein targets for breast cancer

The human cytochrome P450 aromatase receptor protein (PDB ID: 3EQM) was obtained from the Protein Data Bank as shown in Figure 3.47. CMoleytochrome P450 aromatase is the only enzyme in vertebrates that catalyzes the production of all estrogens from androgens. Therefore, aromatase inhibitors are a first-line treatment for estrogen-dependent breast cancer. To prepare the protein, water molecules were removed while hydrogen atoms and cleaved amino acids were added[95, 96].

As shown in Table (3.13), several compounds showed good activity against the studied protein Compared to 4-Androstene-3-17-Dione as control in Figure 3.48.

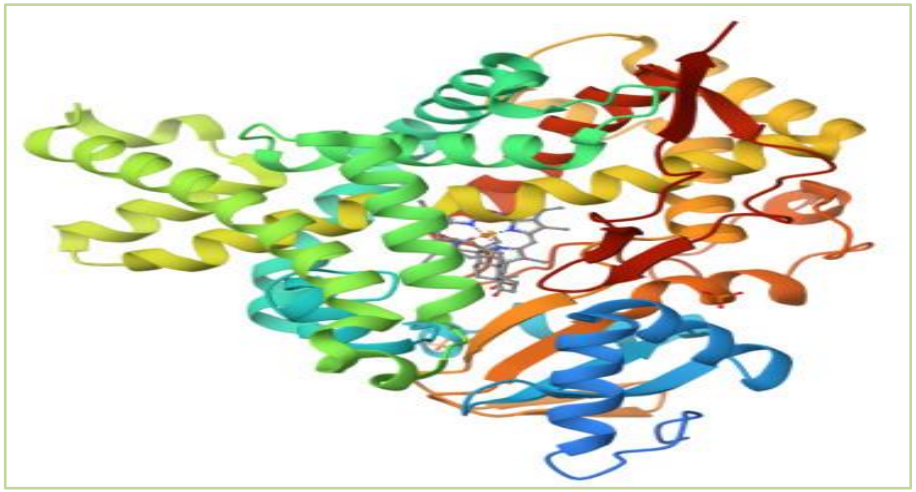

Figure 3.47: Human aromatase cytochrome P450 receptor protein (PDB ID: 3EQM).

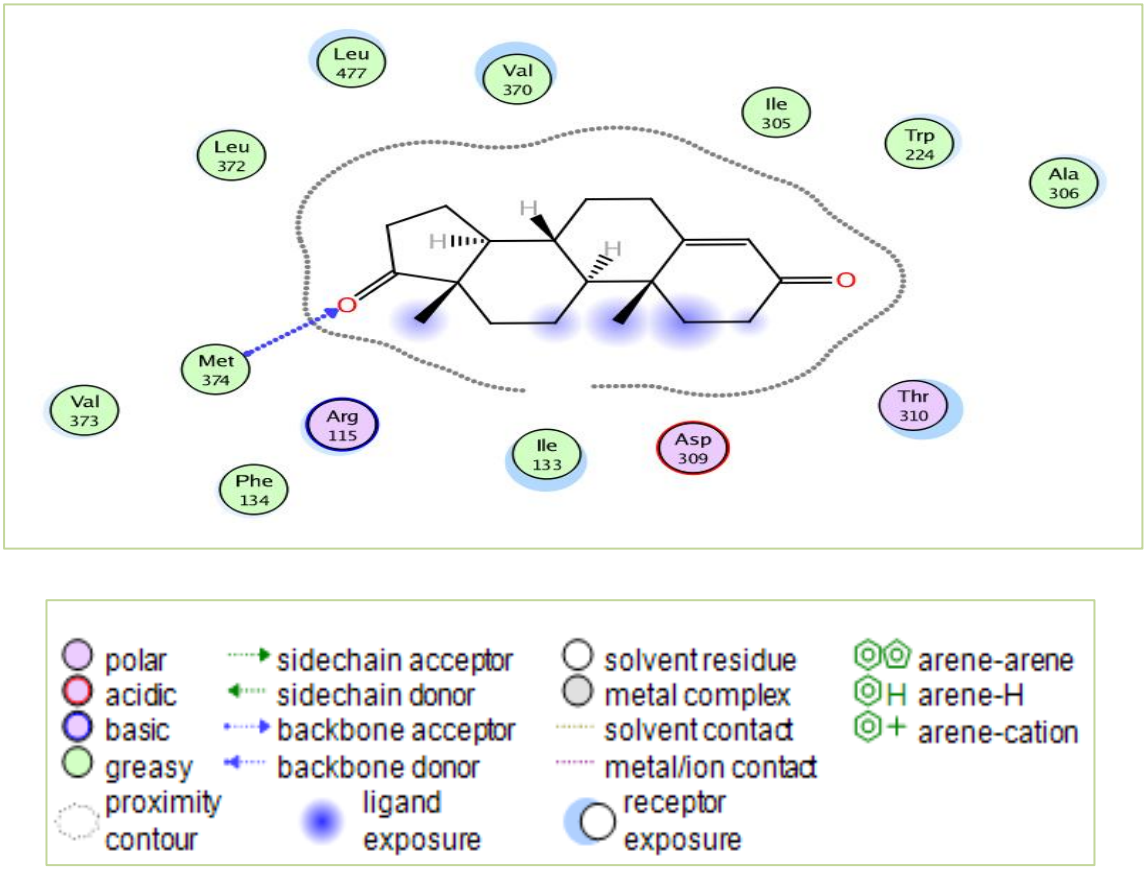

Figure 3.48: The binding poses of 4-Androstene-3-17-Dione on 3eqm.

Table 3. 13: Molecular docking for anti-cancer of the prepared derivatives.

Compound (Ligands)	Target protein: Oxidoreductase (3EQM)						
	E Binding (Kcal/mol)	RMSD	Position of interaction		Interaction	Distance (A^o)	E (Kcal/mol)
			Ligand	Receptor			
4-Androstene-3-17-Dione	-7.8994	1.5121	O (18)	N (MET 374)	H-acceptor	2.91	-2.7
A1	-7.0946	1.0495	O (7) O (10) Cl (17) 6-ring	O (PRO 429) SD (MET311) SD (MET303) CA (GLY 439)	H-donor H-donor H-donor Pi-H	3.21 3.68 3.80 4.16	- 0.8 - 0.9 - 0.7 - 1.0
A2	-7.7234	1.1507	Cl (16) 6-ring	NH_2 (ARG115 CB (CYS 437)	H-acceptor Pi-H	3.20 4.35	-0.9 -0.6
A3	-7.7245	1.9093	BR (7) Cl (17)	SD (MET 447) NH_2 (ARG 115)	H-donor H-acceptor	3.93 3.22	-0.3 -0.9
A4	-7.1083	1.4817	Cl (17)	NH_2 (ARG 115)	H-acceptor	3.22	-0.8
A5	-7.1083	1.4817	O (20) 6-ring 6-ring	SG (CYS 437) CA (VAL 373) CB (ALA 438)	H-donor Pi-H Pi-H	3.52 4.72 3.93	-1.4 -0.6 -0.6
A6	-8.4791	2.3946	Cl (26) Cl (25)	SD (MET 447) NH_2 (ARG 375)	H-donor H-acceptor	3.76 3.51	-0.2 -0.8
B1	-7.2851	2.5686	O (11)	N (MET 374)	H-acceptor	3.22	-1.8
B2	-7.3495	1.7967	O (9) O (10) 6-ring	N (ALA 438) NH_2 (ARG 115) CB (CYS 437)	H-acceptor H-acceptor Pi-H	3.52 3.11 3.86	-0.6 -0.8 -0.6
B3	-10.3703	1.4371	N (14) O (19) O (20) O (22)	OG1 (THR 310) SD (MET 311) SG (CYS 437) CA (VAL 373)	H-donor H-donor H-donor H-acceptor	2.73 3.08 3.14 3.44	-4.1 1.1 0.4 -0.7
B4	-8.8628	3.2356	6-ring 6-ring	CB (ALA 306) CB (CYS 437)	Pi-H Pi-H	4.18 3.81	-0.7 -0.9

B5	-9.2270	1.0951	O (19) O (20) 6-ring 6-ring	CA (CYS 437) NH_2 (ARG 115) CA (VAL 373) CB (ALA 438)	H-acceptor H-acceptor Pi-H Pi-H	3.35 2.95 4.69 4.04	-0.8 -1.5 -0.6 -0.9
C1	-7.2247	1.2386	O (10) 6-ring 6-ring	N (GLY 439) CB (ALA 306) N (ALA 438)	H-acceptor Pi-H Pi-H	2.82 3.83 4.20	-4.0 -0.7 -0.7
C2	-8.4408	0.8845	6-ring 6-ring	CG1 (ILE 133) N (ALA 438)	Pi-H Pi-H	3.94 4.49	-0.7 -0.9
C3	-9.8786	0.7349	6-ring	CA (GLY 439)	Pi-H	4.56	-0.6

3.4.2. Discussion of molecular docking

Molecular docking and some of the other in silico prediction techniques are widely used to understand the ligand receptor interactions during drug discovery process.

The results were good for the studied compounds in Figures 3.49-3.62, as the Score values ranged between (-10.3703_ -7.0946 Kcal/mol). The most important bonds formed are hydrogen bonds, which are important in enzymatic catalysis of reactions that occur inside the body and are essential bonds in maintaining the structural stability of biological molecules. The RMSD values for most of the studied compounds did not exceed 2.

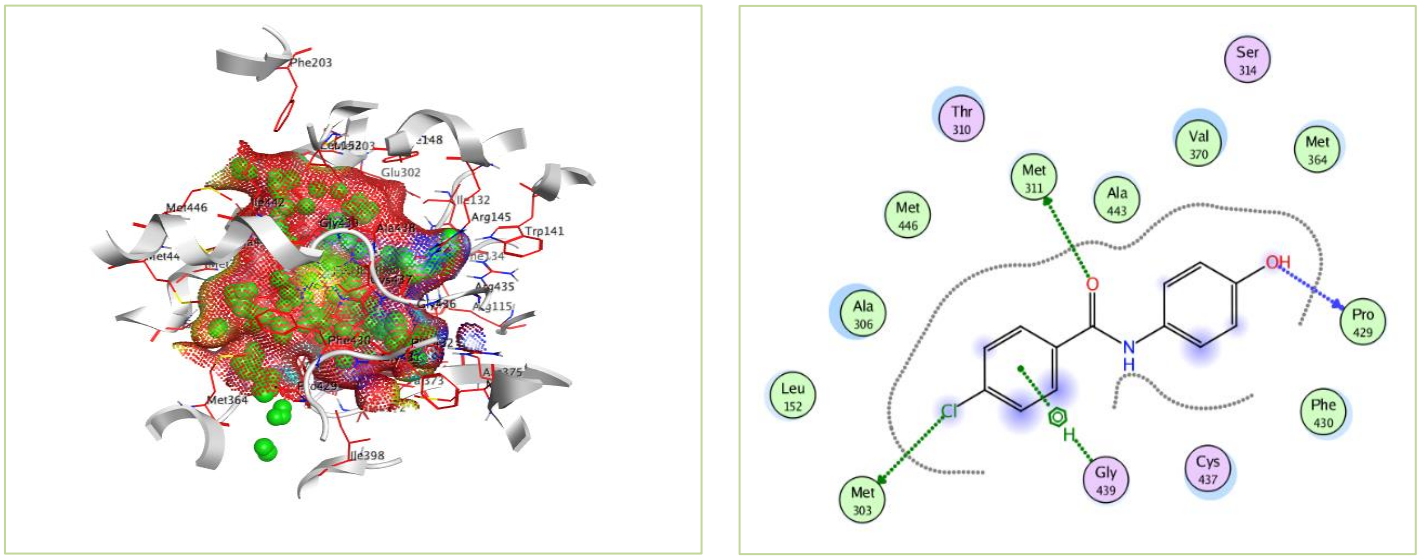

(A) (B)

Figure 3.49: Compound A1 docking: (A) in protein pocket, (B) 2D shape showing the binding sites of the (A1) with the protein (PDB: 3EQM).

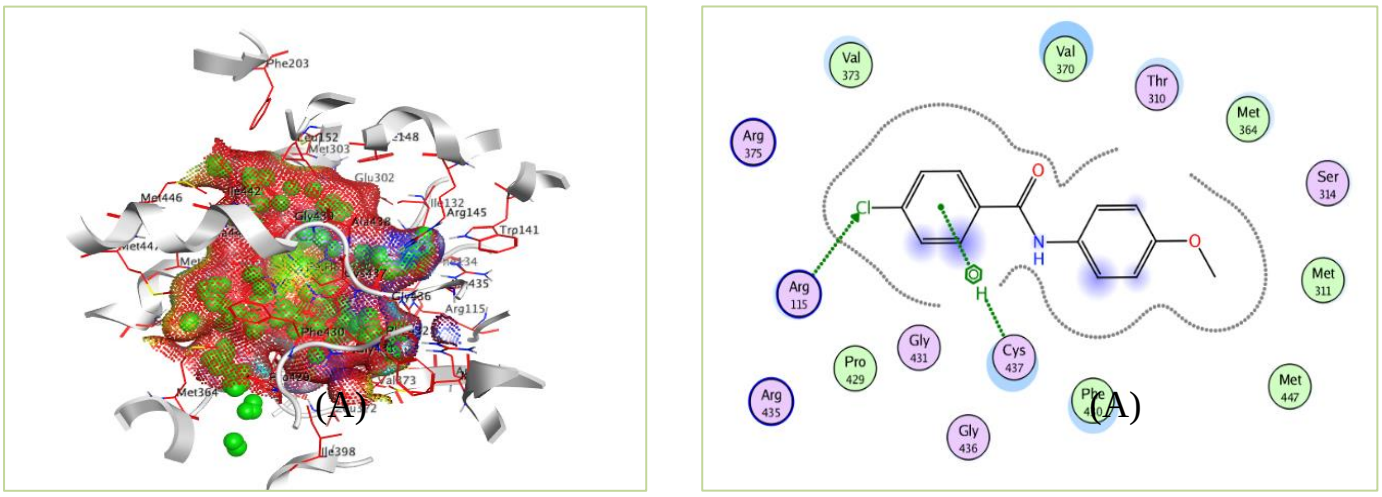

(A) (A)

Figure 3.50: Compound A2 docking: (A) in protein pocket, (B) 2D shape showing the binding sites of the (A2) with the protein (PDB: 3EQM).

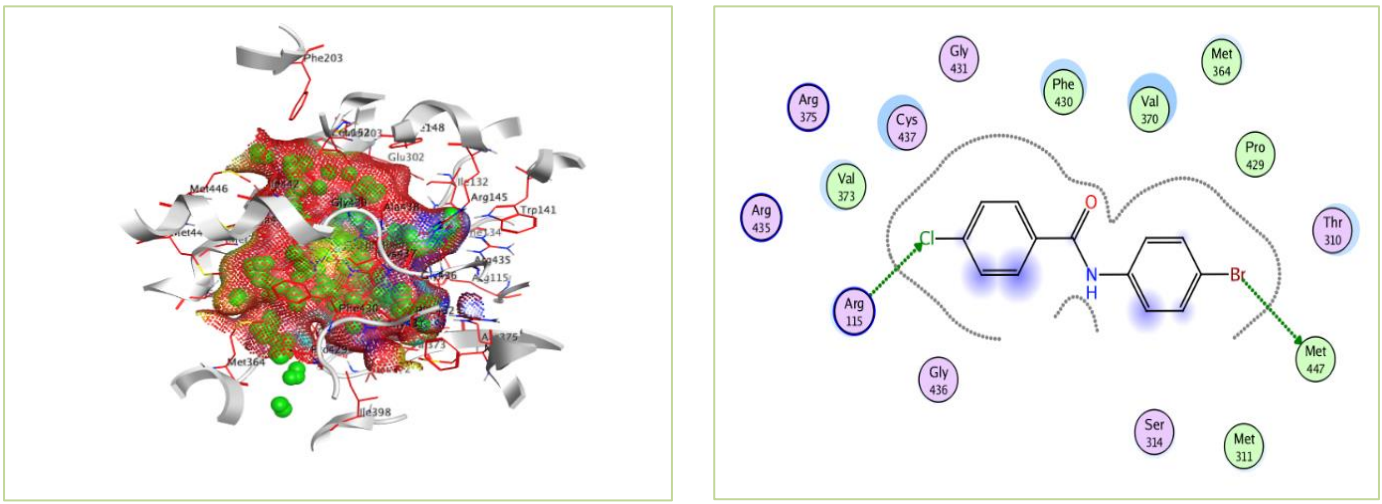

(A) (B)

Figure 3.51: Compound A3 docking: (A) in protein pocket, (B) 2D shape showing the binding sites of the (A3) with the protein (PDB: 3EQM).

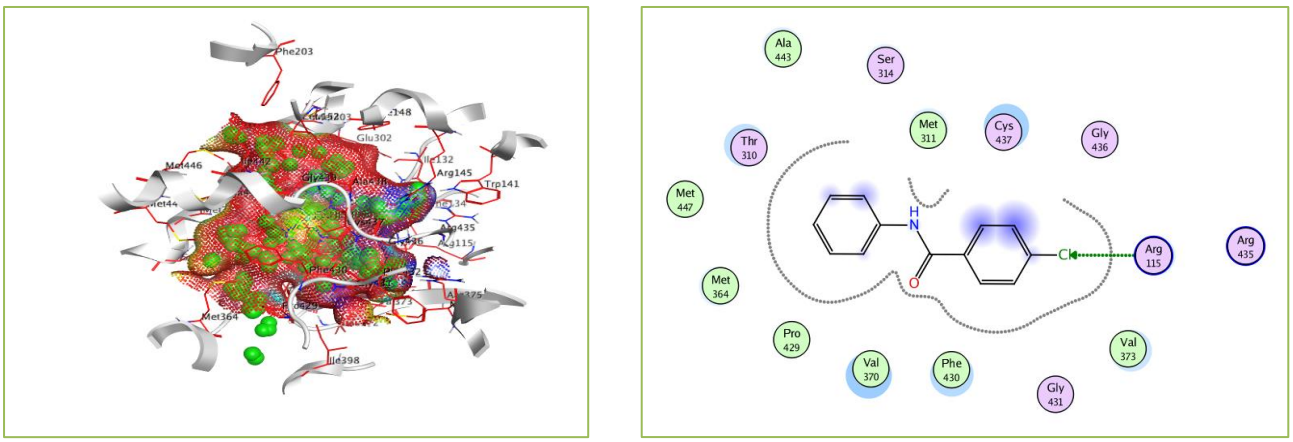

(A) (B)

Figure 3.52: Compound A4 docking: (A) in protein pocket, (B) 2D shape showing the binding sites of the (A4) with the protein (PDB: 3EQM).

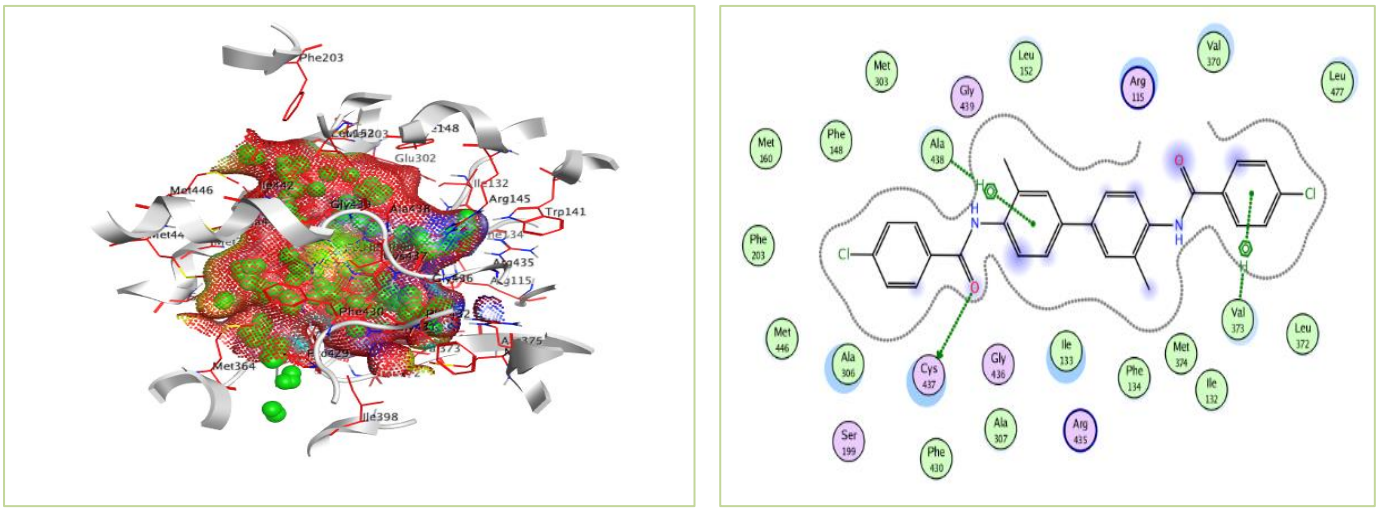

(A) (B)

Figure 3.53: Compound A5 docking: (A) in protein pocket, (B) 2D shape showing the binding sites of the (A5) with the protein (PDB: 3EQM).

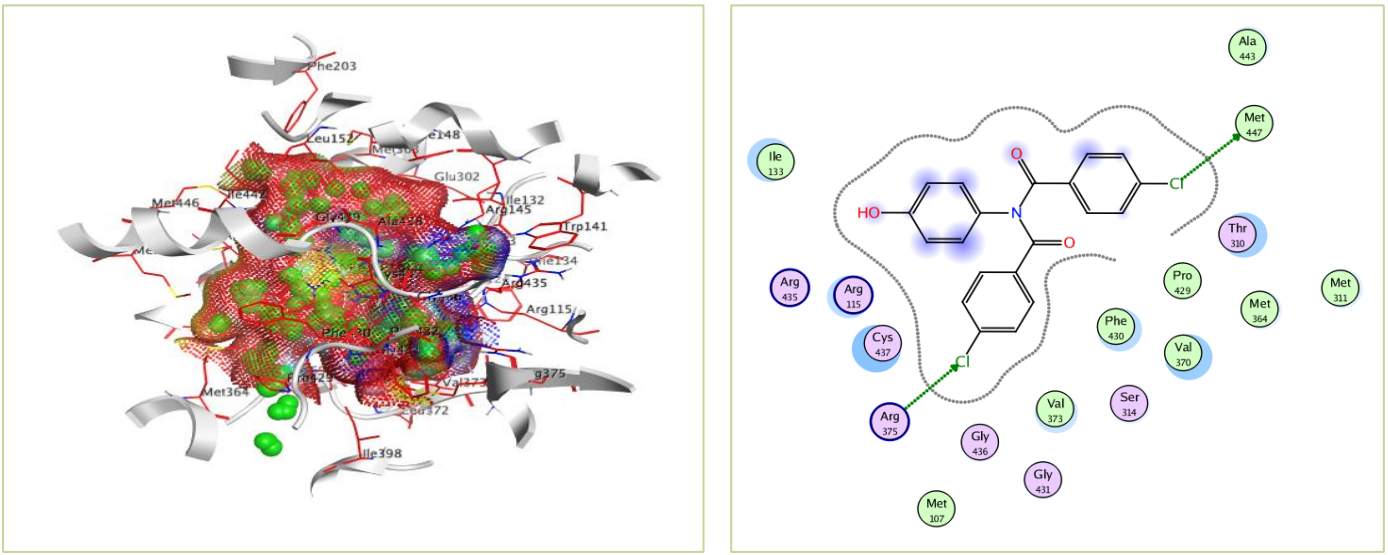

(A) (B)

Figure 3.54: Compound A6 docking: (A) in protein pocket, (B) 2D shape showing the binding sites of the (A6) with the protein (PDB: 3EQM).

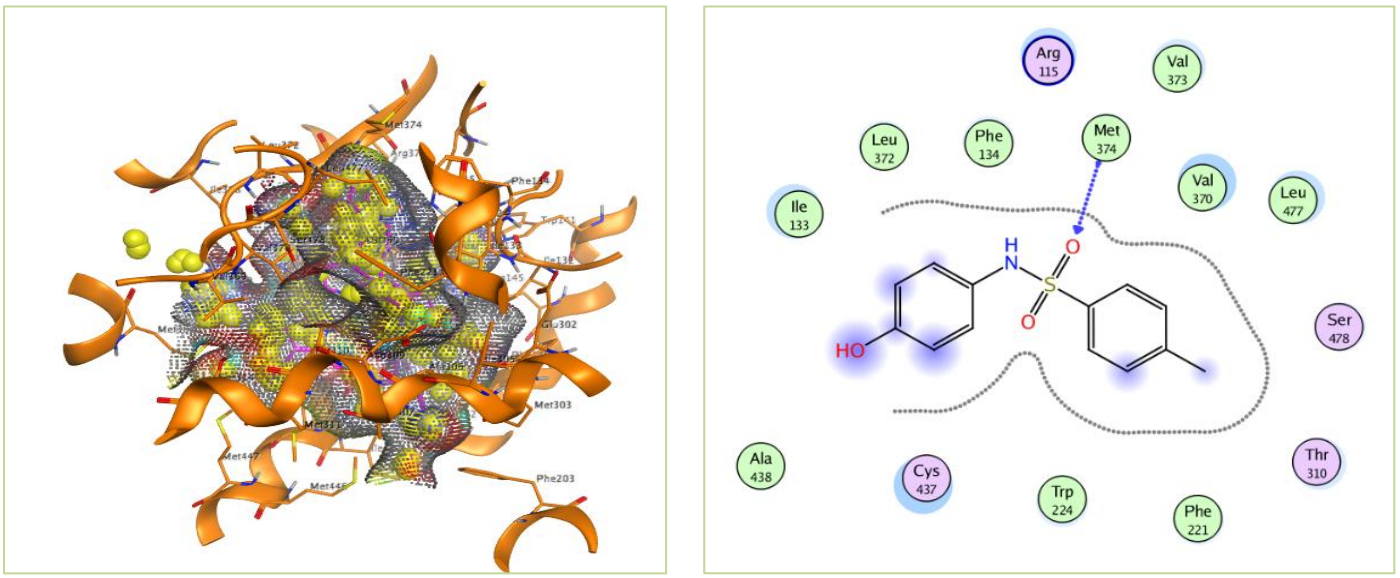

(A) (B)

Figure 3.55: Compound B1 docking: (A) in protein pocket, (B) 2D shape showing the binding sites of the (B1) with the protein (PDB: 3EQM).

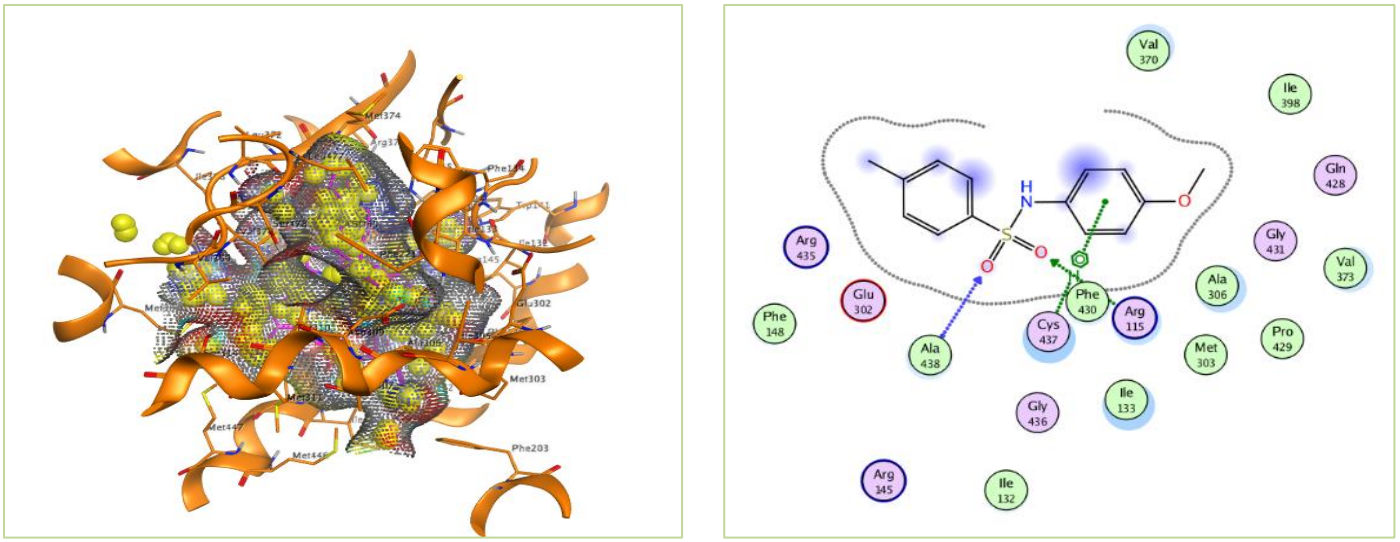

(A) (B)

Figure 3.56: Compound B2 docking: (A) in protein pocket, (B) 2D shape showing the binding sites of the (B2) with the protein (PDB: 3EQM).

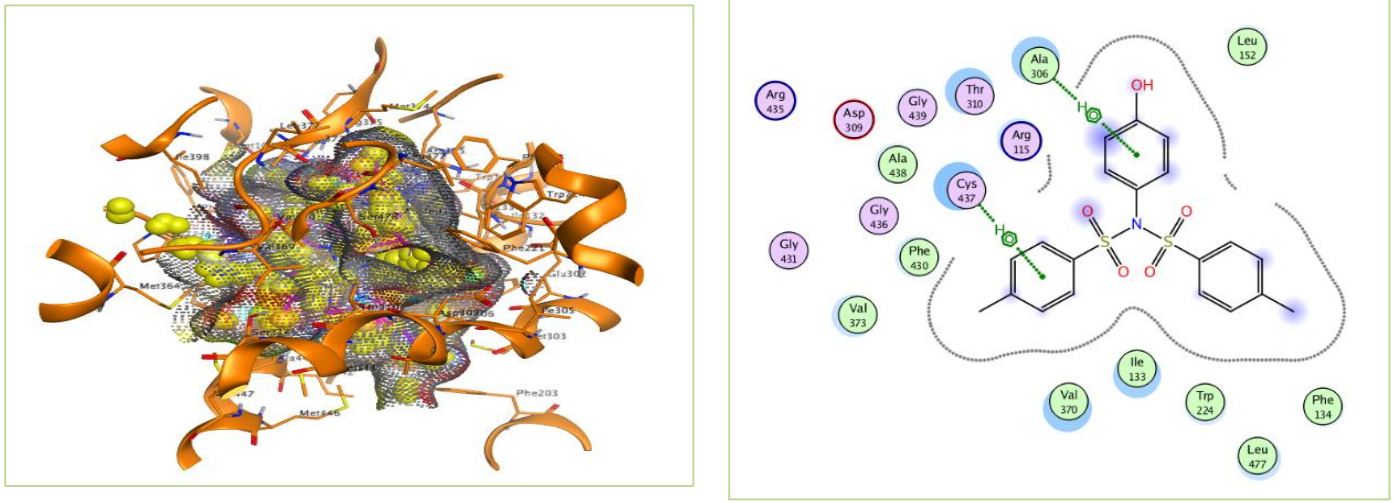

(A) (B)

Figure 3.57: Compound B3 docking: (A) in protein pocket, (B) 2D shape showing the binding sites of the (B3) with the protein (PDB: 3EQM).

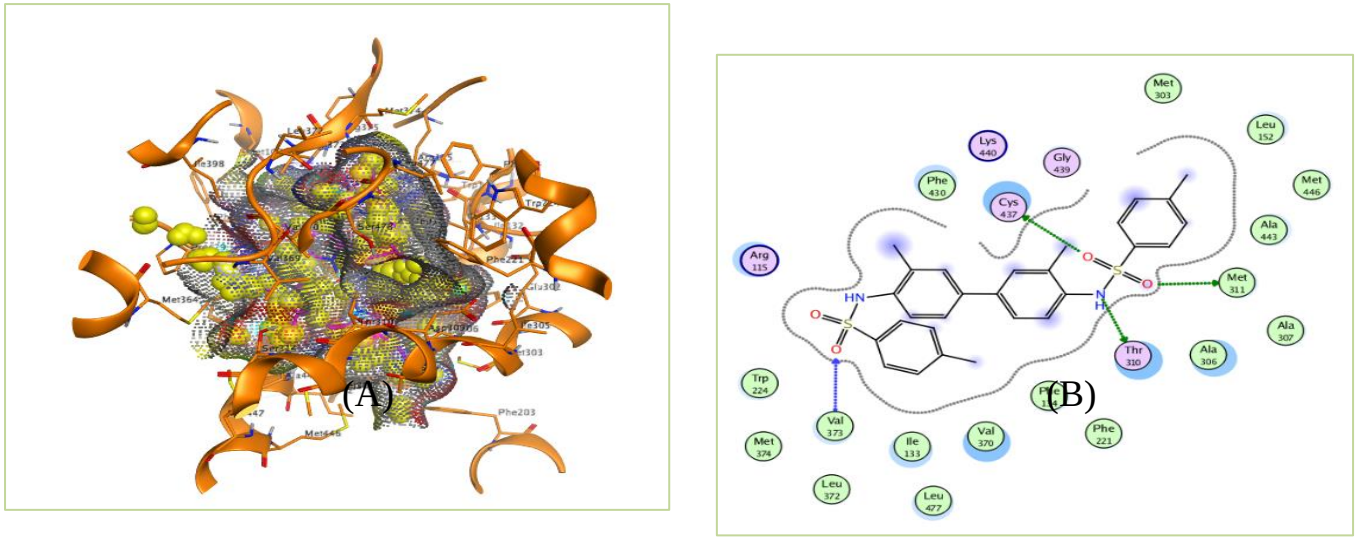

(A) (B)

Figure 3.58: Compound B4 docking: (A) in protein pocket, (B) 2D shape showing the binding sites of the (B4) with the protein (PDB: 3EGM).

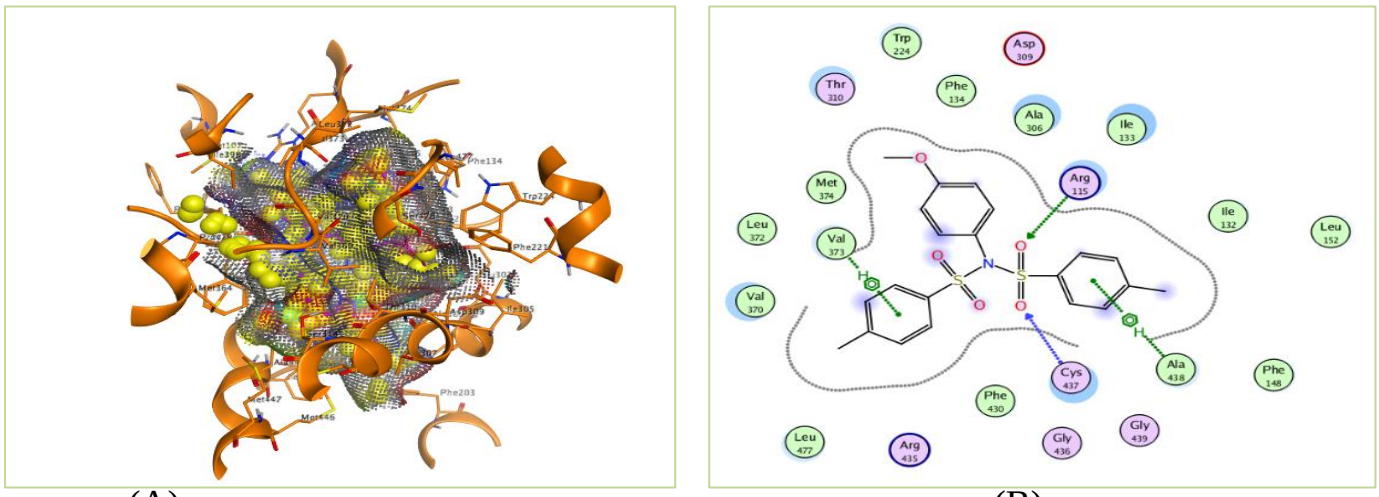

(A) (B)

Figure 3.59: Compound B5 docking: (A) in protein pocket, (B) 2D shape showing the binding sites of the (B5) with the protein (PDB: 3EQM).

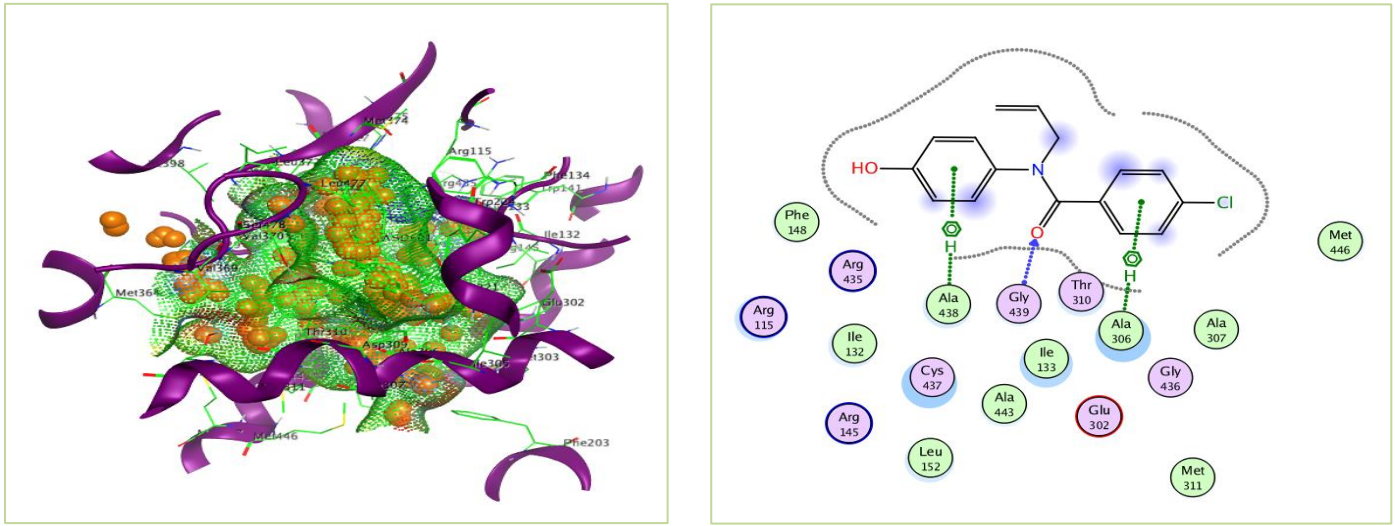

(A) (B)

Figure 3.60: Compound C1 docking: (A) in protein pocket, (B) 2D shape showing the binding sites of the (C1) with the protein (PDB: 3EQM).

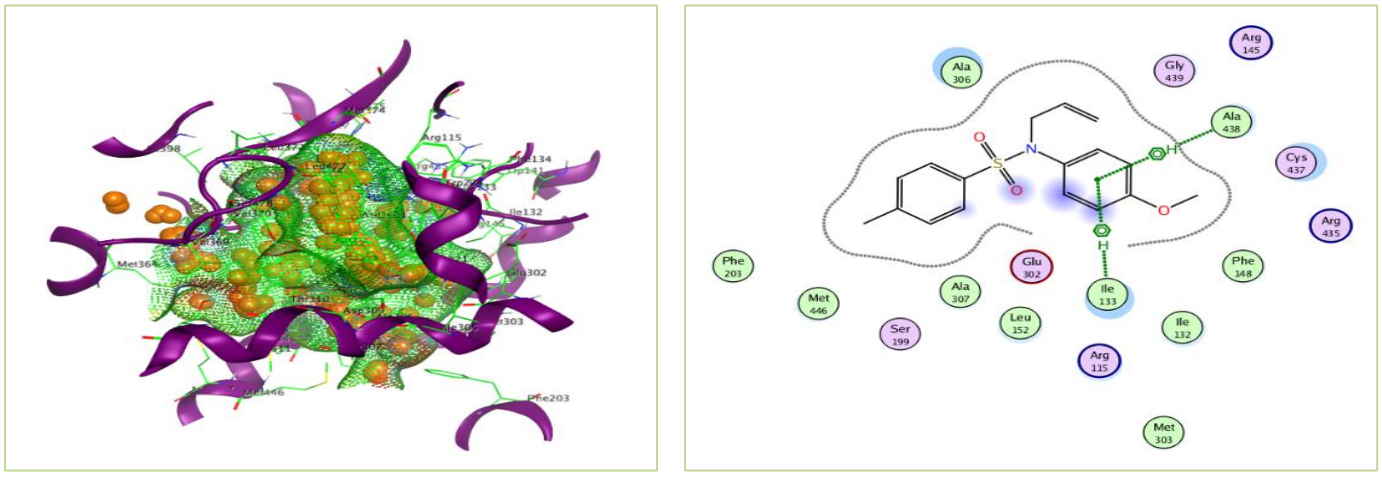

(A) (B)

Figure 3.61: Compound C2 docking: (A) in protein pocket, (B) 2D shape showing the binding sites of the (C2) with the protein (PDB: 3EQM).

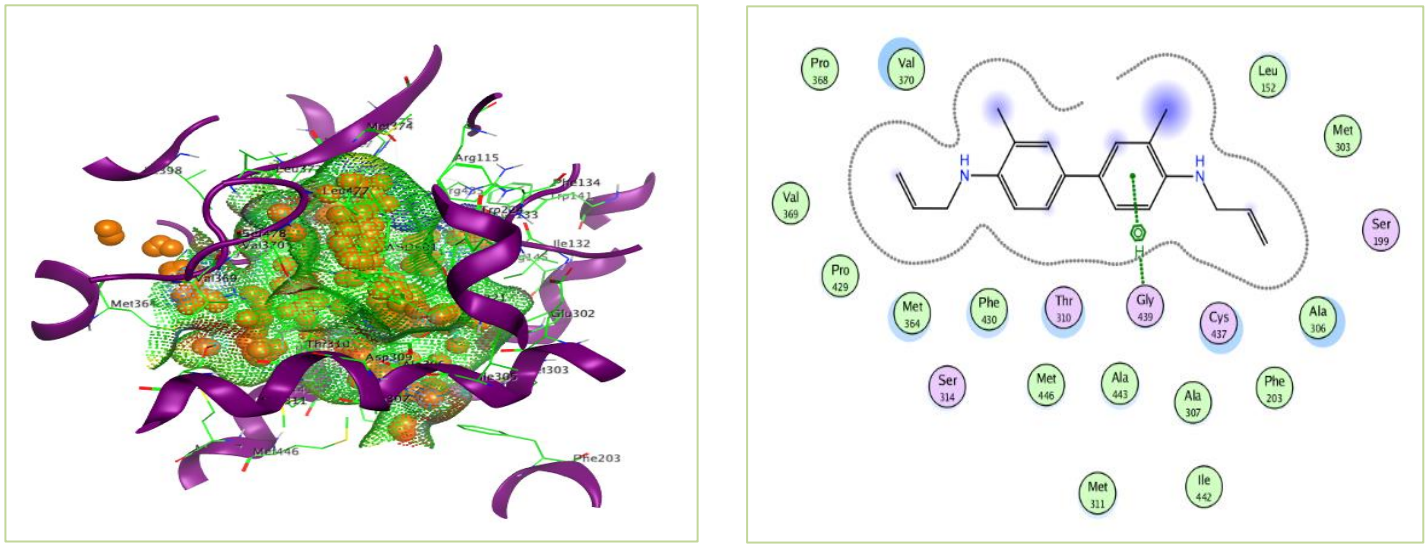

(A) (B)

Figure 3.62: Compound C3 docking: (A) in protein pocket, (B) 2D shape showing the binding sites of the (C3) with the protein (PDB: 3EQM).

3.5. Biological Activity

3.5.1. The cytotoxic activity of (A1, A2, A3, A4, A5, B4, B5) against human breast cancer cells line (MCF-7) in Vitro Using MTT Assay.

In widely used, the concept of IC_{50} is perceive as an inhibition efficiency indicator of a biological and biochemical material in the pharmaceutical field, and its value shows the inhibitory concentration that is required to halve a specific biological substance or biochemical function. The high IC_{50} values indicate low inhibitory activity with the material in contrast to the materials with low IC_{50} values. In this study, the MCF-7 cell line was used to assay the antiproliferative activity of different compounds. The cytotoxic impact of (A1, A2, A3, A4, A5, B4, B5) on the breast cancer cell line (MCF-7) was determined using the 3-(dimethylthiazol-2-yl)-2,5-diphenyltetrazolium bromide (MTT) assay. Using different compound concentrations, the MTT Assay was conducted to determine the cell viability and inhibition rate on the tumor cell line. The cytotoxic effect of (A1, A2, A3, A4, A5, B4, B5) in concentration ranged from (7.4-600) μg/ml on MDA-MB-231 cells. Table (3.14) presented a decrease in cell viability in a dose-dependent pattern. The cell viability is reduced by increasing the concentration of (A1, A2, A3, A4, A5, B4, B5). The compound B5 exhibited significantly the most potent cytotoxic activity with good values (47.39 μg/mL) of IC50 for MDA-MB-231 cells line, **Figure 3.63**. In the other hand, the compound A2 was the lowest in potency with IC_{50} value of 8112.57 μg/mL, **Figure 3.63**. Most of the synthesized compounds (A1, A2, A3, A4, A5, B4, B5) exhibited cytotoxic activity against MCF-7 cell lines with IC_{50} value in the range of (47.39–8112.57 μg/mL). The

microscopically examination of the tested compounds in the cell line at 100 µg/mL used to confirm the calculation of the IC_{50}, **Figure 3.64**.

Table 3.14: Growth inhibition percentages of breast cancer against different concentrations of the studied compounds.

Sample ID	A1								MCF7 24h	
Concentration (µg/mL)	7.4		22.22		66.66		200		600	
absorption at 570 nm	0.741	0.718	0.606	0.646	0.533	0.565	0.519	0.532	0.429	0.480
Viability (%)	89.17	86.40	72.92	77.74	64.14	67.99	62.45	64.02	51.62	57.76
Average Viability (%)	87.79		75.33		66.06		63.24		54.69	
Standard Deviation (±)	1.96		3.40		2.72		1.11		4.34	

Sample ID	A2								MCF7 24h	
Concentration (µg/mL)	7.4		22.22		66.66		200		600	
absorption at 570 nm	0.825	0.829	0.810	0.793	0.767	0.759	0.652	0.682	0.540	0.550
Viability (%)	99.28	99.76	97.47	95.43	92.30	91.34	78.46	82.07	64.98	66.19
Average Viability (%)	99.52		96.45		91.82		80.26		65.58	
Standard Deviation (±)	0.34		1.45		0.68		2.55		0.85	

Sample ID	A3								MCF7 24h	
Concentration (µg/mL)	7.4		22.22		66.66		200		600	
absorption at 570 nm	0.626	0.654	0.592	0.580	0.538	0.490	0.428	0.499	0.413	0.427
Viability (%)	75.33	78.70	71.24	69.80	64.74	58.97	51.50	60.05	49.70	51.38
Average Viability (%)	77.02		70.52		61.85		55.78		50.54	
Standard Deviation (±)	2.38		1.02		4.08		6.04		1.19	

Sample ID	A4								MCF7 24h	
Concentration (µg/mL)	7.4		22.22		66.66		200		600	
absorption at 570 nm	0.817	0.689	0.641	0.689	0.607	0.546	0.571	0.520	0.408	0.498
Viability (%)	98.32	82.91	77.14	82.91	73.04	65.70	68.71	62.58	49.10	59.93
Average Viability (%)	90.61		80.02		69.37		65.64		54.51	
Standard Deviation (±)	10.89		4.08		5.19		4.34		7.66	

Sample ID	A5								MCF7 24h	
Concentration (µg/ml)	7.4		22.22		66.66		200		600	
absorption at 570 nm	0.803	0.703	0.701	0.689	0.608	0.607	0.560	0.536	0.494	0.478
Viability (%)	96.63	84.60	84.36	82.91	73.16	73.04	67.39	64.50	59.45	57.52
Average Viability (%)	90.61		83.63		73.10		65.94		58.48	
Standard Deviation (±)	8.51		1.02		0.09		2.04		1.36	

Sample ID	B4								MCF7 24h	
Concentration (µg/mL)	7.4		22.22		66.66		200		600	
absorption at 570 nm	0.769	0.710	0.641	0.655	0.447	0.478	0.348	0.306	0.201	0.148
Viability (%)	92.54	85.44	77.14	78.82	53.79	57.52	41.88	36.82	24.19	17.81
Average Viability (%)	88.99		77.98		55.66		39.35		21.00	
Standard Deviation (±)	5.02		1.19		2.64		3.57		4.51	

Sample ID	B5								MCF7 24h	
Concentration (µg/mL)	7.4		22.22		66.66		200		600	
absorption at 570 nm	0.759	0.815	0.645	0.685	0.172	0.123	0.101	0.108	0.068	0.054
Viability (%)	91.34	98.07	77.62	82.43	20.70	14.80	12.15	13.00	8.18	6.50
Average Viability (%)	94.71		80.02		17.75		12.58		7.34	
Standard Deviation (±)	4.77		3.40		4.17		0.60		1.19	

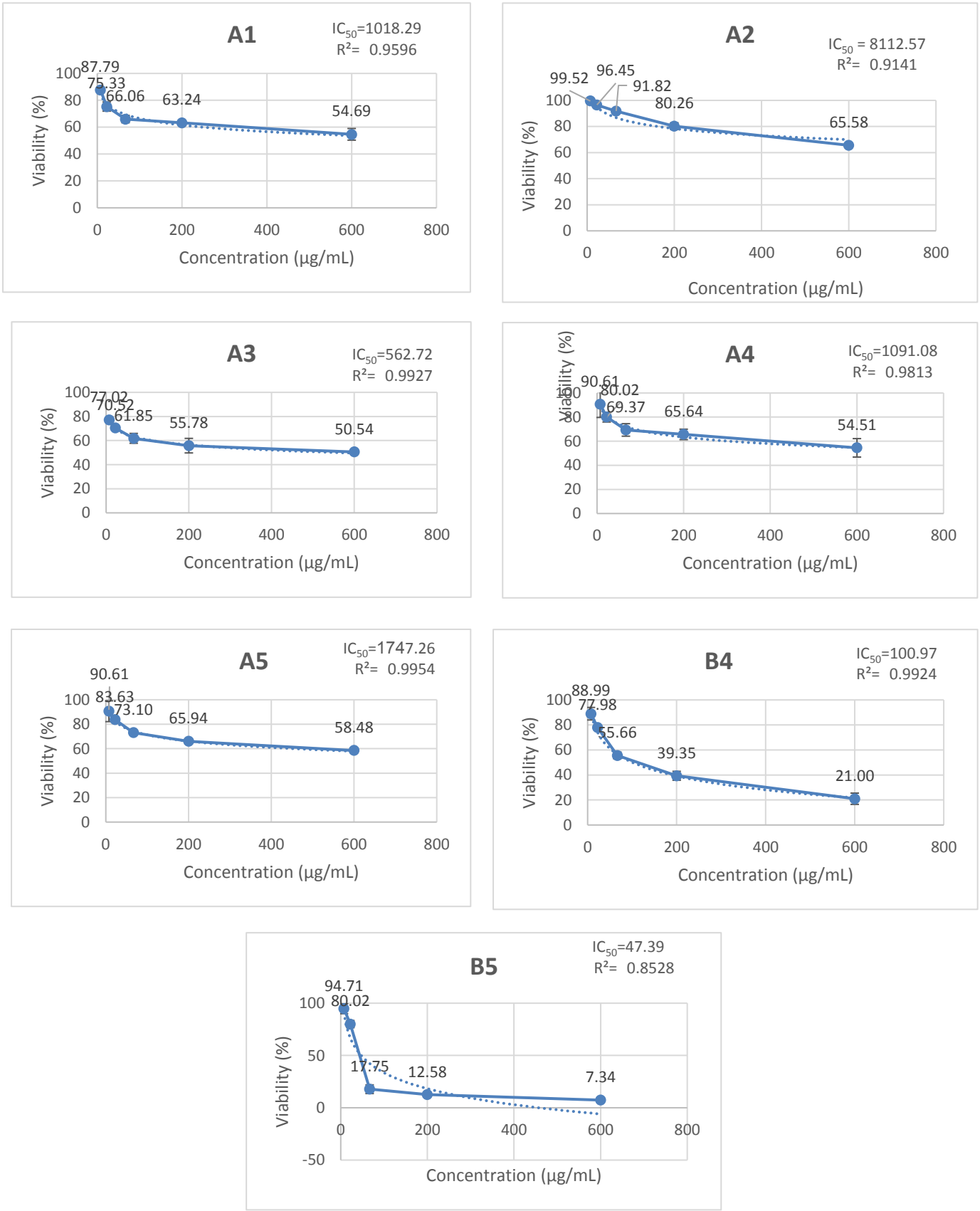

Figure 3.63: The Values of IC50 for synthesis compounds against MCF-7 Cell line.

	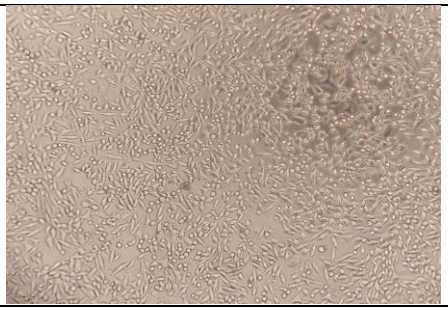	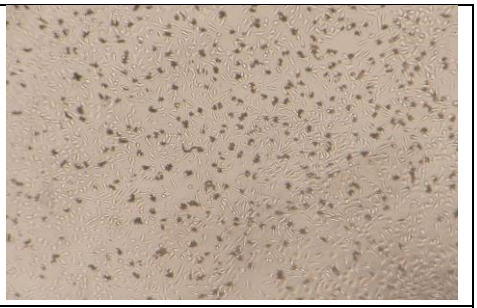
(A). MCF-7 cell lines treated with A1 inhibition activity 7.4 µg/mL	(B). MCF-7 cell lines treated with A1 inhibition activity 22.22 µg/mL	(C). MCF-7 cell lines treated with A1 inhibition activity 66.66 µg/mL
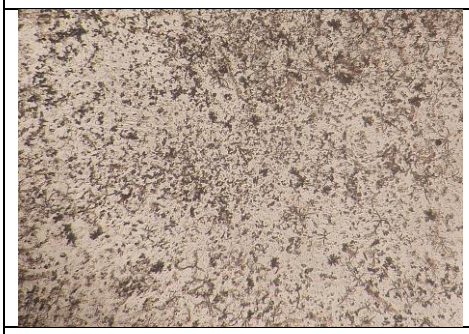	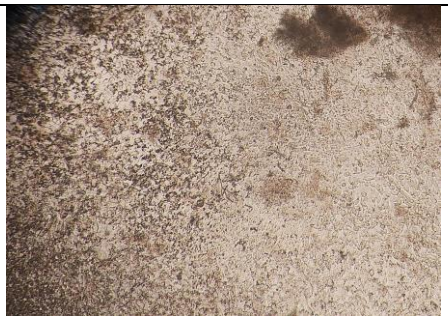	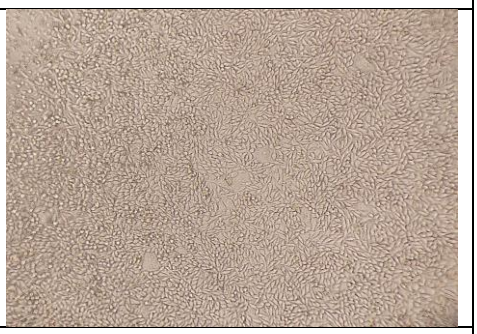
(D). MCF-7 cell lines treated with A1 inhibition activity 200 µg/mL	(E). MCF-7 cell lines treated with A1 inhibition activity 600 µg/mL	(A). MCF-7 cell lines treated with A2 inhibition activity 7.4 µg/mL
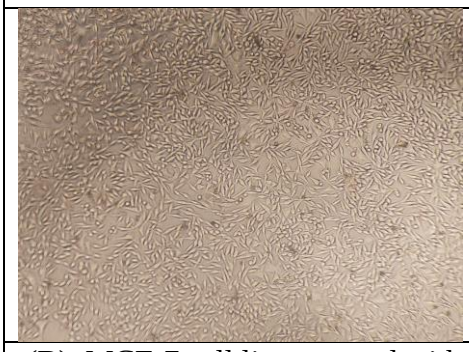		
(B). MCF-7 cell lines treated with A2 inhibition activity 22.22 µg/mL	(C). MCF-7 cell lines treated with A2 inhibition activity 66.66 µg/mL	(D). MCF-7 cell lines treated with A2 inhibition activity 200 µg/mL
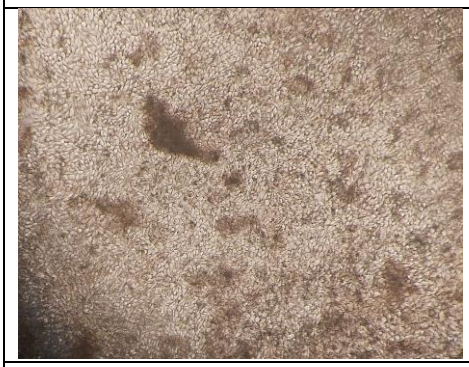	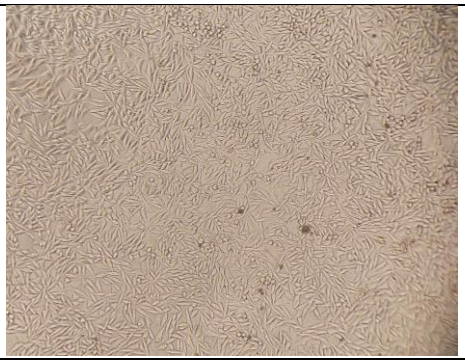	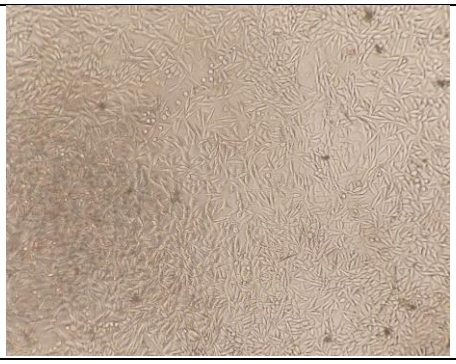
(E). MCF-7 cell lines treated with A2 inhibition activity 600 µg/mL	(A). MCF-7 cell lines treated with A3 inhibition activity 7.4 µg/mL	(B). MCF-7 cell lines treated with A3 inhibition activity 22.22 µg/mL

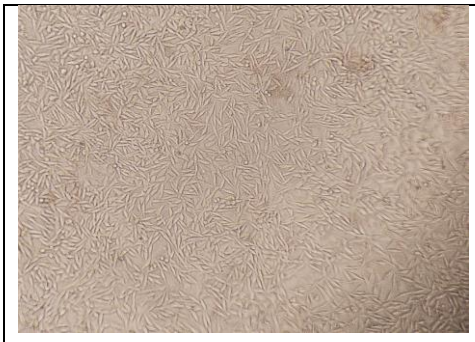	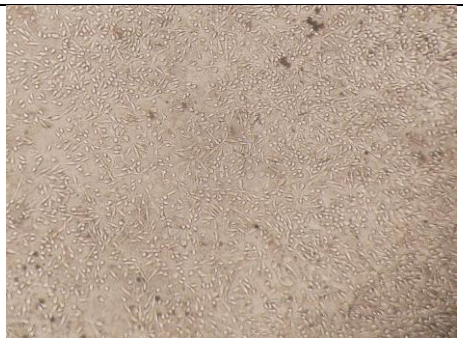	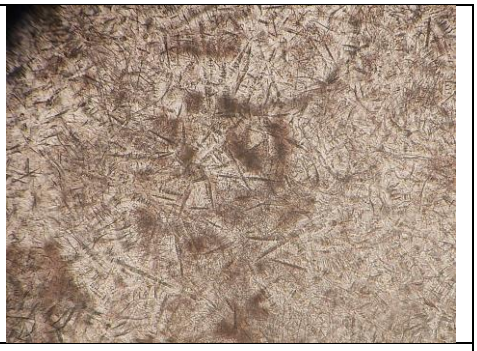
(C). MCF-7 cell lines treated with A3 inhibition activity 66.66 µg/mL	(D). MCF-7 cell lines treated with A3 inhibition activity 200 µg/mL	(E). MCF-7 cell lines treated with A3 inhibition activity 600 µg/mL
		
(A). MCF-7 cell lines treated with A4 inhibition activity 7.4 µg/mL	(B). MCF-7 cell lines treated with A4 inhibition activity 22.22 µg/mL	(C). MCF-7 cell lines treated with A4 inhibition activity 66.66 µg/mL
		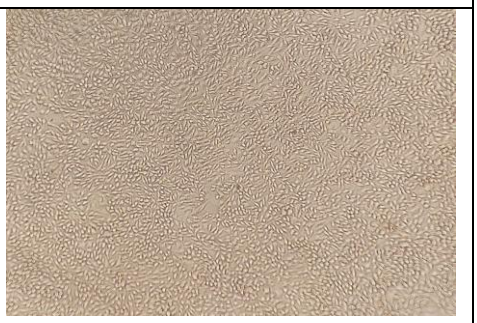
(D). MCF-7 cell lines treated with A4 inhibition activity 200 µg/mL	(E). MCF-7 cell lines treated with A4 inhibition activity 600 µg/mL	(A). MCF-7 cell lines treated with A5 inhibition activity 7.4 µg/mL
	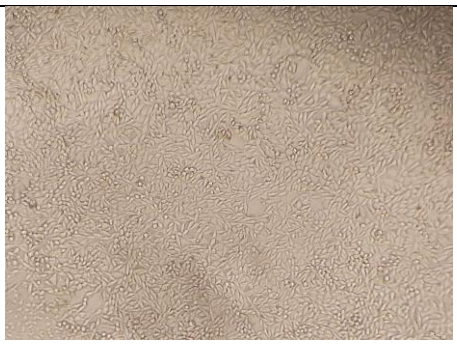	
(B). MCF-7 cell lines treated with A5 inhibition activity 22.22 µg/mL	(C). MCF-7 cell lines treated with A5 inhibition activity 66.66µg/mL	(D). MCF-7 cell lines treated with A5 inhibition activity 200 µg/mL

		
(E). MCF-7 cell lines treated with A5 inhibition activity 600 µg/mL	(A). MCF-7 cell lines treated with B4 inhibition activity 7.4 µg/mL	(B). MCF-7 cell lines treated with B4 inhibition activity 22.22µg/mL
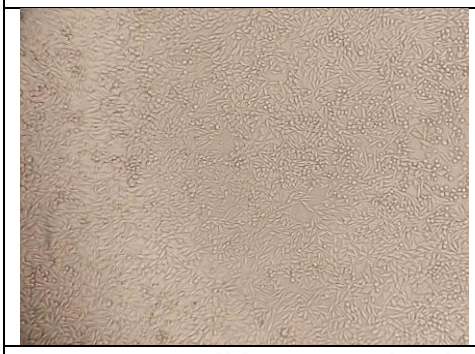		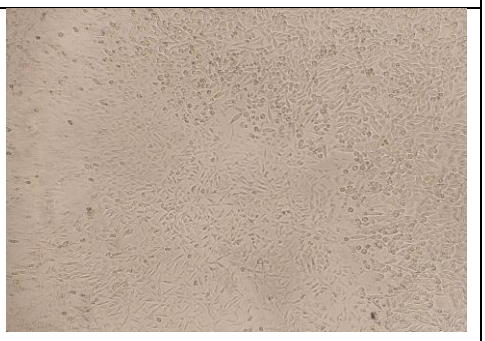
(C). MCF-7 cell lines treated with B4 inhibition activity 66.66 µg/mL	(D). MCF-7 cell lines treated with B4 inhibition activity 200 µg/mL	(E). MCF-7 cell lines treated with B4 inhibition activity 600 µg/mL
	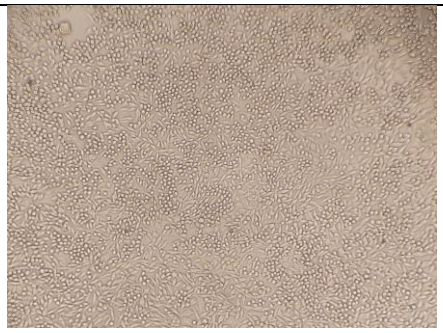	
(A). MCF-7 cell lines treated with B5 inhibition activity 7.4 µg/mL	(B). MCF-7 cell lines treated with B5 inhibition activity22.22µg/mL	(C). MCF-7 cell lines treated with B5 inhibition activity 66.66 µg/mL
		
(D). MCF-7 cell lines treated with B5 inhibition activity 200 µg/mL	(E). MCF-7 cell lines treated with B5 inhibition activity 600 µg/mL	

Figure 3.64: MCF-7 cell line microscopic examination of compounds at 100 µm concentration.

3.5.2.Antioxidant activity of the DPPH scavenging assay.

This assay is a rapid, simple and vastly used method to measure the ability of compounds to act as free radical scavengers or hydrogen donors. After abstracting hydrogen from corresponding donor, the radical losses its characteristic deep violet color and turns to yellow. The IC_{50} values were used to compare the antiradical scavenging activity of different analyzed samples with those of standard antioxidant compound. The IC_{50} values cleared that **A1** compound exhibited the highest antiradical scavenging activity with the lowest IC_{50} value (6.9 µg/mL), while the **A2** had the lowest capacity to scavenge the radical with the highest IC_{50} value (31019.2 µg/mL). Antioxidant drugs facilitate the conversion of DPPH into a stable diamagnetic molecule[97], DPPH, by electron or hydrogen transfers. A change in the color from purple to yellow signifies an increase in the radical scavenging activity of the compounds being examined. The capacity of DPPH radicals to be reduced was assessed by quantifying the decrease in absorbance at 515 nm resulting from the presence of antioxidants. However, it is commonly recognized that organic compounds with electron-donating groups (such as amine, methoxy, and hydroxyl) can function as agents that scavenge free radicals[98].

The results of the antioxidant activity test with DPPH were expressed as % inhibition Table 3.15, which was then linked to a series of samples or standard concentrations to produce a curve, as shown in Figure 3.64 .

Table 3.15: Free radical scavenging activity result of synthesis compounds.

compounds	Radical Scavenging Activity % (RSA) at eight different concentrations (µg/mL)							
	800	**400**	**200**	**100**	**50**	**25**	**12.4**	**6.25**
A1	86.8	80.9	73.3	65.6	63.2	62.3	59.7	45.5
A2	4.5	3.3	2.9	2.7	2.1	1.1	0.8	0.2
A3	35.0	25.8	20.4	17.6	7.7	3.4	2.2	2.2
A4	11.4	9.2	6.8	6.6	4.8	1.9	1.5	1.4
A5	34.8	31.1	27.9	20.4	17.7	15.4	10.1	10.5
B4	94.8	93.9	86.5	71.0	53.3	48.2	21.9	8.6
B5	30.0	28.7	26.8	21.9	20.5	20.1	14.5	15.2

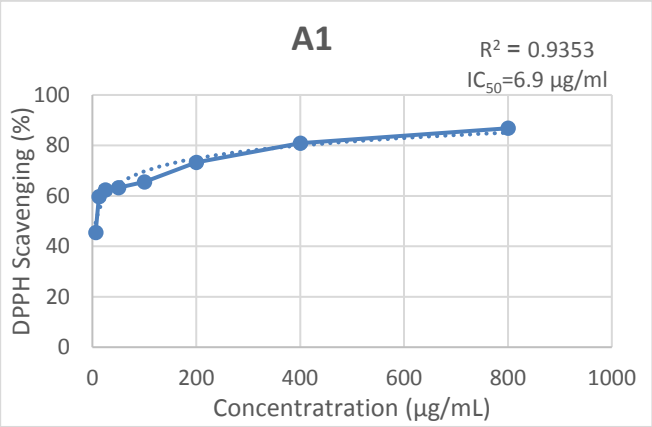

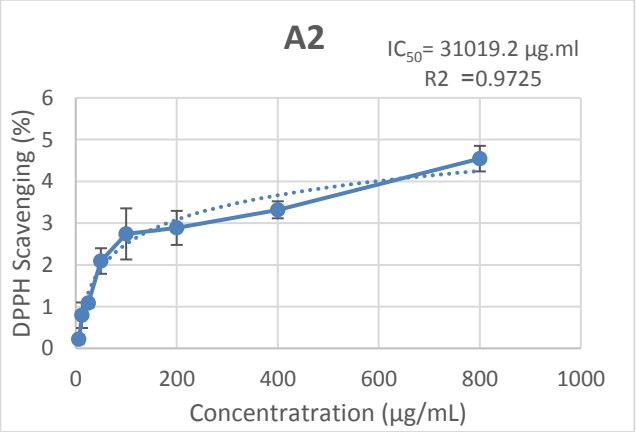

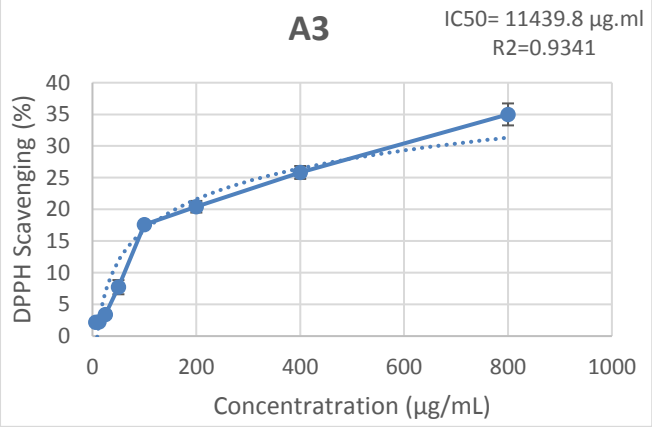

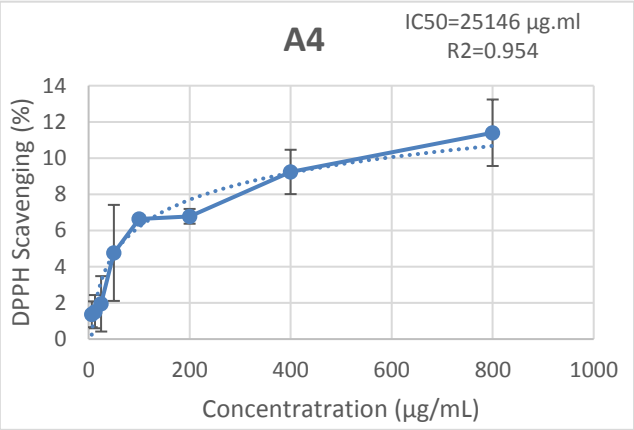

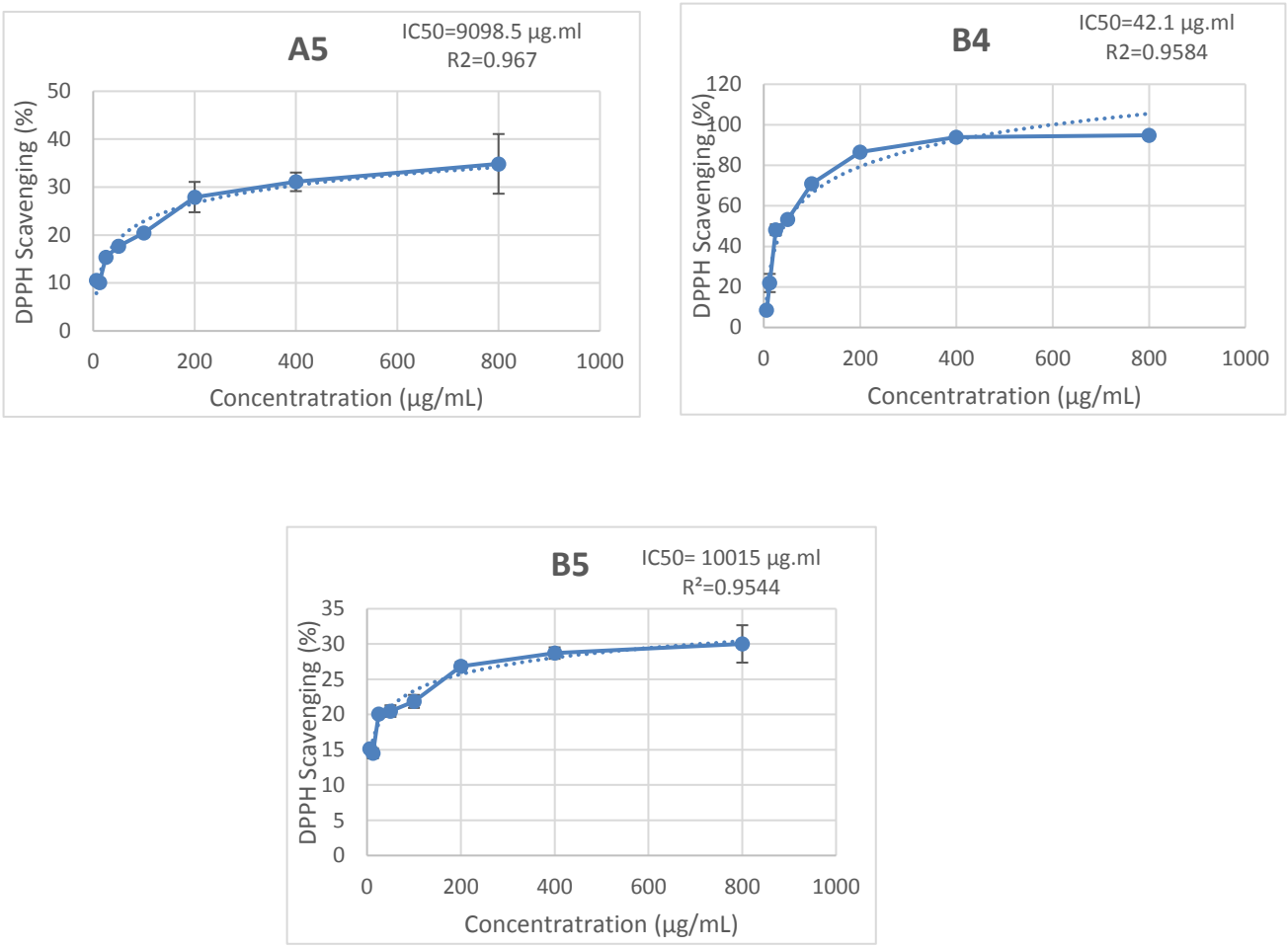

Figure 3.65: Radical scavenging activity (RSA) for the derivative (A1-A5, B4, B5) on DPPH.

Conclusions

1-The di-substituted (A5, A6) benzamide derivatives gave higher yields than the mono-substituted (A1-A4) derivatives.

2-The number of substituted sulfonyl groups, whether mono or di, in the derivatives B1-B5 didn't appear to have any effect on the yield.

3-In allyl derivatives, it is shown that the mono-substituted (C1, C2) derivatives give higher yields than di-substituted derivatives (C3).

4-It was notice that the sulfonyl derivatives B4 exhibited significantly the most potent cytotoxic activity with good value (47.39) of IC_{50} for MAD-MB-231 cells line, while the rest of the derivatives (A1-A4, B5) showed different values for IC_{50}.

5-A1 compound exhibited the highest anti radicals scavenging activity with the lowest IC_{50} value, while the A2 had the lowest capacity to scavenge the radical with the highest IC_{50} value

6-Study molecular docking and the compounds (A1, A5, B2, B3, B5, C1) showed good activity

Recommendations

1-Carboxylic acid can be used as starting materials to prepare new derivatives containing sulfonyl, allyl, or vinyl groups.

2-This work can be modified by reacting the benzoyl chloride with chalcone compounds for the purpose of improving the biological activity.

3-Our study recommends to complete the estimation of IZ, MIC, and LD_{50} of the prepared derivatives.

References

1. DeRuiter J. Amides and related functional groups. *Princ Drug Action 1*. Published online 2005:1-16.

2. Huda Bukheet Hassan. Energy Gap and Infrared Frequencies of Benzamide and Di-Chlorine Benzamide from Density Functional Calculations. *Res J Pharm Tech*. 2018;11(10):4263-4266.

3. Chen H, Zhang Y, Wen Y, et al. Production of constrained L-cyclo-tetrapeptides by epimerization-resistant direct aminolysis. *Nat Commun*. 2024;15(1):1-11. doi:10.1038/s41467-024-49329-3

4. De Berardinis L, Vitali D, Cerea P, Bertolini G, Cabri W, Stucchi M. Rediscovery of an Old Named Reaction: From Micellar Catalysis to Unusual Schotten-Baumann Conditions. *Org Process Res Dev*. Published online 2024:1-22. doi:10.1021/acs.oprd.4c00100

5. Cui HYZX, Zhao ،zLZX. Selective hydrolysis of α-oxo ketene N,S-acetals in water: switchable aqueous synthesis of β-keto thioesters and β-keto amides. *Beilstein J Org Chem*. 2024;20:2225-2233.

6. Zhihui Xu, Tianbao Yang, Niu Tang, Yifeng Ou, Shuang-Feng Yin, Nobuaki Kambe and RQ. UV-Light-Induced N-Acylation of Amines with α-Diketones. *Org Lett*. 2021;23:5329-5333.

7. Li X, Cheng Z, Liu J, Zhang Z, Song S, Jiao N. Selective desaturation of amides: a direct approach to enamides. *Chem Sci*. 2022;13(31).

8. Jiwei Wu, Yuting Zhang, Jingyi Yang, Lingxiang Yu, Shaoqing Zhang, Jie Zhou, Zirong Li, Xiaolan Xu HX. Decarboxylative N-Formylation of Amines with Glyoxylic Acid Promoted by H_2O_2. *J Org Chem*. 2023;88(19):13590-13597.

9. Darmani, NissaBelkacemi L, A. R. Dopamine receptors in emesis: Molecular mechanisms and potential therapeutic function. *Pharmacol Res*. 2020;161:105124. doi:10.1016/j.phrs.2020.105124

10. Fatin Fadhel Mahmood. Optimization Geometry of Benzamide and Di-Fluorine Benzamide Molecules. *Res J Pharm*. 2018;11(9):3978-3982.

11. Dan Liu , Ling Luo, Zhengxing Wang XM and XG. Design, Synthesis and Antifungal/Nematicidal Activity of Novel 1,2,4-Oxadiazole Derivatives Containing Amide Fragments. *Int J Mol Sci*. 2022;23(3):1596.

12. Li H, Wang C, Sanchez T, et al. Amide-containing diketoacids as HIV-1 integrase inhibitors: Synthesis, structure-activity relationship analysis, and biological activity. *Bioorganic Med Chem*. 2009;17(7):2913-2919. doi:10.1016/j.bmc.2009.01.077

13. Xing-Yue Ji , Hui-Qiang Wang , Lan-Hu Hao, Wei-Ying He, Rong-Mei Gao, Yan-Ping Li , Yu-Huan Li JDJ and ZRL. Synthesis and Antiviral Activity of N-Phenylbenzamide Derivatives, a Novel Class of Enterovirus 71 Inhibitors. *Molecules*. 2013;18(3):3630-3640.

14. Silvana Vasile , Anders Hallberg , Jessica Sallander , Mathias Hallberg JÅ and HG de T. Evolution of Angiotensin Peptides and Peptidomimetics as Angiotensin II Receptor Type 2 (AT2) Receptor Agonists. *Biomolecules*. 2020;10(4):649.

15. Qasim ZS, Abbas KS. Benzamine Derivatives: Synthesis, Characterization and Biological Activity Study. *Chem Probl*. 2024;22(4):411-435. doi:10.32737/2221-8688-2024-4-411-435

16. Shteinberg L, Marshalova V V., Dibrova VM, Shein SM. Effect of the benzoic acid additives on the catalytic activity of tetrabuthoxytitanium in the synthesis of benzanilide. *Russ J Gen Chem*. 2011;81(9):1839-1844.

17. Dar BA, Pandey N, Singh S, Kumar P, Farooqui M, Singh B. Solvent-free, scalable and expeditious synthesis of benzanilides under microwave irradiation using clay doped with palladium nanoparticles as a recyclable and efficient catalyst. *Green Chem Lett Rev*. 2015;8(2):1-8.

18. L. Bannwart, S. Abele, S. Tortoioli. Metal-Free Amidation of Acids with Formamides and T3P Synthesis. *Synthesis (Stuttg)*. 2016;48(12):2069-2078. doi:10.1055/s-0035-1561427

19. Donnier-Maréchal M, Carato P, Larchanché PE, et al. Synthesis and pharmacological evaluation of benzamide derivatives as potent and selective sigma-1 protein ligands. *Eur J Med Chem*. 2017;138:964-978.

20. Pengcheng GaoMd, Mahbubur Rahman, Alfredo Zamalloa, Jessica Feliciano MS. Classes of Amides that Undergo Selective N–C Amide Bond Activation: The Emergence of Ground-State Destabilization. *J Org Chem*. 2022;88(19).

21. Ling L, Chen C, Luo M, Zeng X. Chromium-Catalyzed Activation of Acyl C-O Bonds with Magnesium for Amidation of Esters with Nitroarenes. *Org Lett*. 2019;21(6):1912-1916.

22. Saito S. Diboron-Catalyzed Dehydrative Amidation of Aromatic Carboxylic Acids with Amines. *Org Lett*. 2018;20:4397-4400.

23. Ramachandran PV, Hamann HJ. Ammonia-borane as a Catalyst for the Direct Amidation of Carboxylic Acids. *Org Lett*. 2021;23(8):2938-2942.

24. Jin Bai, Shangzhang Li, Riqian Zhu YL and WL. $B2(OH)_4$-Mediated Reductive Transamidation of N-Acyl Benzotriazoles with Nitro Compounds En Route to Aqueous Amide Synthesis. *J Org Chem*. 2023;88:3714-3723.

25. Zahraa S.Qasim.M.SC.Thesis, Misan University (2024).

26. Hameed AD, Al-Fatlawi AAY, Al-Fatlawi AAY. Synthesis and Biological Activity of New Sulfonamide Derivatives. *Int J Drug Deliv Technol*. 2021;11(4):1394-1398.

27. Baran W, Adamek E, Ziemiańska J, Sobczak A. Effects of the presence of sulfonamides in the environment and their influence on human health. *J Hazard Mater*. 2011;196:1-15.

28. York N, Macmillan T. pituitary gland. 2015;(5):2015.

29. Mohammed S, AL-Hadedi A, Abood S. The Role of Sulfa Drugs in our Life. *Rafidain J Sci*. 2022;31(3):64-74.

30. G. Domagk D med. W. No Title. 1935;61:250.

31. J. Trefouel, Mme. Trefouel, F. Nittie, D. Bovet CRSB. No Title. 1935;120:756.

32. Mostafa M. Ghorab, Aiten M. Soliman, Gharieb S. El-Sayyad, Maged S. Abdel-Kader and AIEB. Synthesis, Antimicrobial, and Antibiofilm Activities of Some Novel 7-Methoxyquinoline Derivatives Bearing Sulfonamide Moiety against Urinary Tract Infection-Causing Pathogenic Microbes. *Int J Mol Sci*. 2023;24(10):8933.

33. Takayoshi Awakawa, corresponding author Lena Barra and IA. Biosynthesis of sulfonamide and sulfamate antibiotics in actinomycete. *J Ind Microbiol Biotechnol*. 2021;48:3-4.

34. Nielsen MK, Ugaz CR, Li W, Doyle AG. PyFluor: A low-cost, stable, and selective deoxyfluorination reagent. *J Am Chem Soc*. 2015;137(30):9571-9574.

35. Müller N, Myint AM, Krause D, Weidinger E, Schwarz MJ. Anti-inflammatory treatment in schizophrenia. *Prog Neuro-Psychopharmacology Biol Psychiatry*. 2013;42:146-153.

36. Livia Puljak, Ana Marin, Davorka Vrdoljak, Filipa Markotic, Ana Utrobicic PT. Celecoxib for osteoRowan-Robinson, Katearthritis. *Br J Community Nurs*. 2019;24(10):501-502.

37. Widiarti W, Saputra PBT, Ariyanto MV, et al. The Role of Subcutaneous Furosemide in Heart Failure Management: A Systematic Review. *Curr Cardiol Rep*. 2024;(0123456789).

38. Giles A, Foushee J, Lantz E, Gumina G. Sulfonamide Allergies. *Pharmacy*. 2019;7(3):132.

39. Yoshino T, Sono M, Yazumi S. Usefulness of sulfasalazine for patients with refractory-ulcerative colits. *BMJ Open Gastroenterol*. 2016;3(1):1-8.

40. Scott FI, Osterman MT. Medical management of crohn disease. *Clin Colon Rectal Surg*. 2013;26(2):67-74. doi:10.1055/s-0033-1348043

41. Alani BG, Salim KS, Mahdi AS, Al-Temimi AA. Sulfonamide derivatives: Synthesis and applications. *Int J Front Chem Pharm Res*.2024;4(1):001-015.

42. Moon DO. Exploring the Role of Surface and Mitochondrial ATP-Sensitive Potassium Channels in Cancer: From Cellular Functions to Therapeutic Potentials. *Int J Mol Sci*. 2024;24(4):2129.

43. King NM, Prabu-Jeyabalan M, Nalivaika EA, Wigerinck P, de Béthune MP, Schiffer CA. Structural and Thermodynamic Basis for the Binding of TMC114, a Next-Generation Human Immunodeficiency Virus Type 1 Protease Inhibitor. *J Virol*. 2004;78(21):12012-12021.

44. Cox VC, Zed PJ. Once-Daily Cefazolin and Probenecid for Skin and Soft Tissue Infections. *Ann Pharmacother*. 2004;38(3):458-463.

45. Yan J, Li J, Cheng D. Novel and efficient synthesis of 1-iodoalkynes. *Synlett*. 2007;(15):2442-2444.

46. Luca L De, Giacomelli G. 27 An Easy Microwave-Assisted Synthesis of Sulfonamides Directly from Sulfonic Acids Sulfonamides from Sulfonic Acids An easy and handy synthesis of sulfonamides directly from sulfonic acids or its sodium salts is reported . The reaction is performed unde. *J Org Chem*. 2008;73(c):3967–3969.

47. Bahrami K, Khodaei MM, Soheilizad M. Direct conversion of thiols to sulfonyl chlorides and sulfonamides. *J Org Chem*. 2009;74(24):9287-9291.

48. Shyam PK, Jang HY. Synthesis of Sulfones and Sulfonamides via Sulfinate Anions: Revisiting the Utility of Thiosulfonates. *J Org Chem*. 2017;82(3):1761-1767.

49. Roy T, Lee JW. Cyanide-Mediated Synthesis of Sulfones and Sulfonamides from Vinyl Sulfones. *Synlett*. 2020;31(5):455-458.

50. Chen K, Chen W, Han B, Chen W, Liu M, Wu H. Sequential C-S and S-N Coupling Approach to Sulfonamides. *Org Lett*. 2020;22(5):1841-1845.

51. Zuilhof AFJ van den B and H. Sulfur-Phenolate Exchange as a Mild, Fast, and High-Yielding Method toward the Synthesis of Sulfonamides. *Org Lett*. 2023;25:788-793.

52. Jassim Hussein HS, Abbas KS, Abdul-Saheb YS. Synthesis of some new aryl sulfonyl derivatives and study of their biological activity. *Eurasian Chem Commun*. 2023;5(5):450-465.

53. Stauffer SR, Hartwig JF. Fluorescence resonance energy transfer (FRET) as a high-throughput assay for coupling reactions. Arylation of amines as a case study. *J Am Chem Soc*. 2003;125(23):6977-6985.

54. Salvatore RN, Yoon CH, Jung KW. Synthesis of secondary amines. *Tetrahedron*. 2001;57(37):7785-7811.

55. Liu Y, Chen W, Feng C, Deng G. Ruthenium-catalyzed one-pot aromatic secondary amine formation from nitroarenes and alcohols. *Chem - An Asian J*. 2011;6(5):1142-1146.

56. Aitor Bermejo-López, Man Li , N.V.R. Aditya Dharanipragada , Majken Raeder , A. Ken Inge , Fahmi Himo BMM. A general catalyst for the base-free mono-N-alkylation of aromatic and aliphatic amines with alcohols. *Org Chem*. 2024;5(9):101991.

57. Yang SC, Tsai YC, Shue YJ. Direct platinum-catalyzed allylation of anilines using allylic alcohols. *Organometallics*. 2001;20(25):5326-5330.

58. Du Z, Wei X, Zhang W, Zhang Y, Xue Q. Catalyst-free and highly selective N,N-diallylation of anilines in aqueous phase. *J Chem*. 2013;2013(Scheme 1):1-6.

59. Luciana Cicco, Sara Urselli, Claudia Favia FMP. Iron-Based Deep Eutectic Solvents: Key Players for Amide and Sulfonamide Synthesis and Alcohol Oxidation. *European J Org Chem*. 2024;27(24):300.

60. Chen H, Zhang T, Qian C, Chen X. A novel method for N-alkylation of aliphatic amines with ethers over γ-Al2O3. *Chem Pap*. 2010;64(4):537-540.

61. Marzaro G, Guiotto A, Chilin A. Microwave-promoted mono-N-alkylation of aromatic amines in water: A new efficient and green method for an old and problematic reaction. *Green Chem*. 2009;11(6):774-777.

62. Saurabh C. Khadse VAC. Synthesis of benzamides by microwave assisted ring opening of less reactive dimethylaminobenzylidene oxazolone. *Arab J Chem*. 2017;10(1):S859-S863.

63. Zhu M, Fujita KI, Yamaguchi R. Simple and versatile catalytic system for N-alkylation of sulfonamides with various alcohols. *Org Lett*. 2010;12(6):1336-1339.

64. Wallach DR, Chisholm JD. Alkylation of Sulfonamides with Trichloroacetimidates under Thermal Conditions. *J Org Chem*. 2016;81(17):8035-8042.

65. Zhu M hui, Yu C long, Feng Y lan, et al. Detosylative (Deutero)alkylation of Indoles and Phenols with (Deutero)alkoxides. Published online 2019:1-5.

66. Wang Z, Zeng H, Li C jun. Dearomatization − Rearomatization Strategy for Reductive Cross- Coupling of Indoles with Ketones in Water. Published online 2019:1-5.

67. Adhikari P, Bhattacharyya D, Nandi S, Kancharla PK, Das A. Reductive Alkylation of Quinolines to N ‐ Alkyl Tetrahydroquinolines Catalyzed by Arylboronic Acid. Published online 2021.

68. Wang X jun, Sidhu K, Zhang L, et al. Bromo-Directed N -2 Alkylation of NH -1 , 2 , 3-Triazoles : Efficient Synthesis of Poly-Substituted 1 , 2 , 3-Triazoles. 2009;(5):3-6.

69. Ferreira LG, Dos Santos RN, Oliva G, Andricopulo AD. *Molecular Docking and Structure-Based Drug Design Strategies*. Vol 20.; 2015.

70. McNutt AT, Francoeur P, Aggarwal R, et al. GNINA 1.0: molecular docking with deep learning. *J Cheminform*. 2021;13(1):1-20.

71. Aguiar C, Camps I. Molecular Docking in Drug Discovery: Techniques, Applications, and Advancements. *ChemRxiv*. 2024,.

72. Sahu D, Rathor LS, Dwivedi SD, et al. A Review on Molecular Docking As an Interpretative Tool for Molecular Targets in Disease Management. *Assay Drug Dev Technol*. 2024;22(1):40-50.

73. Sahu MK, Nayak AK, Hailemeskel B, Eyupoglu OE. Exploring Recent Updates on Molecular Docking: Types, Method, Application, Limitation & Future Prospects. *Int J Pharm Res Allied Sci*. 2024;13(2):24-40.

74. Ahmed RA, Alawin OA, Sylvester PW. γ-Tocotrienol reversal of epithelial-to-mesenchymal transition in human breast cancer cells is associated with inhibition of canonical Wnt signalling. *Cell Prolif*. 2016;49(4):460-470.

75. Nada A.S. Alwan, Furat N. Tawfeeq and NAGM. Demographic and clinical profiles of female patients diagnosed with breast cancer in Iraq. *J Contemp Med Sci*. 2019;5(1):14-19.

76. Rajib Hossain, Pranta Ray, Chandan Sarkar, Md. Shahazul Islam, Rasel Ahmed Khan, Abul Bashar Ripon Khalipha,' Muhammad Torequl Islam, William C. Cho, Miquel Martorell, Javad Sharifi-Rad, Monica Butnariu, Almagul Umbetova and DC. Natural Compounds or Their Derivatives against Breast Cancer: A

Computational Study. *Biomed Res Int*. 2022;1:5886269.

77. Obeagu EI, Obeagu GU. Breast cancer: A review of risk factors and diagnosis. *Med (United States)*. 2024;103(3):E36905.

78. Munteanu IG, Apetrei C. Analytical methods used in determining antioxidant activity: A review. *Int J Mol Sci*. 2021;22(7).

79. Parcheta M, Świsłocka R, Orzechowska S, Akimowicz M, Choińska R, Lewandowski W. Recent developments in effective antioxidants: The structure and antioxidant properties. *Materials (Basel)*. 2021;14(8):1-24.

80. Barakat A, Ghabbour HA, Al-Majid AM, et al. Synthesis, spectroscopic investigations (X-ray, NMR and TD-DFT), antimicrobial activity and molecular docking of 2,6-bis(hydroxy(phenyl)methyl)cyclohexanone. *Molecules*. 2015;20(7):13240-13263. doi:10.3390/molecules200713240

81. Bernal FA, Coy-Barrera E. Molecular docking and multivariate analysis of xanthones as antimicrobial and antiviral agents. *Molecules*. 2015;20(7):13165-13204. doi:10.3390/molecules200713165

82. Rehman H, Qadir A, Ali Z, Nazir S, Zahra A, Shahzady TG. Synthesis and characterization of novel sulfonamides derivatives and their antimicrobial, antioxidant and cytotoxicity evaluation. *Bull Chem Soc Ethiop*. 2017;31(3):491-498.

83. Tanaka H, Tokumaru Y, Fukui KI, et al. Chemo- and product-selective electrooxidation of 3-(arylthiomethyl)- Δ3-cephems. *Synthesis (Stuttg)*. 2009;(20):3449-3459.

84. Waingeh VF, Ngassa FN, Song J. A Theoretical Study of <i>β</i>-Amino Acid Conformational Energies and Solvent Effect. *Open J Phys Chem*. 2015;05(04):122-131.

85. Alves Lourenço BL, Araújo Santos Silva MV, de Oliveira EB, et al. Virtual Screening and Molecular Docking for Arylalkylamine-N-Acetyltransferase (aaNAT) Inhibitors, a Key Enzyme of <i>Aedes</i> (Stegomyia) <i>aegypti</i> (L.) Metabolism. *Comput Mol Biosci*. 2015;05(03):35-44.

86. Herrera-Ruiz M, López-Rodríguez R, Trejo-Tapia G, et al. A new furofuran lignan diglycoside and other secondary metabolites from the antidepressant extract of Castilleja tenuiflora Benth. *Molecules*. 2015;20(7):13127-13143. doi:10.3390/molecules200713127

87. Nguyen NT, Nguyen TH, Pham TNH, et al. Autodock Vina Adopts More Accurate Binding Poses but Autodock4 Forms Better Binding Affinity. *J Chem Inf Model*. 2020;60(1):204-211.

88. Neubig RR, Spedding M, Kenakin T, Christopoulos A. Update on Terms and Symbols in Quantitative Pharmacology. *Pharmacol Rev*. 2003;55(4):597-606.

89. Chauhan NB, Patel NB, Patel VM, Mistry BM. Synthesis and biological evaluation of coumarin clubbed thiazines scaffolds as antimicrobial and antioxidant. *Med Chem Res*. 2018;27(9):2141-2149.

90. Chaban T, Ogurtsov V, Mahlovanyy A, et al. Antioxidant properties of some novel derivatives thiazolo[4,5-b] pyridine. *Pharmacia*. 2019;64(4):171-180.

91. Nafie MS, Tantawy MA, Elmgeed GA. Screening of different drug design tools to predict the mode of action of steroidal derivatives as anti-cancer agents. *Steroids*. 2019;152(September).

92. El Rhabori S, El Aissouq A, Daoui O, Elkhattabi S, Chtita S, Khalil F. Design of new molecules against cervical cancer using DFT, theoretical spectroscopy, 2D/3D-QSAR, molecular docking, pharmacophore and ADMET investigations. *Heliyon*. 2024;10(3):e24551.

93. El-Bindary AA, Toson EA, Shoueir KR, Aljohani HA, Abo-Ser MM. Metal–organic frameworks as efficient materials for drug delivery: Synthesis, characterization, antioxidant, anticancer, antibacterial and molecular docking investigation. *Appl Organomet Chem*. 2020;34(11):1-15.

94. Liu Z, Liu Y, Zeng G, et al. *Application of Molecular Docking for the Degradation of Organic Pollutants in the Environmental Remediation: A Review*. Vol 203. Elsevier Ltd; 2018.

95. Mohammed AO, Abo-Idrees MI, Makki AA, Ibraheem W, Alzain AA. Drug repurposing against main protease and RNA-dependent RNA polymerase of SARS-CoV-2 using molecular docking, MM-GBSA calculations and molecular dynamics. *Struct Chem*. 2022;33(5):1553-1567. doi:10.1007/s11224-022-01999-9

96. Madhavi Sastry G, Adzhigirey M, Day T, Annabhimoju R, Sherman W. Protein and ligand preparation: Parameters, protocols, and influence on virtual screening enrichments. *J Comput Aided Mol Des*. 2013;27(3):221-234.

97. Sterle M, Durcik M, Stevenson CEM, et al. Exploring the 5-Substituted 2-Aminobenzothiazole-Based DNA Gyrase B Inhibitors Active against ESKAPE Pathogens. *ACS Omega*. 2023;8(27):24387-24395.

98. Baliyan S, Mukherjee R, Priyadarshini A, et al. Determination of Antioxidants by DPPH Radical Scavenging Activity and Quantitative Phytochemical Analysis of Ficus religiosa. *Molecules*. 2022;27(4).

الجزء الرابع: -

تم دراسة الالتحام الجزيئي للمركبات المحضرة باستخدام برنامج MOE2015.10 لتحليل قدرة المركبات على تثبيط سرطان الثدي عن طريق ربطها ببروتين واحد 3EQM وأظهرت المركباتA1,A5, B2, C1 نشاطا جيدا. وبعد ذلك تم تقدير الفعالية البيولوجية لهذه المركبات بعد تصنيعها وتم التشخيص بطرق كيميائية مختلفة، بما في ذلك فعالية مضاد السرطان ومضاد الأكسدة، تم القياس في المختبر باستخدام طريقة السمية الخلوية (طريقة صلاحية الخلية MTT) في خلايا MCF7 للكشف عن فعالية مضاد السرطان، وطريقة DPPH (IC_{50}) لقياس فعالية الطرد ضد الجذور الحرة لتحديد فعالية مضادات الأكسدة.

في هذه الدراسة، تم استخدام الخط الخلوي MCF-7 لفحص فعالية مانع التكاثر الخلوي للمركبات المختلفة، وتم تحديد التأثير السام للمركبات (A1، A2، A3، A4، A5، B4، B5) على خط خلايا سرطان الثدي (MCF-7)، وتراوح التأثير السام للمركبات (A1، A2، A3، A4، A5، B4، B5) بتركيز من (600-7.4) ميكروغرام / مل على خلايا MDA-MB-231. بالإضافة إلى ذلك، تم استخدام قيم IC_{50} لمقارنة فعالية الطرد لمضاد الجذور للعينات المختلفة التي تم تشخيصها مع المركبات المضادة للتأكسد القياسية. أوضحت قيم IC_{50} أن المركب A1 أظهر أعلى فعالية طرد مضاد للجذور الحرة مع أقل قيمة (6.9) IC_{50} ميكروغرام/مل)، في حين أن المركب A2 كان لديه أدنى قدرة على طرد الجذور مع أعلى قيمة (31019.2) IC_{50} ميكروغرام/مل)

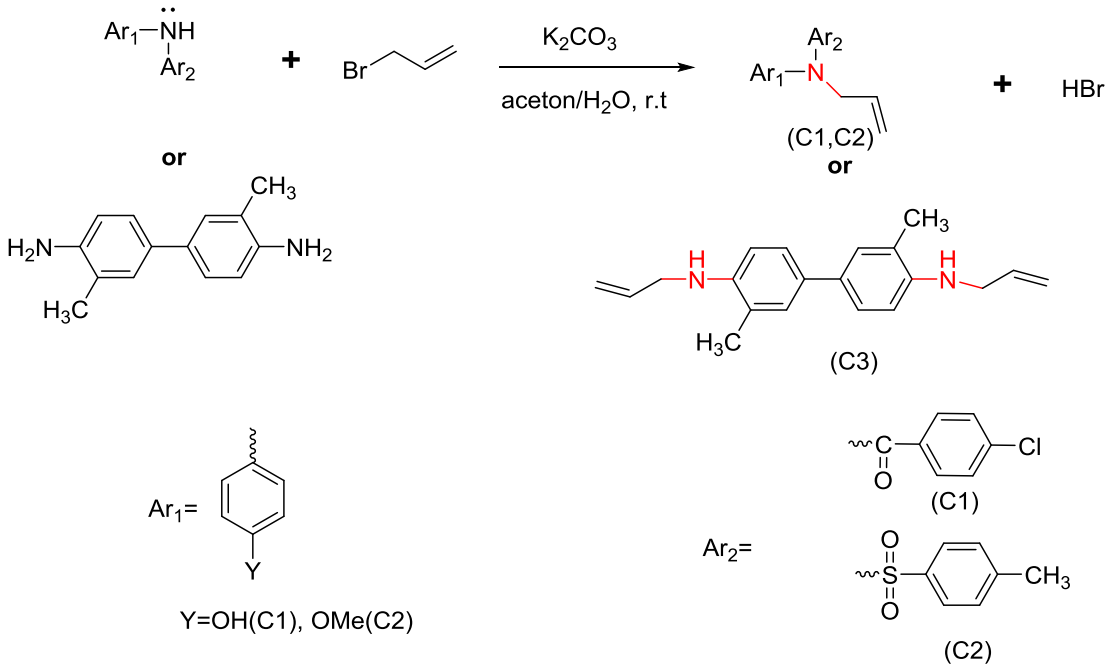

مشتقات البنزآمايد والسلفونامايد والاليل المحضرة شخصت بواسطة عدد من الخواص الفيزياوية كدرجة الانصهار وتقنية كروماتوغرافيا الطبقة الرقيقة بالإضافة إلى التقنيات الطيفية الممثلة ب: الأشعة تحت الحمراء والرنين النووي المغناطيسي للبروتون والرنين النووي المغناطيسي للكاربون وتقنية طيف الكتلة.

أظهرت الدراسة بأن كل البيانات والقيم التي تم الحصول عليها من القياسات الفيزياوية والطيفية أكدت صحة تراكيب المركبات المحضرة في هذه الدراسة.

الملخص

الجزء الأول: -

هذا الجزء يتضمن تحضير من مشتقات البنز آمايد (A1- A6) بواسطة تفاعل انلين معوض في الموقع بارا أو اورثو- توليدين - 4 - كلوروبنزوايل كلورايد بوجود 1,4- دايو كسان كمذيب.

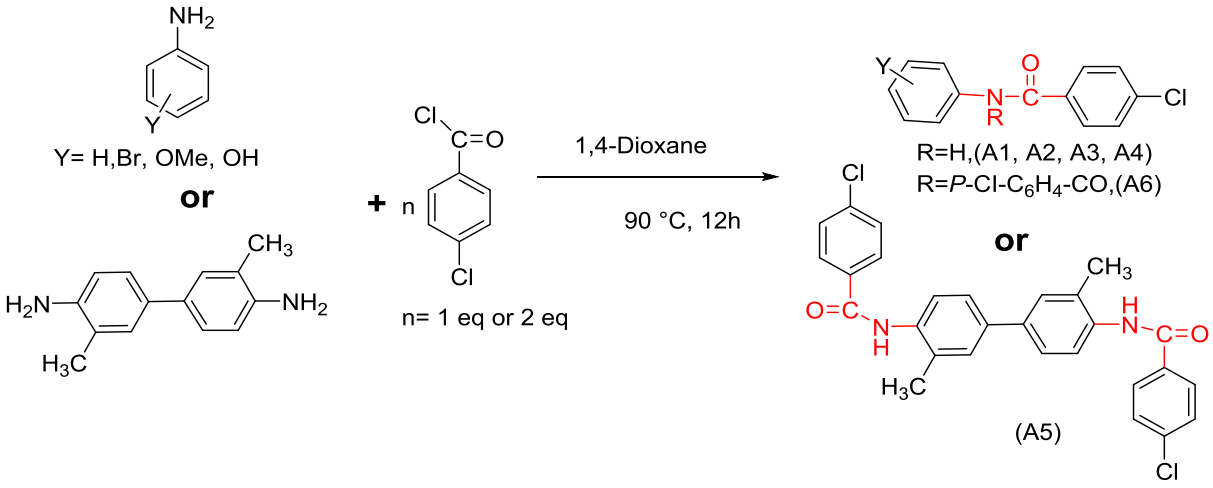

الجزء الثاني: -

بعض من مشتقات السلفونامايد حضرت (B1-B5) حضرت من خلال مفاعلات انيلين معوض في الموقع بارا أو اورثو توليدين مستخدمين DCM كمذيب وEt_3N كعامل مساعد.

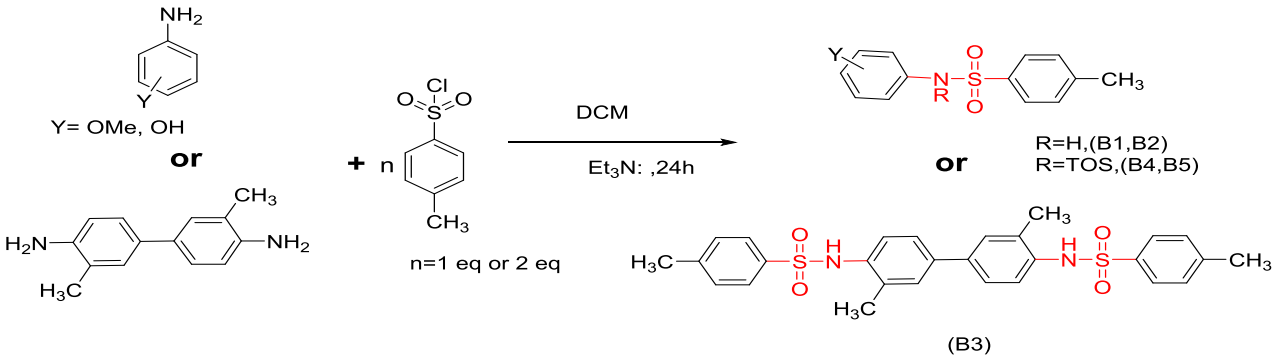

الجزء الثالث:-

هذا الجزء يصف تحضير بعض مشتقات الاليل (C1-C3) بواسطة مزج A1, B2 أو اورثو توليدين مع بروميد الاليل وكربونات البوتاسيوم في الأسيتون والماء.

جامعة ميسان

كلية العلوم

قسم الكيمياء

تحضير وتشخيص ودراسة النشاط البايولوجي والالتحام الجزيئي لبعض مشتقات الانلين الجديدة

الرسالة

مقدمة الى كلية العلوم/جامعة ميسان

لأستيفاء متطلبات الحصول على درجة الماجستير في علوم الكيمياء

من قبل

زهراء صباح شمخي

بكالوريوس علوم كيمياء /جامعة ميسان 2021

بأشراف

أ.د كريم سالم عباس

أ.م.د يسرى صبري عبد الصاحب

2025